PHYSICAL REVIEW
LETTERS

VOLUME 6 JUNE 1, 1961 NUMBER 11

LIFETIMES OF FAST IONS IN THE PLASMA OF DCX

C. F. Barnett, J. L. Dunlap, R. S. Edwards, G. R. Haste, H. Postma,
J. A. Ray, R. G. Reinhardt, W. J. Schill, R. M. Warner, and E. R. Wells
Oak Ridge National Laboratory,* Oak Ridge, Tennessee
(Received May 4, 1961)

Previous publications[1-3] have outlined the general construction of the DCX machine and have described various measurements of the plasma ring formed in DCX by injecting 600-kev diatomic hydrogen ions in the median plane and dissociating them with a vacuum carbon arc. A plasma ring of 300-kev protons concentric with the magnetic axis can also be formed without an arc, since dissociating collisions occur between the diatomic ions and residual gas molecules. In this Letter we report the results of recent lifetime studies for protons trapped in DCX via the latter mechanism, gas dissociation. These studies show mean containment times in the order of seconds at initial proton densities of 10^7 cm^{-3}.

The present experiments were conducted in the DCX 2:1 mirror geometry with an axial midplane magnetic field of 10 kilogauss and an H_2^+ beam of about 1.4 ma. With the H_2^+ beam entering the system, oil diffusion pumps and an evaporated titanium film produced a pressure of 5×10^{-8} mm Hg within the water-cooled copper liner which surrounded the plasma region. The steady-state fast proton density was about 10^7 cm^{-3}, as determined from the expression

$$n_+ = I n_0 \sigma_d L \tau / V,$$

where I is the injected H_2^+ current, n_0 is the neutral gas density, σ_d is the dissociation cross section for proton production, L is the path length of the H_2^+ for dissociations that result in effective trapping (approximately 10 cm), τ is the measured lifetime of the fast protons, and V is the plasma volume (about 10^{+3} cm^3).

A major loss mechanism for the circulating protons is electron-capture collisions with the background gas. The lifetimes of the protons were deduced from measurements of the energetic neutrals resulting from these collisions. This neutral flux is a measure of the charge-exchange reaction rate within the plasma volume, $n_+ n_0 \sigma_{cx} v$, where σ_{cx} is the electron capture cross section and v is the velocity of the circulating protons. The rate at which this neutral flux decays after the H_2^+ beam is interrupted is then the rate at which the fast proton density disappears, since $n_0 \sigma_{cx} v$ is nearly constant during the decay interval. If charge exchange is the only loss process, the proton density and the neutral flux should decrease exponentially with a time constant, $\tau = 1/(n_0 \sigma_{cx} v)$.

In these experiments a portion of the energetic neutrals was passed through a 10^{-5}-inch thick nickel foil and then monitored by a Faraday cup. This foil thickness is sufficient to insure a statistical charge state equilibrium of the ions and neutrals escaping the back surface. For energies of 300 kev the emerging beam is greater than ninety-nine percent protons. Particle beams with energies greater than 150 kev are not attenuated by this thickness. The current from the Faraday cup was amplified by a transistor circuit and then displayed on an oscilloscope.

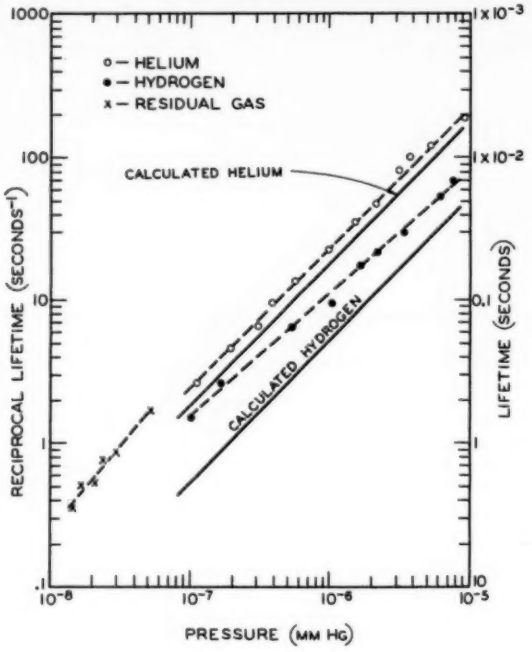

FIG. 1. Reciprocal lifetime as a function of hydrogen, helium, and residual gas pressure.

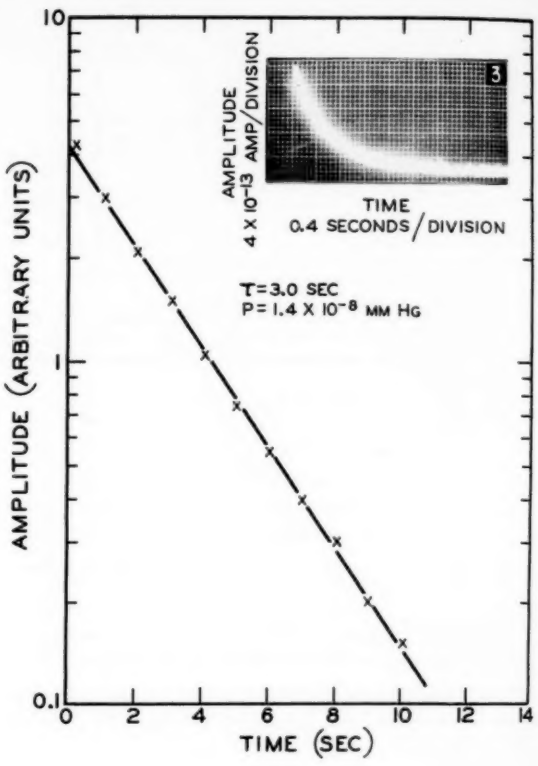

FIG. 2. Amplitude of neutral-particle detector signal as a function of time.

Photographs of the oscilloscope trace decay after interruption of the H_2^+ beam provided curves of the decay of the fast proton density.

The pressure responses of the decay traces to helium and hydrogen were determined in the range from base pressure to 1×10^{-5} mm Hg. The decay curves were exponential through this pressure range. Figure 1 shows the reciprocal lifetimes observed during the helium and hydrogen runs, along with the reciprocal lifetimes expected from the loss of 300-kev protons by charge-exchange collisions in each gas. The deviation of the hydrogen curve from a 45-degree slope results from the presence of background gas contaminants which possess larger electron capture cross sections. The cross sections of helium and the contaminants seem to be about equal, and the helium curve has a 45-degree slope. For helium the measured lifetimes are 80% of the calculated. For hydrogen at the higher pressures, where the effects of the contaminants are the smallest, the measured lifetimes are 60% of the calculated. The discrepancy is attributed to small errors in measurements and to the energy lost (approximately 10 kev) by the protons through ionization and excitation collisions with the gas.

The residual gas curve of Fig. 1 was obtained by cooling the liner which surrounded the plasma region with liquid nitrogen and photographing the decay traces as the pressure decreased. Figure 2 shows a typical decay trace obtained at the lowest pressure. The semilog plot shows an exponential decay with a time constant of 3 seconds. That the decay traces are exponentials constitutes evidence for a single loss mechanism.

Linear plots of the measured reciprocal lifetimes as functions of pressure show that the helium and residual gas data extrapolate to infinite lifetime at zero pressure, as is expected if proton loss is due solely to charge exchange. As a result of the higher average electron capture cross section of the background gas contaminants, the hydrogen data extrapolate to a finite lifetime.

We believe that the present experiment is significant in that we have shown that a mirror machine is capable of containing a plasma for seconds at densities of 10^7 cm^{-3} with charge exchange as the only apparent mechanism for particle loss. Our future work will be undertaken to increase the density of stored ions, to study the extent of orbital disorganization, and to investigate the homogeneity of the ion distribution.

*Operated by Union Carbide Corporation for the U. S. Atomic Energy Commission.

[1]C. F. Barnett et al., Proceedings of the Second United Nations International Conference on the Peaceful Uses of Atomic Energy, Geneva, 1958 (United Nations, Geneva, 1958), Vol. 31, p. 298.

[2]A. H. Snell, Fourth International Conference on Ionization Phenomena in Gases, Uppsala, Sweden, 1959 (North-Holland Publishing Company, Amsterdam, 1960), Vol. II, pp. 997-1001.

[3]J. L. Dunlap, IRE Trans. on Nuclear Sci. NS-7, No. 4, 19 (1960).

EVIDENCE ON THE LAMINAR NATURE OF THE EXOSPHERE OBTAINED BY MEANS OF GUIDED HIGH-FREQUENCY WAVE PROPAGATION

R. M. Gallet and W. F. Utlaut
National Bureau of Standards, Boulder, Colorado
(Received May 1, 1961)

The purpose of this Letter is to report the results of a series of experiments which take advantage of the laminar structure of the exosphere for testing the existence and properties of the sheets at large distances above the earth. In addition, it is suggested that this new mode of propagation may be useful for observing, in a quasi-continuous manner from ground observations, the characteristics of the permanent ring current, recently observed in Explorer VI and Pioneer V measurements.[1]

It has been known for some years[2] that the structure of the earth's exosphere seems to be somewhat fibrous, in the sense that the electron density distribution has slight increases distributed in thin sheets or columns along the magnetic field lines. This property is evidenced mainly by the observations made on "whistlers."[3] These are a very specific type of natural radio signals of very low frequencies propagating along the curved magnetic lines of force and generated by lightning discharges. The observations show that quite often the signals are guided along several, well-separated, discrete paths. Also, the existence of long trains of echoes, in which the signal is reflected back and forth many times between the two ends of the line of force with a remarkably small total attenuation, requires that the waves be guided very efficiently within such columns or sheets, in a way similar to the guided propagation of light in long glass fibers ("light pipes") or radio waves in dielectric waveguides. In the whistler mode the frequency of the signal has to be smaller than the electron gyrofrequency, $\omega_H = eH/mc$, and smaller than the angular plasma frequency, ω_p, given by $\omega_p^2 = 4\pi N_e e^2/m$. Under such conditions, the refractive index is usually very large (from 7 to 30 within the exosphere) and there are strong refraction effects, complicated by a great anisotropy and a large dispersion.

The energetic particles comprising the outer Van Allen belt have also been observed by Pioneer IV[4] and by Explorer VII,[5] the latter under disturbed conditions, to be distributed in thin layers which are remarkably sharp. The relationship between the density distribution of the high-energy electrons of the Van Allen radiation, which have a low space density, and the more numerous thermal electrons forming the bulk of the exosphere is, however, not yet determined.

The present series of experiments was stimulated by the suggestion made by Obayashi[6] of the possibility of high-frequency wave guidance through the exosphere. In this case, the frequency is well above the plasma frequency and gyrofrequency, and the refractive index is almost equal to unity; consequently, the wave velocity is very nearly that for free space. We believe, however, that guidance along the line of force is afforded by a relatively small gradient of electron density transverse to the field under circumstances where the gradient is sufficient to produce the slight bending equal to the curvature of the line of force. Also it is neces-

sary that the wave enter the exosphere in a direction tangential to the magnetic field.

It is interesting to note, historically, that Pedersen in a 1929 paper[7] suggested the possibility of propagation along a band of electrons or ions which connects the northern and southern polar areas and he considered such bands to be formed by the magnetic field of the earth. This mode of propagation was suggested by Pedersen to provide an explanation of the long-delay echoes observed at Oslo, Norway, in 1927 by Hals[8] and later by Van der Pol and Størmer at a frequency of 9.56 Mc/sec.[9] A later search for such echoes, on frequencies of 13.455 Mc/sec (30 kw) and 20.675 Mc/sec (9 kw), was made in the period 1947-1949 by Budden and Yates,[10] and during this period echoes considered to be of long delay were not observed. Observations, however, were made at several selected intervals of an hour or two in length one day each fortnight only and, if conditions permitting such echoes exist for short periods, a small percentage of time, the relatively infrequent periods of observation may explain why long-range echoes were not detected.

The experimental work of Obayashi was performed in Japan at a geomagnetic latitude of 26°. The magnetic line originating there is about 7000 km in length and, at most, reaches a height above the magnetic equator of 1500 km. Thus, most of the propagation path lay below the exosphere in the normal ionosphere. In order to test better the properties of the exosphere, experiments conducted at a much higher geomagnetic latitude are necessary so that the radio wave may traverse sufficiently far into the exosphere. Fortunately, a transmitter located near Washington, D. C. (geomagnetic latitude 50.2°) was available for use in the present series of observations. The line of force beginning at this point, computed using spherical harmonic analysis of the geomagnetic field with 48 terms included (see Vestine and Sibley[11]), has a maximum height above the earth's surface of 10 460 km (2.64 earth radii measured from the center of the earth) and a length of 33 650 km to the corresponding magnetically conjugate point in the South Pacific.

Attempts were made on various occasions during a two-month period from late April to June of 1960 to observe the signal propagating via the suggested mode and backscattering from the ground at the point in the other hemisphere which is the magnetic conjugate of the transmitter. A high-frequency radar having a peak-pulse power output of approximately 100 kw was used. To aid in signal identification a special pulse group of two one-millisecond pulses separated in time by 8 milliseconds was transmitted at a group repetition rate of 2.5 cps. A superheterodyne receiver, with a bandwidth of approximately 1 kc/sec, was used in conjunction with a low-noise preamplifier to receive the signal of which range-time and range-amplitude presentations were photographically recorded. The antenna used for both transmitting and receiving was an array of two vertically polarized 3-element Yagis which had been designed to operate on a frequency of 13.7 Mc/sec. This was tipped upward 71° to align it with the earth's magnetic field. Observations were made only during the nighttime, because of the limited frequency range of operation imposed by the antenna and because of the marginal sensitivity of the radar, so that the benefits of low critical frequency and low absorption of the ionosphere could be utilized. Table I summarizes the periods of observations and gives the radar range and times during which a clearly recognized signal was detected.

Backscatter echoes were found to exist for a length of time ranging from a few minutes up to a period in excess of 50 minutes. The received signals were weak, and it is estimated that the transmission loss for these signals exceeded 200 db. Two echo characteristics of interest are their sharpness and range stability. Pulse broadening much greater than that caused by the receiver circuitry has not been observed. This is in contrast to the large amount of pulse elongation found in normal ground backscatter echoes propagated via the ionosphere, where energy is returned from a large area of the earth, and suggests a selective mechanism of wave guidance such that only those waves whose normals lie very close to the direction of the magnetic field are propagated via this mode. The range of an echo usually remained constant throughout the period during which it was detectable but, as may be seen in Table I, echo ranges differed from one time of occurrence to another. Figure 1 is a good example showing the stability of echo range as well as the sharpness of echo return. This record was made between the hours of 0200 and 0300 U.T. on June 9, 1960, during which time an echo at a range of 27 600 km was found to exist for more than 45 minutes, gradually weakening in strength and finally disappearing. The total propagation path distance of this echo

Table I. Summary of one set of data.

Observation period U.T. Date	Start	Stop	Echo return U.T. Start	Stop	Approximate range (km)
April 22	0100	0513			
22	0558	1309	1000	1040	25 000
25	0440	1240			
27	0500	1244			
28	0630	1149			
30	0930	1241			
May 2	0536	1205			
3-4	2235	1226	0140	0142	20 000
			0220	0222	20 000
5	0456	1225			
6	0520	1156	0645	0648	21 500
			0700	0704	22 000
			0951	0953	22 100
9	0444	1234			
10	0445	1104			
12	0529	1202	0530	0532	21 500
			0630	0635	21 500
13	0330	0950	0405	0420	24 100
			0800	0802	25 200
16	0344	0907			
18	0325	0846			
23	0346	1005			
25	0308	1026			
26	0254	0302			
28	0312	0906	0802	0815	21 600
31	0315	1006			
June 1	0325	1003			
7	0434	0903			
8	0244	0904	0605	0608	20 600
			0637	0640	20 600
			0650	0653	20 600
			0710	0729	20 600
9	0200	1007	0204	0250	27 600
10	0116	1008			
11	0319	0945	0730	0732	24 500
15	0307	0805			
16	0138	1003			
19	0409	1105			
20	0219	0900			
21	0249	0902	0300	0400	24 000

(55 200 km) exceeded by at least 13 000 km the range of round-the-world echoes which have been found by various observations made in the high-frequency and the very-low-frequency bands to range from 41 160 to 42 000 km.[12,13]

The characteristics of the echoes described above differ from those reported by Obayashi and shown in Fig. 8 of reference 6. His echoes, at ranges of about 7000 km, show continuous fluctuations in range with time and are not sharp but instead are spread out. Their characteristics and range are very similar to those of normal ionospherically propagated backscatter echoes shown by several investigators[14,15] and the trans-equatorial echoes reported by Stanford observers.[16]

All exospheric echoes received at Washington, D. C., were found at ranges which were less than the calculated field-line length and different ranges from echo to echo were observed. Shortening of field lines may be explained in terms of the combined effect of the diamagnetism and drift currents, observed at altitudes beyond 6 earth radii (Explorer VI and Pioneer V).[1] Time variations of the intensity and position of the currents are, perhaps, sufficient to account quantitatively for the change in length of the line of force even though they probably do not cause a detectable change in the strength of the magnetic field observed at the surface of the earth. Thus, it is possible that this new method of exploring the exosphere may be able to provide information on the characteristics of the diamagnetism and drift currents from observations made on the ground. An additional quantity which is measurable by this type of experiment, if our concept of the method of wave guidance is correct, is the gradient of electron density transverse to the magnetic field and in the plane containing the magnetic line. Under the conditions of our experiment (i.e., frequency and latitude) it has

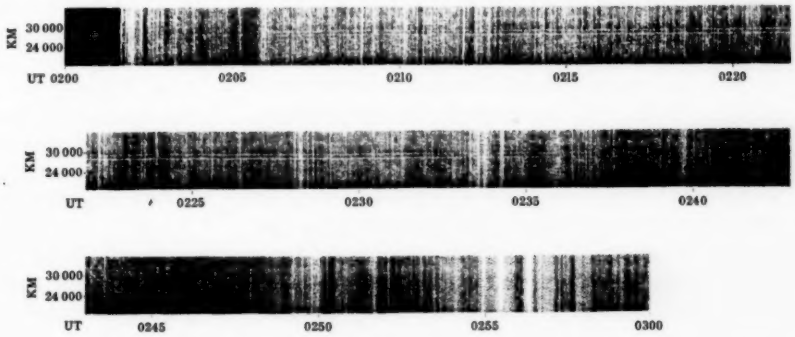

FIG. 1. Exospheric backscatter, June 9, 1960, 0200-0300 U.T.

been calculated that an electron density gradient equal to or greater than 8.1×10^{-2} electron/cc cm transverse to the field was needed for wave guidance.

Continuation of this experiment, at the same and at higher geomagnetic latitudes and transmitting nearly simultaneously on several different frequencies, is planned to permit further investigation of the variations of transverse electron density gradient and the effects of the ring current. Observations of one-way propagation, with transmitter and receiver located at magnetic conjugate points such as New Zealand and southern Alaska, are also being considered.

A more complete discussion of the conditions necessary for the high-frequency exospheric mode of propagation and the resulting information which can be deduced concerning the exosphere is planned for publication in the future.

[1]E. J. Smith, P. J. Coleman, D. L. Judge, and C. P. Sonett, J. Geophys. Research 65, 1858 (1960).

[2]R. M. Gallet, Twelfth General Assembly of Union Radio-Scientifique Internationale, Symposium on whistlers and very low frequency emissions, September, 1957, Boulder, Colorado (unpublished).

[3]L. R. O. Storey, Phil. Trans. Roy. Soc. (London) A246, 113 (1953).

[4]J. A. Van Allen and L. A. Frank, Nature 184, 219 (1959).

[5]B. J. O'Brien, J. A. Van Allen, F. E. Roach, and C. W. Gartlein, J. Geophys. Research 65, 2759 (1960). See also B. J. O'Brien and G. H. Ludwig, J. Geophys. Research 65, 2695 (1960); R. L. Arnoldy, R. A. Hoffman, and J. R. Winckler, J. Geophys. Research 65, 1361 (1960).

[6]T. Obayashi, J. Rad. Research Lab. Japan 6, 603 (1959).

[7]P. O. Pedersen, Proc. Inst. Radio Engrs. 17, 1750 (1929).

[8]Carl Størmer, Nature 122, 681 (1928).

[9]Balth Van der Pol, Nature 122, 878 (1928).

[10]K. G. Budden and G. G. Yates, J. Atmospheric and Terrest. Phys. 2, 272 (1952).

[11]E. H. Vestine and W. L. Sibley, J. Geophys. Research 65, 1967 (1960).

[12]H. A. Hess, Proc. Inst. Radio Engrs. 36, 981 (1948).

[13]M. Desirant and J. L. Michiels, Electromagnetic Wave Propagation (Academic Press, Inc., New York, 1960).

[14]W. L. Hartsfield and R. Silberstein, Proc. Inst. Radio Engrs. 40, 1700 (1952).

[15]W. Dieminger, Avionics Research (Pergamon Press, New York, 1958).

[16]O. G. Villard, Jr., S. Stein, and K. C. Yeh, J. Geophys. Research 62, 399 (1957).

ELECTRICAL CONDUCTION AND BREAKDOWN IN HIGH-PRESSURE RARE GASES

R. Forman

Parma Research Laboratory, Union Carbide Corporation, Parma, Ohio

(Received March 29, 1961)

Some novel results have been obtained in the study of electrical conduction and breakdown effects in high-pressure inert gases (1-300 mm of Hg) using a high-temperature thermionic emitter as a cathode.

Two types of diodes have been used in these measurements. The first is a cylindrical-type diode which consists of a 0.010-inch diameter filament about 3.5 cm long and a cylindrical anode 1 cm in diameter and 1.25 cm long. The second type consists of a horizontal filament about 1.25 cm long and 0.010 inch in diameter with a disk anode, 1.5 cm in diameter, placed 0.5 cm above the filament. The filament was in general of tungsten, although similar results have been obtained on tantalum and rhenium. The anode material was either tungsten or tantalum sheet.

The diode assembly was mounted in a Pyrex envelope and evacuated on an ultrahigh-vacuum system. The high-vacuum pump consisted of a forepump, three-stage water-cooled oil diffusion pump and a liquid nitrogen cold trap. Included in the high-vacuum system was an Alpert-type metal valve, a molybdenum getter tube, a purified break-seal argon bottle, the tube under test, and a Bayard-Alpert ionization gauge. The system was baked out at 400°C for 8-10 hours and after degassing the pressure in the system was below 10^{-9} mm of mercury. The filaments were degassed by heating to 2500°-3000°K and the anodes were degassed at about 1000°C by electron bombardment.

After the tubes had been processed as described, anode voltage vs anode current vacuum data were taken on these diodes. The filaments were heated by a dc voltage source. The points shown as dark squares in Fig. 1 illustrate

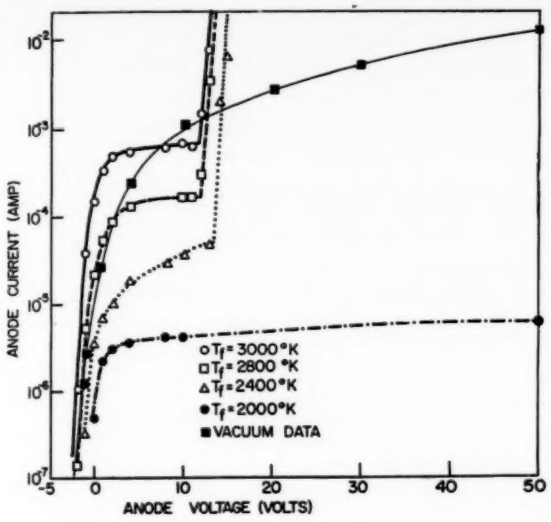

FIG. 1. Anode current-voltage characteristics of Tube 7B at vacuum and at an argon pressure of 107 mm of mercury. This tube is a cylindrical diode with a 0.01-inch diameter tungsten filament and a 1.0-cm diameter tungsten cylindrical anode. The vacuum data are shown by the solid squares. The other data illustrate the diode characteristics in argon as a function of filament temperature.

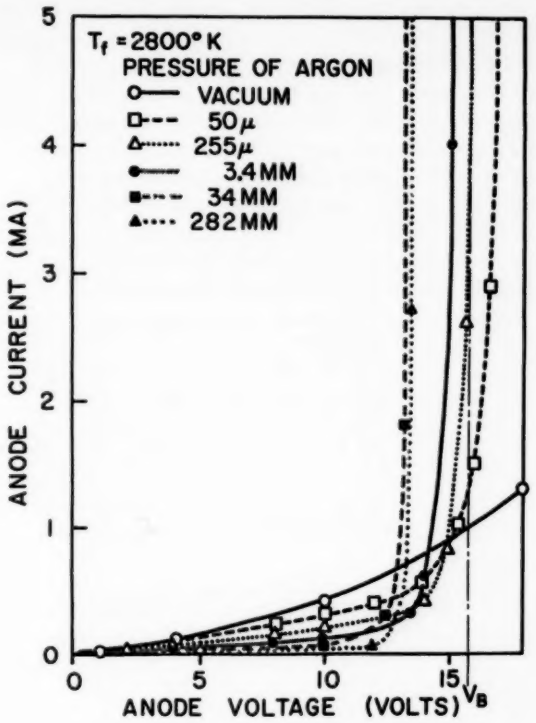

FIG. 2. Anode current-voltage characteristics of Tube 8A at a given filament temperature with the pressure of argon as the other parameter. This tube has a disk tantalum anode and a 0.01-inch diameter tungsten filament.

these data taken on a cylindrical-type diode with a filament temperature of 2800°K. This curve is representative of space-charge data and above +1 volt is the same for all filament temperatures between 2400°-3000°K. However, if a high pressure of high-purity argon is the ambient, some very different anode current vs anode voltage curves are obtained. These are illustrated in Fig. 1 for the case where the tube was filled with argon to 107 mm of mercury. The space-charge-limited vacuum data, described previously, are in the same figure for comparison.

The high pressure—high temperature data of Fig. 1 have some unusual features. One obvious effect is that the current vs voltage curves at the high pressure do not follow a space-charge relation. They are extremely temperature dependent. In addition, at temperatures of 2400°K and above, the gas breaks down before the anode potential reaches the ionization potential of the gas. These measurements were made with dc on the filament where the negative end of the filament was always the common terminal for the dc power supply in the anode circuit. Under these conditions the maximum accelerating voltage in the tube was the anode voltage and this type of arrangement eliminated any possibility of having the filament voltage contribute to early breakdown.

Figure 2 is a plot of the anode current vs anode voltage for a diode, with a filament temperature of 2800°K. The ambient pressure of argon is the variable parameter. This tube had a 0.01-inch diameter tungsten filament and a tantalum disk anode. The vacuum line follows the usual $V^{3/2}$ space-charge equation. One should note that, at pressures above 1 mm, there is no doubt that the gas breaks down before ionization potential is reached. At lower pressures (250 μ and below), breakdown occurs at ionization potential or above.

Similar results have been obtained in xenon and krypton but not in helium or neon.

The highest temperature current-voltage curve of Fig. 1 resembles those obtained on a gas plasma with a Langmuir probe and can be analyzed on this basis to yield very reasonable values of the parameters. This plasma-like behavior strongly suggests that there are positive ions being generated in the gas below breakdown which neutralize the electron space charge. From the data in Fig. 1 it is also obvious that if this assumption is correct, there are a greater number of ions being generated at a higher temperature than at the lower ones, because the measured electron current rises with increasing temperature.

A possible mechanism for the production of these ions is the thermal ionization of the inert gas at or in the vicinity of the hot filament. In addition, it is probable that some of the high electrical conduction properties of the gas, shown in Figs. 1 and 2, can be partly attributed to the generally low collision cross section for electrons in the inert gases.

A more complete report will be published in the Journal of Applied Physics.

NEW ALLOTROPIC FORM OF He^3†

A. F. Schuch and R. L. Mills

Los Alamos Scientific Laboratory, University of California, Los Alamos, New Mexico

(Received May 8, 1961)

The occurrence in solid He^4 of a change in phase from hexagonal closest packing to the face-centered cubic structure[1,2] at a temperature and pressure above 14.9°K and 1100 atmospheres has prompted an investigation of the high-pressure and temperature structure of He^3.

This investigation employed the cryostat and x-ray diffraction arrangement used in the He^4 study.[2] However, because higher pressures were required, the He^3 was solidified in a beryllium cell with a slightly thicker wall. The cell was a cylinder with a 0.8-mm bore and a 0.5-mm wall. The pressure was measured with a Bourdon gauge which was calibrated with a free piston gauge. The temperature was measured with a hydrogen vapor pressure thermometer fastened to the sample cell. A four-stage mercury piston pump designed by Edeskuty[3] was used to compress the gas from 4 psi to the required pressure. The diffraction patterns were obtained with copper and with molybdenum radiation and were photographed on a 4×5-inch flat film placed 5 cm from the sample. During the exposure the cell was oscillated through an angle of thirty degrees.

The He^3 was analyzed with a mass spectrometer. The impurities found were 0.04% He^4 and 0.04% of a mixture of hydrogen isotopes. The remaining 99.92% was He^3.

The sample was first prepared by cooling the cell to the neighborhood of 20°K and then compressing the helium into it at the desired pressure of the experiment. The gas was then solidified by slowly cooling it. The intention was always to have the solid at a temperature and pressure near the melting curve.

It was found that He^3 under high pressure also transforms to the face-centered cubic structure. The data from a diffraction photograph of He^3 at 18.74°K and 1693 atmospheres are listed in Table I. In the table, d is the interplanar spacing found and a_0 is the length of the edge of the cubic unit cell derived from it.

The average cell edge obtained from seven photographs of helium at an average temperature and pressure of 18.76°K and 1690 atmospheres is $a_0 = 4.242 \pm 0.016$ A. This dimension gives a molar volume of 11.50 cc, which is to be compared to 11.54 cc computed from the measurements of Grilly and Mills.[4]

The hcp-fcc transition occurs at a higher pressure than it does for He^4. Where the transition line joins the melting curve has not been deter-

Table I. Data from one diffraction photograph.

hkl	d (A)	a_0 (A)
111	2.425	4.200
200	2.138	4.276
220	1.495	4.228
131	1.283	4.255
222	1.221	4.230
		Average = 4.238

mined in this study. It was observed, however, that He^3 at 15.98°K and 1341 atm still has the hexagonal close-packed structure. The cell dimensions and molar volume at this condition are: $c_0 = 4.986$ A, $a_0 = 0.046$ A, $c_0/a_0 = 1.637$, and $V = 12.07$ cc. The computed[4] molar volume is 12.09 cc.

The new phase has been designated the γ phase.

We wish to acknowledge the many contributions of Donald F. Clinton and the members of his staff shop in the construction and repair of items of equipment used in this research.

---

†Work performed under the auspices of the U. S. Atomic Energy Commission.

[1]J. S. Dugdale and F. E. Simon, Proc. Roy. Soc. (London) A218, 291 (1953).

[2]R. L. Mills and A. F. Schuch, Phys. Rev. Letters 6, 263 (1961).

[3]F. J. Edeskuty, Ind. Eng. Chem. 51, 69(A) (1959).

[4]E. R. Grilly and R. L. Mills, Ann. Phys. 8, 1 (1959).

SIMPLE MODEL FOR THE MAGNETIC BEHAVIOR OF SUPERCONDUCTORS OF NEGATIVE SURFACE ENERGY

B. B. Goodman

Institut Fourier, Grenoble, France

(Received April 12, 1961)

It is well known that for certain superconductors the magnetic field H_c^* required for the complete suppression of the superconducting state considerably exceeds the critical field H_c. Interest in this question has been revived by the discovery that, well below their transition temperatures, exceptionally high values of H_c^* are found for Mo_3Re[1] (≈ 15 kgauss) and Nb_3Sn[2] (> 88 kgauss). While inhomogeneous strains and chemical inhomogeneities in a superconductor are known to influence its behavior, probably owing to a resulting spatial variation of the surface energy of a normal-superconducting boundary, it is the purpose of this Letter to propose a simplified model for the magnetic behavior of a homogeneous strain-free superconductor, in which a spatially independent negative surface energy could lead to large values of H_c^*/H_c.

Suppose that a superconductor of negligible demagnetizing coefficient divides itself, in the presence of a magnetic field H, into thin normal and superconducting laminas, of thickness d_n and d_s, respectively. Let us add to the resulting expression for g, the Gibbs free energy per unit volume,[3] an additional contribution arising from a configurational interphase surface energy, $\Delta' H_c^2/8\pi$. One then obtains

$$g = (H_c^2/8\pi)\left\{-x\left[1 - \frac{q}{p} - h^2\left(1 - \frac{\tanh p}{p}\right)\right] - h^2\right\}, \qquad (1)$$

where $H_c^2/8\pi$ is the difference in free energy per unit volume between the normal state and the superconducting state in zero field, $h = H/H_c$, $x = d_s/(d_n + d_s)$ is the fraction of the specimen in the superconducting state, $p = d_s/2\lambda$, and $q = \Delta'/\lambda$, λ being the penetration depth of the magnetic field. Equation (1) supposes that the London equation is obeyed in the superconducting laminas, a hypothesis we shall comment on later. As London pointed out,[3] the condition for Eq. (1) to lead to the well-known magnetic behavior of a so-called ideal superconductor is that $q > 1$. Hence $\Delta = \Delta' - \lambda$, the total surface energy usually measured experimentally, is then positive. Pippard[4,5] has suggested that Δ' should be of the order of ξ, the coherence distance in the superconducting state. For pure superconductors, ξ tends towards a limiting value ξ_0 characteristic of the metal; while for very impure superconductors ($l \ll \xi_0$), ξ is of the order of l, the electronic mean free path.[6]

For $q < 1$, corresponding to a superconductor of negative total surface energy, Eq. (1) leads to the existence of two transition fields. For h less than the lower transition field h', given by $h' = q^{1/2}$, one finds $x = 1$ and $p = \infty$, so that here the specimen exhibits a Meissner effect, while for $h > h''$, where h'' is given by

$$q = h'' + (1 - h''^2)\tanh^{-1}(h''^{-1}), \qquad (2)$$

the normal state is stable. For $q \ll 1$, Eq. (2) becomes $h'' = 2/3q$. For intermediate fields the laminar structure is stable, the thickness of the

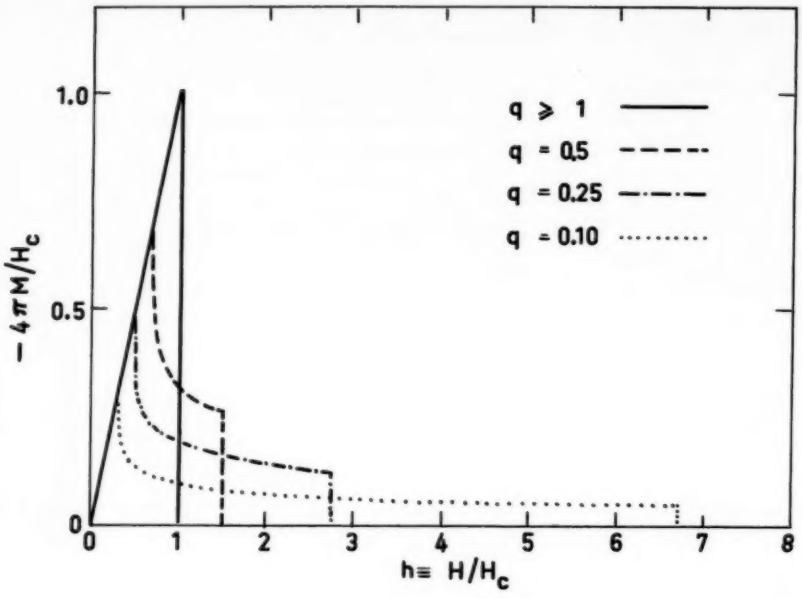

FIG. 1. Reduced magnetization curves for the present model of a superconductor, for different values of q.

superconducting laminas being determined by the equation $qh^{-2} = \tanh p - p\,\mathrm{sech}^2 p$, while that of the normal laminas remains negligible ($x = 1$). The magnetization M, given by $-4\pi M = xH[1 - (\tanh p)/p]$, leads to the curves given in Fig. 1 for different values of q. We may note that, since the surface energy does not contribute to g either for $h = 0$ or for $h > h''$, the area under each magnetization curve is independent of q and satisfies the thermodynamic condition,

$$\int_0^\infty M dH = -H_c^{\,2}/8\pi.$$

It is tempting to correlate the prediction of two transition fields for $q < 1$ with the observation of Doidge[7] and Davies[8] that in dilute tin alloys the magnetic and resistive transitions become distinct when $l \lesssim \lambda$. However, the magnetic transitions observed by these authors went practically to completion at the lower transition field. The inadequacy of the present model, when l is not small compared with λ, is hardly surprising, since here the London equation is known to be inexact,[6] and furthermore it is physically unreasonable to assume, as we have done, that the normal laminas can be of negligible thickness.

However, these limitations should be much less serious for very impure superconductors, for which l is small, and Fig. 2 shows magnetization curves based on the present model which have been fitted to the hysteresis-free results obtained by Calverley and Rose-Innes[9] for a single mixed crystal of composition $Ta_{36}Nb_{64}$. It has here been assumed that the fields H_c^* quoted for the complete suppression of superconductivity correspond to the predicted discontinuous disappearance of M at h''. In fact, it is more probable that, owing to a field dependence of λ which we have not considered, the observed magnetization went to zero continuously, as has been found for superconducting thin films and colloids.[10,11] The results of these authors suggest that the effect of allowing λ to vary with H would probably be to distort the magnetization curves in Fig. 1 in such a way as (a) to yield a continuous disappearance of M, h'' being increased by at most a factor of about $\sqrt{2}$, and (b) to decrease the fitted values of H_c in Fig. 2 by not more than 10%. The correction required by the field dependence of λ has therefore been ignored.

By extrapolation of the values of H_c to 0°K one obtains $H_0 = 1600 \pm 100$ gauss, so that $H_0/T_c = 230$ gauss deg^{-1}, which is within 20% of the values found for this quantity for pure Ta and Nb. The value obtained for q, which is expected to be close to l/λ, may be discussed by using standard expressions relating λ, ξ_0, l/σ (σ being the conductivity of the specimen $= 2.5 \times 10^{-4}$ emu), and T_c (its transition temperature = 6.9°K) to the properties of the Fermi surface.[12] These lead to $\lambda = 800$ A

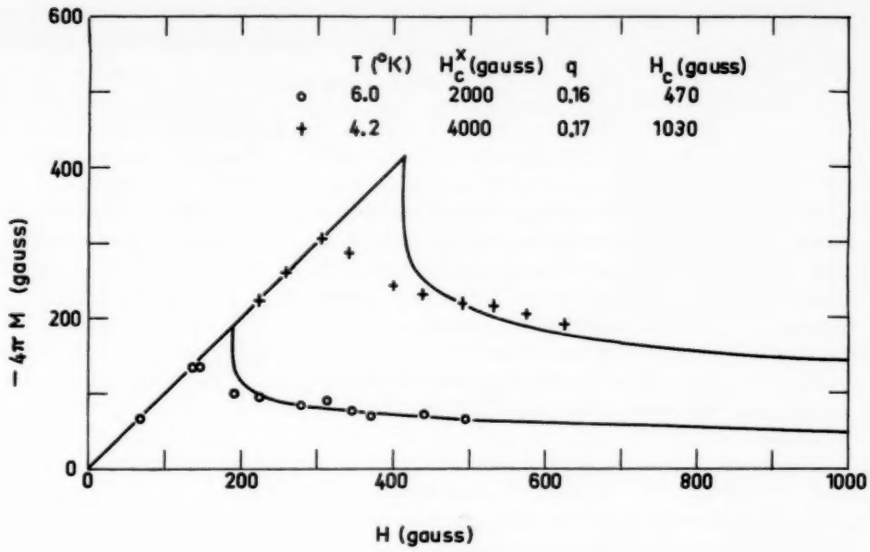

FIG. 2. Fit of the present model to the magnetization curves of Calverley and Rose-Innes' specimen of $Ta_{36}Nb_{64}$.

and $l = 76(S/S_0)^{-1}$ A, where S is the free area of the Fermi surface in the alloy and S_0 the area it would have if the five conduction electrons per atom were perfectly free. Thus the result $q = 0.16$ suggests that (S/S_0) should be somewhat less than unity, which does not seem unreasonable in view of the values of this order of magnitude which have been found for several other metals.[13]

The present model therefore seems to give a plausible account of the results of Calverley and Rose-Innes, and it confirms the impression that their magnetization curves represent a new type of magnetic behavior characteristic of homogeneous strain-free superconductors of negative surface energy. The magnetic field needed for the complete suppression of superconductivity, $h''H_C$, appears as a true thermodynamic variable, rather than as a property associated with certain individual lattice flaws. According to this model, for large h'', $h'' = 2/3q \approx 2\lambda/3\xi$, while using a different model, which takes into account the field dependence of λ, Pippard[5] finds a value which is only slightly larger: $h'' = (f\sqrt{6})\lambda_{H=0}/\pi\xi$; here f depends on the details of the model and lies between 1 and $\sqrt{2}$. Since for $l \ll \lambda$, we have $\lambda \propto l^{-1/2}$ and $\xi \approx l$, we may expect that, other things being equal, $h'' \propto l^{-3/2}$. The persistence of superconductivity in high magnetic fields, brought about by the existence of a negative surface energy, should therefore be favored by a short electronic mean free path, and thus a high resistivity, in the normal state.

[1]J. E. Kunzler, E. Buehler, F. S. L. Hsu, B. T. Matthias, and C. Wahl, J. Appl. Phys. 32, 325 (1961).
[2]J. E. Kunzler, E. Buehler, F. S. L. Hsu, and J. H. Wernick, Phys. Rev. Letters 6, 89 (1961).
[3]F. London, Superfluids (John Wiley & Sons, Inc., New York, 1950), Vol. I, pp. 125-130.
[4]A. B. Pippard, Proc. Cambridge Phil. Soc. 47, 617 (1951).
[5]A. B. Pippard, Phil. Trans. Roy. Soc. (London) 248, 97 (1955).
[6]A. B. Pippard, Proc. Roy. Soc. (London) A216, 547 (1953).
[7]P. R. Doidge, Phil. Trans. Roy. Soc. (London) 248, 553 (1956).
[8]E. A. Davies, Proc. Roy. Soc. (London) A255, 407 (1960).
[9]A. Calverley and A. C. Rose-Innes, Proc. Roy. Soc. (London) A255, 267 (1960).
[10]J. M. Lock, Proc. Roy. Soc. (London) A208, 391 (1951).
[11]C. S. Whitehead, Proc. Roy. Soc. (London) A238, 175 (1956).
[12]T. E. Faber and A. B. Pippard, Proc. Roy. Soc. (London) A231, 336 (1955).
[13]R. G. Chambers, Proc. Roy. Soc. (London) A215, 481 (1952).

EFFECT OF MAGNETIC FIELD ON THERMAL CONDUCTIVITY AND ENERGY GAP OF SUPERCONDUCTING FILMS*

D. E. Morris and M. Tinkham†
Department of Physics, University of California, Berkeley, California
(Received April 27, 1961)

We have measured the change in the thermal conductivity of superconducting tin and indium films upon application of a magnetic field in the plane of the film. These experiments were undertaken to explore the dependence of the energy gap and the penetration depth upon magnetic field, and to determine the thermodynamic order of the field-induced superconducting transition in films.

Sample films are evaporated onto glass substrates held at 77°K, after ion-bombardment cleaning of the substrate surface. During an experiment, a typical temperature drop along the film is 0.1°K with ~10^{-7} watt total heat transport along the sample film and substrate. Because of its relatively large thickness (~0.01 cm), the substrate carries most of the heat despite its very low thermal conductivity. The change from superconducting to normal alters the temperature drop by ~0.001°K. Changes of ~2 microdegrees in the temperature drop along the film are detectable. This extreme differential temperature sensitivity is achieved by use of a carbon resistor heater-thermometer at one end of the film, connected in a bridge circuit with an identical reference thermometer located at the opposite end of the film. A copper rod connects the latter end to a helium bath whose temperature is controlled to ~0.001°K by a vapor pressure regulator. Balance of the thermometer bridge is measured by a dc microvoltmeter. Fields up to 1000 oersteds are produced by a water-cooled Helmholtz pair, and the angle of the field with respect to the surface of the film can be adjusted to within 0.02° by auxiliary coils. In practice, field tilts of ±0.4° produce negligible changes in the experimental results. To reach the high critical fields of very thin films, we use an iron-core electromagnet. The film thickness is estimated from the measured critical field and published data[1] relating the critical field to thickness.

Experimental results for films of tin and indium of thickness ~700 A are shown in Fig. 1. For both metals the thermal conductivity increases nearly as H^2 up to the critical field. At the critical field, the thermal conductivity in the superconducting state joins smoothly onto the field-independent conductivity of the normal metal. This indicates that the superconducting transition in a magnetic field is second order for films of this thickness, in contrast to the first-order transition of bulk superconductors in a field.

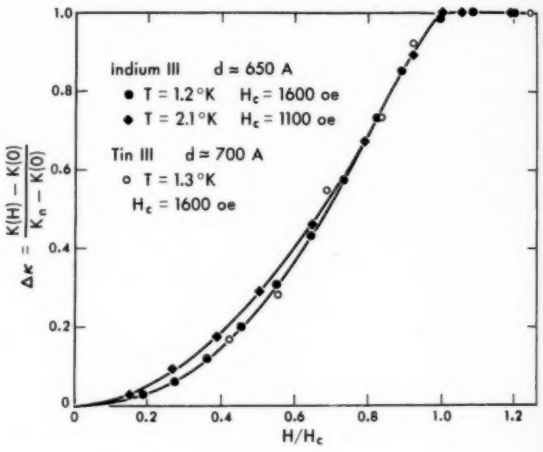

FIG. 1. Change of thermal conductivity of thin superconducting films with magnetic field.

Orientation of the field parallel and perpendicular to the direction of heat flow in the film produces the same effect upon the thermal conductivity to within the experimental accuracy, for films ranging between 700 and 2800 A. Since the induced diamagnetic currents in the superconductor are perpendicular to the field, our data also indicate that the thermal conductivity does not depend upon the angle between the thermal gradient and the diamagnetic current. Thus, if the observed variation of the thermal conductivity is explained in terms of a decrease of the energy gap of the BCS theory[2] with increasing field, the modified gap remains essentially isotropic. This result is interesting in view of the theoretical prediction[3] of a $\vec{p}_F \cdot \vec{v}_{drift}$ term in the excitation spectrum of a superconductor carrying a uniform current. The absence of an observable effect of this sort might be due to the

fact that in these films the two equal and opposite surface currents are only slightly separated in space. Alternately, the short-mean-free path in these "dirty" samples may upset the simple prediction. The lack of anisotropy is important in evaluating the results of Giaever and Megerle[4] concerning the magnetic field dependence of the tunnel effect between superconductors, since their method can only determine the energy gap normal to the surface of the film, which is perpendicular to the directions of both the applied magnetic field and induced current.

The results of Fig. 1 may be used to compute a dependence of the energy gap upon field in a simple way if the electronic term K_e dominates the thermal conductivity, and if K_e is primarily limited by electron scattering by lattice imperfections. Under these conditions the ratio of the thermal conductivity in the superconducting state K_{es} to that in the normal state K_{en} is given by Bardeen, Rickayzen, and Tewordt[5] as their Eq. (3.6). This may be written

$$\frac{K_{es}}{K_{en}} = G(\epsilon_0/kT) = \int_{\epsilon_0}^{\infty} E^2(\partial f/\partial E)dE \Big/ \int_0^{\infty} E^2(\partial f/\partial E)dE,$$

where $f(E/kT)$ is the Fermi function. If we assume that the effect of a field upon the superconducting state can be adequately represented as a change of the ϵ_0 of BCS, then the observed quantity $\Delta\kappa$ plotted in Fig. 1 should be given by

$$\Delta\kappa = \frac{K_{es}(H) - K_{es}(0)}{K_{en} - K_{es}(0)} = \frac{G[\epsilon_0(H)/kT] - G[\epsilon_0(0)/kT]}{1 - G[\epsilon_0(0)/kT]}.$$

This relation was used to invert the experimental data on indium III to yield $\epsilon_0(H)$, with the result shown in Fig. 2. Because $G(\epsilon_0/kT)$ initially drops only quadratically as ϵ_0/kT increases from zero, the gap must drop more steeply to zero near H_c than the approach of $K_{es}(H)$ to K_{en} there. The difficulty of distinguishing between a broadened transition because of film inhomogeneity and a truly rounded approach to K_{en} because of the form of $G(\epsilon_0/kT)$ results in an uncertainty in the choice of H_c. The bars on the plotted experimental points in Fig. 2 indicate the size of this uncertainty.

Our results for the dependence of the energy gap upon magnetic field in a thin film are qualitatively similar to those from the more direct measurements of Giaever and Megerle,[4] although their data were taken on a thicker film at a much higher reduced temperature (T/T_c) and in a different metal (aluminum). From our data in Fig. 2, $\epsilon_0(H)/\epsilon_0(0)$ seems to approach $1-(H/H_c)^2$ at low temperatures, but it is moderately well fitted at $T/T_c = 0.63$ by $\epsilon_0(H)/\epsilon_0(0) = [1-(H/H_c)^2]^{1/2}$. The latter form is that given by Douglass[6] based on the Landau-Ginzburg-Gorkov theory, which is expected to hold near T_c.

With thicker films, new features appear as shown in Fig. 3. The thickest film, tin II with

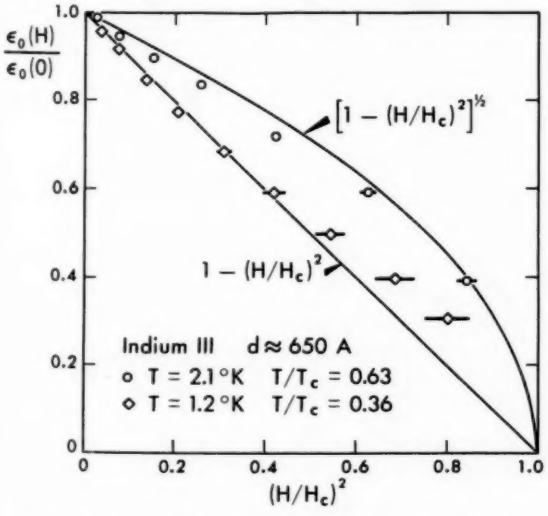

FIG. 2. Magnetic field dependence of superconducting energy gap computed from data of Fig. 1.

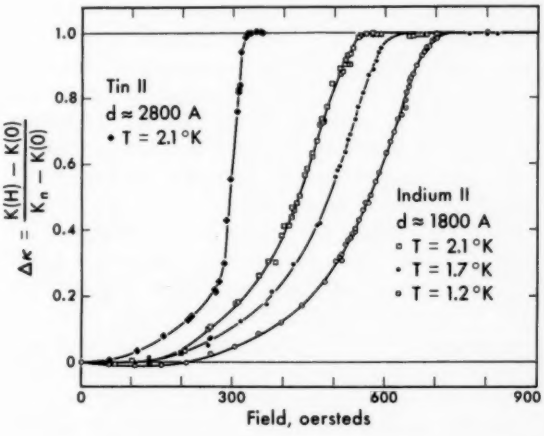

FIG. 3. Change of thermal conductivity of superconducting films of intermediate thickness with magnetic field.

$d \approx 2800$ A, has $\Delta\kappa \sim H^2$ up to the vicinity of H_c, where it reaches only ~25%; then K appears to rise discontinuously to K_n, indicating that the transition is first order in films of this thickness. By our method of analysis, we find that $\epsilon_0(H)/\epsilon_0(0)$ drops abruptly from ~0.83 to 0. If we apply the theory of reference 6, the observed critical field ratio for this film, $H_c/H_c(\text{bulk}) \approx 1.53$, implies that $d/\lambda \approx 3.6$ and $\epsilon_0(H_c)/\epsilon_0(0) \approx 0.78$. The agreement with the above value of 0.83 is quite good considering the limited accuracy and the fact that the gap will not be completely uniform in a film as thick as this one. The film indium II, of intermediate thickness $d \approx 1800$ A, is still thin enough to display a second-order transition, but the increase of K near H_c is much faster than H^2. This behavior may be explained in terms of an increase of the penetration depth λ as the gap decreases, as would be expected on the basis of sum-rule arguments.[7] Since the film thickness is smaller than a coherence length ξ_0, we expect the energy gap to be nearly independent of position in the film. We may then apply the approach of Pippard,[8] considering the balance between condensation energy and magnetic energy to determine the gap (or order parameter) as a function of field. Taking account of the dependence of film susceptibility on (d/λ) and of the dependence of λ on ϵ_0, one is led to expect a change in the form of $\epsilon_0(H/H_c)$ of the observed sense for films with $d > \lambda$. A similar conclusion follows from the explicit theory of reference 6. Only in a film thin enough ($d \ll \lambda$) so that the penetration is always nearly complete will there be a definite limiting relation between $\epsilon_0(H)/\epsilon_0(0)$ and H/H_c.

In indium II at the lowest temperature we see an apparent initial decrease of thermal conductivity with field. We believe that this represents a decrease in the phonon conductivity K_g, produced by increased electronic scattering of phonons as the energy gap is decreased. This interpretation is reasonable, as the initial decrease is seen at the lowest temperatures and in a relatively thick film, both conditions favoring K_g over K_e, and it is observed in indium, having a lower Debye Θ than tin. The observed K_n indicates an electronic mean free path limited by defect scattering to $l \sim 200$ A. Then K_g, limited only by boundary scattering, should be comparable in magnitude to K_e, as required for the validity of this interpretation.

*Supported in part by the National Science Foundation, the Alfred P. Sloan Foundation, and the Office of Naval Research.

†Member of the Miller Institute for Basic Research in Science.

[1]D. Shoenberg, Superconductivity (Cambridge University Press, New York, 1952), Fig. 71(b) on p. 169.

[2]J. Bardeen, L. N. Cooper, and J. R. Schrieffer, Phys. Rev. 108, 1175 (1957).

[3]N. N. Bogoliubov, J. Exptl. Theoret. Phys. (U.S.S.R.) 34, 58 (1958) [translation: Soviet Phys. - JETP 7, 41 (1958)].

[4]I. Giaever and K. Megerle, Phys. Rev. 122, 1101 (1961).

[5]J. Bardeen, G. Rickayzen, and L. Tewordt, Phys. Rev. 113, 982 (1959).

[6]D. H. Douglass, Jr., Phys. Rev. Letters 6, 346 (1961).

[7]M. Tinkham and R. A. Ferrell, Phys. Rev. Letters 2, 331 (1959).

[8]A. B. Pippard, Phil. Mag. 43, 273 (1952).

GROUND-STATE ENERGY OF AN ELECTRON GAS IN A LATTICE OF POSITIVE POINT CHARGES

A. Bellemans and M. De Leener*
Faculty of Sciences, University of Brussels, Brussels, Belgium
(Received February 27, 1961; revised manuscript received May 4, 1961)

The ground-state energy of an electron gas in a rigid lattice of positive point charges has been studied using the quantum statistical formalism of Bloch and de Dominicis.[1,2] The grand partition function of the system was expanded in powers of the coupling parameter between (i) the electrons and the lattice and (ii) pairs of electrons; this parameter is of course the square of the electronic charge. On account of the long-range forces, a certain number of divergences are met within this expansion; as usual one gets rid of them by (a) taking into account the electroneutrality of the whole system, and (b) summing infinite series of divergent terms.

Finally, taking the limit of zero temperature, one obtains the ground-state energy which can be conveniently expressed in terms of the parameter r_s, related to the density ρ of the electron gas by

$$r_s = (3/4\pi)^{1/3}\rho^{-1/3}. \tag{1}$$

Using as units the Bohr radius for r_s and the rydberg for the energy, we found the following expression of the ground-state energy for the case of a simple cubic lattice:

$$\epsilon(r_s) = \frac{3}{5}\left(\frac{9\pi}{4}\right)^{2/3}\frac{1}{r_s^2} - \frac{1}{3}\left(\frac{3\nu}{\pi}\right)^{2/3}\left(\frac{9\pi}{4}\right)^{1/3}\frac{1}{r_s}\chi - \frac{3}{2\pi}\left(\frac{9\pi}{4}\right)^{1/3}\frac{1}{r_s} + \{0.0622\ln r_s - 0.096\} - \frac{1}{6\pi^2}\sum_{\vec{u}\neq 0}\frac{1}{u^4}\left\{\frac{1-u^2}{2u}\ln\left|\frac{1+u}{1-u}\right| + 1\right\} + O(r_s \ln r_s). \tag{2}$$

ν is the ratio of the charge of a lattice point to the electron charge; the vector $\vec{u}$ is equal to $(\pi/3\nu)^{1/3}\vec{n}$, where (n_x, n_y, n_z) are integral numbers; χ is a constant defined as

$$\chi = -\sum_{\vec{\lambda}}\frac{1}{r_{\vec{\lambda}}} + \int\frac{1}{r}\,d\vec{r}, \tag{3}$$

where $\vec{\lambda}$ is a lattice vector.

The physical meaning of the various terms of (2) is the following: (a) The first term is the kinetic energy of a free electron gas; (b) the second term is the Madelung energy [see Eq. (3)] of a lattice of positive point charges in a uniform negative background; (c) the third term is the exchange energy of the electron gas, as calculated by Wigner[3]; (d) the fourth term is the correlation energy of the electron gas, as calculated by Gell-Mann and Brueckner[4]; and (e) the fifth term is the polarization energy of the free electron gas by the lattice, in the linear approximation.

The sum of terms (a), (c), and (d) in Eq. (2) is just the ground-state energy of an electron gas in a positive continuum; terms (b) and (e) arise from the lattice.

Expression (2) is plotted on Fig. 1 (curve I) for the special case $\nu = 1$; strictly speaking, this would correspond to "metallic hydrogen." The importance of the "structural" terms (b) and (e) in $\epsilon(r_s)$ is apparent when one compares curve I to curve II, the latter corresponding to an electron gas in a uniform positive background.[4] (For body-centered and face-centered cubic lattices, curves very similar to curve I are obtained.)

The ground-state energy of "metallic hydrogen" has been investigated before by Wigner and Huntington[5]; they first looked for approximate Bloch wave functions for independent electrons and next calculated exchange and correlation corrections. This method of approach is rather different from ours, which treats electron-lattice and electron-electron interactions in a symmetric way. It is then quite remarkable that the curve for $\epsilon(r_s)$ derived by Wigner and Huntington is very close to our curve I, as can be seen from Fig. 1. The abcissas and ordinates at the minimum are, respectively: $r_s = 1.64$, $\epsilon(r_s) = -1.05$ and $r_s = 1.59$, $\epsilon(r_s) = -0.99$. We may further expect that the exact minimum value of $\epsilon(r_s)$ for "metallic hydrogen" is near to (and probably somewhat below) -1 rydberg. This indicates that expansions for $\epsilon(r_s)$ like (2) converge satisfactorily in the region $r_s < 2$. This seems to be supported by the calculations of Dubois[6] for the term $O(r_s \ln r_s)$ of the correlation energy of an electron gas in a positive uniform background and also by our own rough estimations of the polarization energy $O(r_s)$ of the electrons by the lattice.

A detailed account of the results reported above

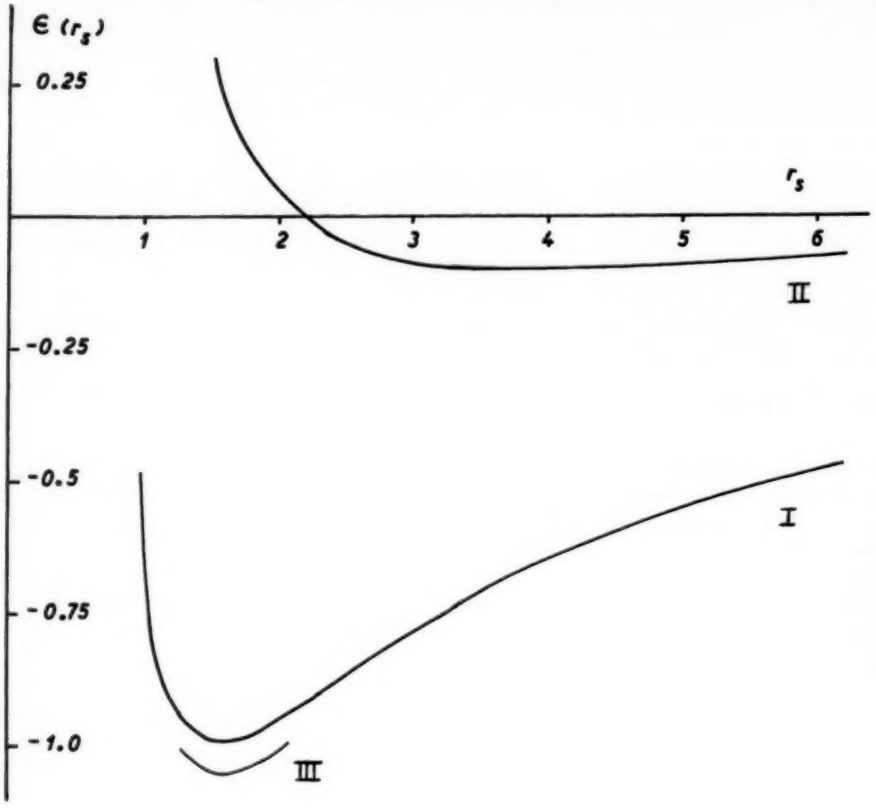

FIG. 1. Graph of $\epsilon(r_s)$ (in rydbergs). (I) Equation (3) for $\nu = 1$; (II) electron gas in uniform positive background[4]; (III) curve of Wigner and Huntington.[5]

will be published elsewhere. The authors wish to thank Professor I. Prigogine for his constant interest in this work.

*Aspirant au F.N.R.S.

[1]C. Bloch and C. de Dominicis, Nuclear Phys. 7, 459 (1958).

[2]C. Bloch and C. de Dominicis, Nuclear Phys. 10, 181 (1959).

[3]E. P. Wigner, Phys. Rev. 46, 1002 (1934).

[4]M. Gell-Mann and K. A. Brueckner, Phys. Rev. 106, 364 (1957).

[5]E. P. Wigner and H. B. Huntington, J. Chem. Phys. 3, 764 (1935).

[6]D. F. Dubois, Ann. Phys. 7, 174 (1959).

SPLITTING OF THE EMISSION LINES OF RUBY BY AN EXTERNAL ELECTRIC FIELD

W. Kaiser, S. Sugano, and D. L. Wood
Bell Telephone Laboratories, Murray Hill, New Jersey
(Received May 9, 1961)

The fluorescence emission of ruby ($Al_2O_3 + Cr^{3+}$) has been investigated in great detail in recent years and it is now well understood.[1] In highly diluted pink ruby with chromium concentrations below 0.05%, the emission consists essentially of two lines at $R_1 = 14\,421$ cm^{-1} and $R_2 = 14\,450$ cm^{-1} corresponding to transitions from the split components of the $t_2^3\ ^2E$ state to the ground state $^4A_2$, respectively. Since the ground state is split by 0.38 cm^{-1},[2] both emission lines are actually doublets, which can easily be observed at 77°K with a high-resolution grating instrument.

We have superimposed an external electric field upon the internal crystal field and observed a new additional splitting of the emission lines, which is much larger than expected from a superficial consideration of the Stark effect. Ruby plates of 1-mm thickness with a chromium concentration of approximately 0.01% were cut from a large single crystal parallel and perpendicular to the optic axis. The samples were immersed in liquid nitrogen and illuminated with a 100-watt Hg lamp. The emission of the crystal was focused on the entrance slit of a Bausch and Lomb grating spectrometer with a 50 000-line/in. grating. With this system the ground-state splitting of the R_1 and R_2 lines was clearly visible (see Fig. 1 top). Upon application of an external electric field parallel to the optic axis of the ruby, a surprisingly strong effect on the emission pattern was observed. Both components of the R_1 and R_2 lines exhibit a distinct splitting which is shown in Fig. 1 for the R_1 line for several electric fields. On the top (no field) and the bottom ($E_0 = 1.58\times10^5$ v/cm) of this figure, actual microphotometer traces of the photographic plate are presented; at intermediate fields, only the positions of the individual components are indicated. The frequency shift is so large that the two center lines pass the midpoint between the two original R_1 components at a field of about 65 kv/cm and cross over at still higher fields. It is interesting to note that the center of the split lines does not shift with applied electric field; furthermore, both components of the R_1 (see Fig. 1) and R_2 lines split by the same amount. It can be seen from Fig. 2 that the splitting $\Delta\nu$ is directly proportional to the electric field. At a field of 1.7×10^5 v/cm, $\Delta\nu$ reaches a value of one wave number (3×10^{10} cps). With increasing electric field, the emission lines slightly broaden. No detailed study was made of this effect. Polarizers in the light beam indicated that the polarization is unaltered by the electric field. In specimens with the electric fields perpendicular to the optic axis, no change in the emission pattern could be observed for fields as high as 1.7×10^5 v/cm.

The observed splittings of the R_1 and R_2 fluorescence lines in the presence of an electric field are not normal Stark splittings. This is because both the initial and final states of the fluorescence are Kramers doublets whose degeneracies may not be removed in the presence of any electric field. In what follows, we shall show that the apparent splittings are due to the opposite Stark shifts of the energy levels of chro-

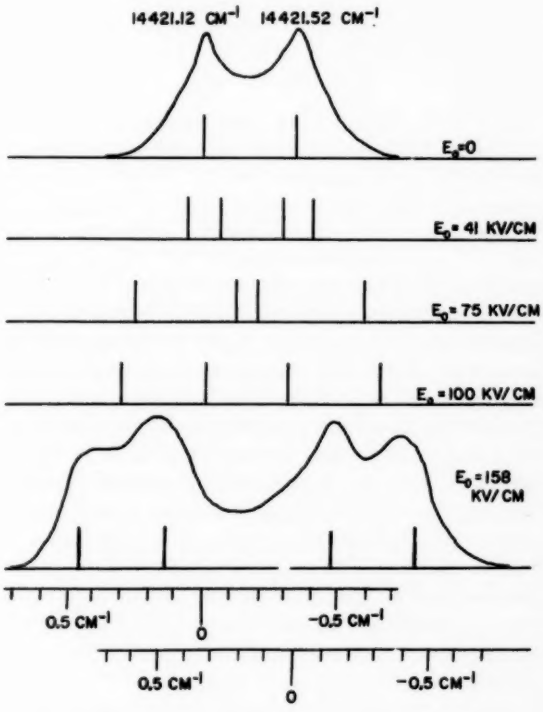

FIG. 1. Splitting of the R_1 line in an electric field parallel to the optical axis.

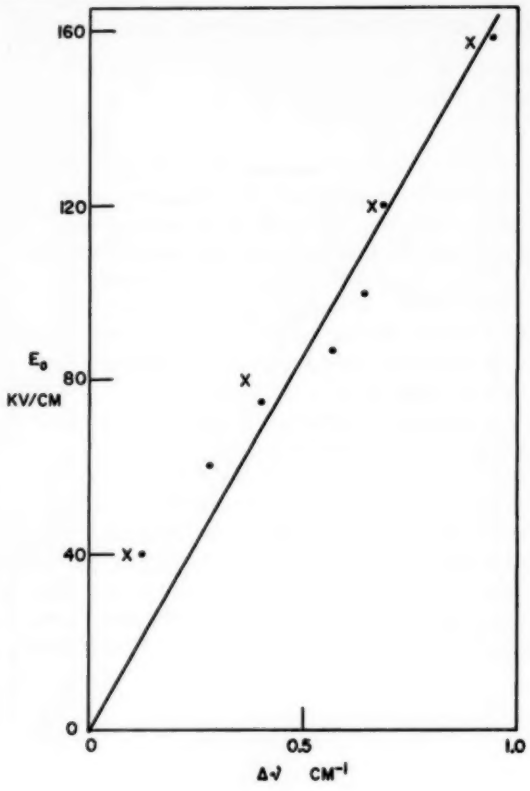

FIG. 2. Pseudo-Stark splitting $\Delta\nu$ of ruby vs applied electric field E_0. Data are obtained from the R_1 (•) and R_2 (×) lines.

mium ions at different lattice sites.

It is well known that in ruby there are two kinds of chromium sites, A and B.[3] Transformation of the A site into the B site is only possible by symmetry operations involving inversion around the chromium ion, while transformation of A to A or B to B is achieved solely by translation or by both translation and rotation around the optic axis. The A and B sites are energetically equivalent in the absence of an electric field. This circumstance may be simply expressed by the fact that the odd-parity crystal field associated with the A site, $V_u(A)$, is equal to minus the odd crystal field at the B site, $V_u(B) = -V_u(A)$.

Let us consider the local electric field acting on the chromium ions. The local field may be written in the form, $\alpha \cdot \vec{E}_0$, where $\vec{E}_0$ is the applied electric field and α is generally a tensor determined by the dielectric properties of crystals. Polarization effects due to ionic displacements and deformation of electron clouds in crystals are taken into account in the tensor α. For a uniaxial crystal such as ruby, the term in the Hamiltonian for the interaction of the chromophoric electrons with the local electric field produced by the external applied field is given by

$$V_S = \sum_i [\alpha_{\parallel} z_i E_{0z} + \alpha_{\perp}(x_i E_{0x} + y_i E_{0y})],$$

where x, y, and z are the electron coordinates and the z axis is taken along the optic axis.

Since V_S belongs to odd parity, the crystal field levels of chromium ions are perturbed by the combined action of V_u and V_S. This perturbation produces the Stark shift. Because of the opposite sign in the odd-parity crystal fields at the A and B sites, the Stark shifts for these sites are expected in opposite directions. This gives the pseudo-Stark splittings observed in our experiment. Furthermore, since V_u corresponds to the z component of the equivalent irreducible tensor,[4] a simple symmetry consideration shows that the Stark shifts are vanishing when E_0 is perpendicular to the optic axis.

The accurate calculation of this type of Stark shift is as difficult as that of the absolute intensities of the crystal field spectrum. It is, however, possible to estimate the order of magnitude of the Stark shift $\Delta\nu$ by using the relation $\Delta\nu \sim \alpha_{\parallel} \times E_{0z} \langle V_u \rangle \langle z \rangle / \Delta$, where $\langle V_u \rangle$ is the matrix element of V_u between the state relevant to the fluorescence and the high excited state of odd parity, $\langle z \rangle$ the similar matrix element of z, and Δ the energy difference between the two states appearing in the matrix elements. Putting $\alpha_{\parallel} \sim 1$, $\langle V_u \rangle \sim 1000$ cm^{-1}, $\langle z \rangle \sim 1$ A, and $\Delta \sim 50\,000$ cm^{-1}, we obtain $\Delta\nu \sim 0.1$ cm^{-1} at $E_{0z} = 10^5$ volts/cm.

The above-mentioned Stark shifts are expected in both the initial and final states of the fluorescence. Therefore, the observed magnitude of the pseudo-Stark splitting should be compared with twice the difference of the Stark shifts in the initial and final states of the fluorescence. This would not change the estimated order of the magnitude, as the shifts are not expected to be the same in both states.

The other characteristic features expected from our theory are as follows:

(1) The center of the split components does not shift (no pseudo-Stark shift) because the crystal symmetry gives $|V_u(A)| = |V_u(B)|$. Here we neg-

lect contribution from the V_S^2 term which is very small for the fields achieved in our experiments.

(2) The magnitude of the splittings is expected to be the same for the R_1 and R_2 excited states because the Stark term is independent of spin. The same is true for the initially split ground levels having $M_S = \pm 3/2$ and $M_S = \pm 1/2$.

(3) Optical anisotropies associated with the split components are identical with each other and also with the anisotropy of the original unsplit line. All these points are in agreement with our experiments.

Although we have not given any detailed discussion on the local electric field, experiments of this type are very important because they allow a direct investigation of the local electric field. The quantitative discussion on the local field is only possible after the detailed knowledge of the odd-parity excited states is obtained.

The effect discussed here is expected to be extremely fast (comparable to the optical frequencies of the lattice), and high-frequency modulation of the ruby emission can be anticipated. The application of an ac electric field should allow frequency modulation of the output of a ruby optical maser.[5]

[1]O. Deutschbein, Ann. Physik 14, 712 (1932); S. Sugano and Y. Tanabe, J. Phys. Soc. Japan 13, 880 (1958); F. Varsanyi, D. L. Wood, and A. L. Schawlow, Phys. Rev. Letters 3, 544 (1959).

[2]A. A. Manenkov and A. M. Prokhorov, J. Exptl. Theoret. Phys. (U.S.S.R.) 28, 762 (1955) [translation: Soviet Phys.-JETP 1, 611 (1955)].

[3]R. W. G. Wyckoff, Crystal Structures (Interscience Publishers, New York, 1951).

[4]Y. Tanabe and H. Kamimura, J. Phys. Soc. Japan 13, 394 (1958).

[5]T. H. Maiman, Brit. Commun. and Electronics 7, 674 (1960); R. J. Collins, D. F. Nelson, A. L. Schawlow, W. Bond, C. G. B. Garrett, and W. Kaiser, Phys. Rev. Letters 5, 303 (1960).

ANISOTROPY OF THE MAGNETOELECTRIC EFFECT IN Cr_2O_3

V. J. Folen, G. T. Rado, and E. W. Stalder
U. S. Naval Research Laboratory, Washington, D. C.
(Received May 8, 1961)

On the basis of earlier considerations of magnetic crystal symmetry effects by Landau and Lifshitz,[1] Dzyaloshinskii[2] showed that a magnetoelectric effect (i.e., a magnetic moment produced by an externally applied electric field or an electric moment produced by an externally applied magnetic field) may exist in antiferromagnetic Cr_2O_3. In his development of the thermodynamic potential which is compatible with the magnetic symmetry, Dzyaloshinskii obtained the relation[2]

$$4\pi\phi_{me} = -\alpha_{\parallel} E_z H_z - \alpha_{\perp}(E_x H_x + E_y H_y), \qquad (1)$$

where ϕ_{me} is the magnetoelectric part of the thermodynamic potential, and $\alpha_{\parallel}$ and $\alpha_{\perp}$ are the magnetoelectric parameters for the directions parallel and perpendicular to the crystallographic c axis, respectively. From this potential, one obtains (using $4\pi\partial\phi/\partial\vec{H} = -\vec{B}$) the linear relations

$$B_z = \alpha_{\parallel} E_z, \quad B_x = \alpha_{\perp} E_x, \quad \text{and} \quad B_y = \alpha_{\perp} E_y. \qquad (2)$$

As a result of measurements on a nonoriented Cr_2O_3 single crystal, Astrov[3] obtained evidence that the magnetoelectric effect does exist in Cr_2O_3, and that the effect is a linear function of the electric field in accord with Eq. (2).

In this Letter, we report measurements of the magnetoelectric effect (resulting from an applied electric field) in two x-ray-oriented single-crystal disks of Cr_2O_3, and show that a large anisotropy exists both in the magnitude and temperature dependence of this effect. One of the disks was fabricated with its plane surfaces parallel to the crystallographic c axis, and the second disk with its plane surfaces perpendicular to the c axis. In the former case, the surfaces were parallel to the (110) plane. The plane surfaces were coated with silver paint to provide uniform electrical contact with the specimen. The apparatus used to measure the magnetic moment was similar to that used by Astrov.[3] However, we found it necessary to make the measurements in vacuum in order to avoid electrical breakdown in the vicinity of the electrodes. The magnetic moment was obtained by applying to the sample a 1000-cps alternating electric field and using a narrow-band amplifier of approximately 0.15-μv sensitivity to measure the voltage induced in a 10 000-turn pickup coil surrounding the sample. The largest values of $\alpha_{\perp}$ and $\alpha_{\parallel}$ correspond to induced rms voltages of

8.35 μv and 124.7 μv, respectively. Electrostatic shielding was provided by inserting a grounded brass cylinder between the pickup coil and the assembly consisting of the sample and electrodes. A Lavite disk having approximately the same conductivity as the Cr_2O_3 disks was used to show that the electrostatic shielding is adequate and that extraneous current effects are absent. Low temperatures were obtained by immersing a cylinder containing the sample and electrodes into a liquid nitrogen bath. High temperatures were obtained with a furnace or heated water bath. In all the measurements the temperature was determined by means of a copper-constantan thermocouple in thermal contact with one of the silver electrodes on the sample. The copper thermocouple wire also served as the ground connection for this electrode. Considerable care had to be taken to avoid electrical breakdown in the vicinity of the electrodes, particularly at the lower temperatures. Such breakdown even occurred when a helium atmosphere was used in the apparatus, and consequently the measurements had to be made in vacuum so that no breakdown occurred.

Figure 1 shows the results of our measurements on the temperature dependence of $\alpha_\perp$ and $\alpha_\parallel$. It is seen that there is a large anisotropy of the magnetoelectric effect. The magnitude of $\alpha_\perp$ and its temperature dependence is similar to that obtained by Astrov.[3] His measurements (which were made on a nonoriented crystal) extended down to 250°K only. The curve $\alpha_\parallel$, on the other hand, shows that the magnetoelectric effect goes through a maximum and then becomes zero at 97°K. At slightly lower temperatures it appears to rise again. In both samples, the magnetoelectric effect is zero at 306°K, and remains approximately zero at higher temperatures. Since antiferromagnetic susceptibility measurements by McGuire et al.[4] show the Néel temperature to be 307°K, it appears that the magnetoelectric effect does not exist in the paramagnetic region, in accord with the symmetry considerations of Landau and Lifshitz.[1] Measurements of the magnetoelectric effect in the two disks as a function of applied electric field showed that the effect is linear [in accord with Eq. (2)] for fields ranging from zero to 3200 rms volts/cm. The values of E_z and E_x used in obtaining the results shown in Fig. 1 were 2160 and 2050 rms volts/cm, respectively.

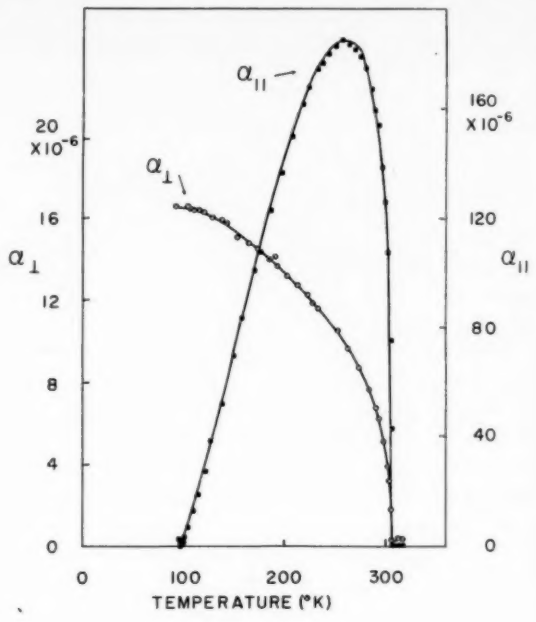

FIG. 1. Temperature dependence of the magnetoelectric parameters $\alpha_\perp$ and $\alpha_\parallel$. The α's are dimensionless in the Gaussian units used.

A theoretical discussion of the temperature dependence of the α's is given in reference 5.

---

[1] L. D. Landau and E. M. Lifshitz, Electrodynamics of Continuous Media (Addison-Wesley Publishing Company, Inc., Reading, Massachusetts, 1960), p. 119. (English translation of a 1958 Russian edition).

[2] I. E. Dzyaloshinskii, J. Exptl. Theoret. Phys. (U.S.S.R.) 37, 881 (1959) [translation: Soviet Phys. - JETP 10, 628 (1960)].

[3] D. N. Astrov, J. Exptl. Theoret. Phys. (U.S.S.R.) 38, 984 (1960) [translation: Soviet Phys. - JETP 11, 708 (1960)].

[4] T. R. McGuire, E. J. Scott, and F. H. Grannis, Phys. Rev. 102, 1000 (1956).

[5] G. T. Rado, following Letter [Phys. Rev. Letters 6, 609 (1961)].

MECHANISM OF THE MAGNETOELECTRIC EFFECT IN AN ANTIFERROMAGNET

George T. Rado
U. S. Naval Research Laboratory, Washington, D. C.
(Received May 8, 1961)

A crystal placed in an applied electric field may experience a magnetization which is proportional to the electric field. This magnetoelectric effect was first observed experimentally by Astrov[1] in a monocrystal of antiferromagnetic Cr_2O_3. Even earlier, Landau and Lifshitz[2] had pointed out the possibility that this effect (and its inverse) may exist in some spin-ordered materials, and Dzyaloshinskii[3] had predicted specifically that it could exist in Cr_2O_3. Both of these theories are based on symmetry arguments and thermodynamics only.

In the present Letter we propose a simple phenomenological theory of the temperature dependence of the magnetoelectric effect. This theory correctly predicts the experimental observations presented in the accompanying Letter[4] for both the parallel ($\parallel$) and perpendicular ($\perp$) orientations of the electric field with respect to the axis of spontaneous antiferromagnetism (z axis). In addition, we tentatively suggest a possible atomic mechanism which conforms to the restrictions imposed by our phenomenological theory. Rough numerical estimates based on this mechanism explain the observed values of the magnetoelectric effect to within an order of magnitude.

We begin by introducing a fictitious magnetic field $\vec{h}$ which we define by the requirement that the magnetization $\vec{M}$ induced by $\vec{h}$ be identical with that induced by the applied electric field $\vec{E}^a$. Since the quantity $\alpha_\parallel/4\pi$, which may be called the "parallel magnetoelectric susceptibility," is defined[3] by $\alpha_\parallel = B_z/E_z{}^a$, our definition of $\vec{h}$ leads to

$$\alpha_\parallel = 4\pi M_z/E_z{}^a = 4\pi\chi_\parallel h_z/E_z{}^a, \tag{1}$$

where the applied magnetic field $\vec{H}^a$ is assumed to be zero (so that $B_z = 4\pi M_z$) and the parallel antiferromagnetic volume susceptibility is denoted by $\chi_\parallel$. If we recall that experimentally M_z is proportional to $E_z{}^a$, and that the magnetoelectric effect vanishes unless the material under consideration possesses an ordered spin arrangement, it seems reasonable to assume that h_z has the form

$$h_z = a_\parallel E_z{}^a \langle S_z \rangle_{\mathrm{av}}, \tag{2}$$

where $\langle S_z \rangle_{\mathrm{av}}$, which is proportional to the zero-field sublattice magnetization M_0, represents the thermal average of the expectation value of the z component of the ionic spin, and $a_\parallel$ is an essentially temperature-independent constant of the material. By combining Eqs. (1) and (2) we obtain

$$\alpha_\parallel = 4\pi a_\parallel \chi_\parallel \langle S_z \rangle_{\mathrm{av}}, \tag{3}$$

and on the basis of analogous arguments we obtain

$$\alpha_\perp = 4\pi a_\perp \chi_\perp \langle S_z \rangle_{\mathrm{av}}. \tag{4}$$

The temperature dependence of $\alpha_\parallel$ and $\alpha_\perp$ is seen to be determined by $\chi_\parallel M_0$ and $\chi_\perp M_0$, respectively. If we express these quantities in terms of the equations resulting from the Néel-Van Vleck molecular field theory[5] of a two-sublattice antiferromagnet, we can make the following predictions: As the temperature T increases from 0°K to the Néel temperature, T_N, the quantity $\alpha_\perp$ should decrease monotonically from some finite value to zero in the manner of the sublattice magnetization; the quantity $\alpha_\parallel$, on the other hand, should increase from zero to some maximum value and then return to zero. Both of these qualitative predictions have been verified experimentally.[4] As shown in Fig. 1, even the quantitative agreement between the calculated and measured α's is satisfactory. The existing discrepancies between theory and experiment are no worse in the case of the α measurements (Fig. 1) than in the case of the χ measurements[6] (Fig. 2 of reference 6). In both cases these discrepancies may at least in part be attributed to the fact that a two-sublattice model is not strictly applicable to Cr_2O_3.

According to the above considerations, electric fields should have "tuning" (and other) effects on antiferromagnetic resonance, and these effects should be calculable by simply using our fictitious $\vec{h}$ in place of (or in addition to) the actual $\vec{H}^a$ throughout the usual resonance equations. We also suggest that by applying a strong magnetic field parallel to the antiferromagnetic axis and making use of the Néel "spin-flop" effect,[5] it should be possible to "switch" from a

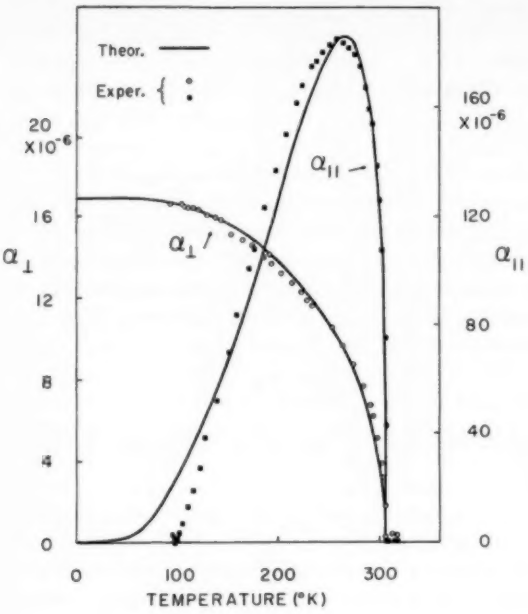

FIG. 1. Comparison of calculated and measured magnetoelectric susceptibilities. The theoretical curves are based on Eqs. (3) and (4) and the following numerical values: $T_N = 360°K$, θ(= Curie-Weiss constant) $= -0.38\,T_N$, $a_{\parallel} = 38.7\times10^{-3}$, and $a_{\perp} = 1.32\times10^{-3}$. The experimental points are taken from Folen, Rado, and Stalder, reference 4.

measurement of $\alpha_{\parallel}$ to a measurement of $\alpha_{\perp}$.

In attempting to explain the physical origin of the magnetoelectric effect, we think of the electron cloud of each magnetic ion as being distorted by $\vec{E}^a$. As a result of spin-orbit coupling, the spins are "aware" of this distortion and hence they may give rise to an induced magnetization. To construct a specific model, we assume that the unperturbed Hamiltonian consists of a part describing the free ion (say, Cr^{+++}), a part describing that portion of the crystalline electric potential which is an even function of the coordinates, and a part describing the Zeeman energy arising from the exchange field. In a material like Cr_2O_3 the ground state is then nondegenerate. We further assume that the perturbing Hamiltonian is linear in the potential arising from $\vec{E}^a$, linear in the potential arising from the constant part $\vec{E}^c$ of the crystalline field, and quadratic in the spin-orbit energy $\lambda\vec{L}\cdot\vec{S}$. Thus the order of magnitude of the fourth-order energy correction is given by

$$W \approx (e\vec{E}^a\cdot\vec{r})(e\vec{E}^c\cdot\vec{r})(\lambda\vec{L}\cdot\vec{S})^2/(\Delta_1\Delta_2\Delta_3), \qquad (5)$$

where Δ_1, Δ_2, Δ_3, are appropriate splittings calculable from the eigenvalues of the unperturbed Hamiltonian. Alternatively, the quantity

$$W = 2\,\mu_B\vec{S}\cdot\vec{h} \qquad (6)$$

may be regarded as the Zeeman shift produced by $\vec{h}$. From Eqs. (5) and (6), it follows that $\vec{h}$ is consistent with Eq. (2) provided we take

$$a \approx e^2E_z{}^c r^2\lambda^2L^2/(2\,\mu_B\Delta_1\Delta_2\Delta_3) \qquad (7)$$

as an approximate measure of either of the (unequal) quantities $a_{\parallel}$ and $a_{\perp}$. The quantity r^2 denotes z^2 and xz in the parallel and perpendicular cases, respectively, and L^2 denotes $L_z{}^2$ and L_xL_z in these two cases. It should be noted that the α's resulting from the substitution of Eq. (7) into Eqs. (3) and (4) do fulfill the requirement of being invariant with respect to the product of the space inversion and time reversal transformations, while being noninvariant with respect to either of these transformations separately. For a very rough numerical estimate applicable to Cr_2O_3, we use $\Delta_1 \approx \Delta_2 \approx 2\times10^4\ cm^{-1}$, $\Delta_3 \approx 1.6\times10^5\ cm^{-1}$ (parity considerations), $r \approx 10^{-8}$ cm, $\lambda \approx 10^2\ cm^{-1}$, and $eE_z{}^c z \approx 1.7\times10^3\ cm^{-1}$ (point charge calculations based on the structure of αFe_2O_3). The value[7] $a \approx 0.6\times10^{-3}$ resulting from Eq. (7) may be consistent with the values $a_{\parallel} = 38.7\times10^{-3}$ and $a_{\perp} = 1.32\times10^{-3}$ required to fit the experimental curves of $\alpha_{\parallel}$ and $\alpha_{\perp}$ by means of Eqs. (3) and (4). More accurate estimates based on actual calculations of the relevant matrix elements are under way.

The writer wishes to thank V. J. Folen and R. D. Myers for helpful discussions.

---

[1]D. N. Astrov, J. Exptl. Theoret. Phys. (U.S.S.R.) 38, 984 (1960) [translation: Soviet Phys.-JETP 11, 708 (1960)].

[2]L. D. Landau and E. M. Lifshitz, Electrodynamics of Continuous Media (Addison-Wesley Publishing Company, Inc., Reading, Massachusetts, 1960), p. 119. (English translation of a 1958 Russian Edition.)

[3]I. E. Dzyaloshinskii, J. Exptl. Theoret. Phys. (U.S.S.R.) 37, 881 (1959) [translation: Soviet Phys.-JETP 10, 628 (1960)].

[4]V. J. Folen, G. T. Rado, and E. W. Stalder, preceding Letter [Phys. Rev. Letters 6, 607 (1961)].

[5]See, for example, T. Nagamiya, K. Yosida, and R. Kubo, Advances in Phys. 4, 1 (1955), paragraph 4.

[6]T. R. McGuire, E. J. Scott, and F. H. Grannis, Phys. Rev. 102, 1000 (1956).

[7]Both a and α are dimensionless in the Gaussian units used in the present paper.

DYNAMIC POLARIZATION ANOMALIES IN ORGANIC FREE RADICALS*

Robert H. Webb

Department of Physics, Stanford University, Stanford, California

(Received May 12, 1961)

As a part of a broader study of exchange effects in various paramagnetic substances, we have found an organic free radical in which the Overhauser effect gives way to a "solid" effect at low temperature, and one in which the two effects are present simultaneously.

The Overhauser effect[1] is produced by saturation of the electron spin resonance (ESR) transition in a system in which the nuclei are coupled to the electrons by a hyperfine interaction. It appears as an enhancement of the nuclear polarization, and therefore of the nuclear magnetic resonance (NMR) signal. The "solid" effect,[2] on the other hand, depends on dipole-dipole coupling between the electrons and nuclei in a solid and requires the saturation of the forbidden transitions at $\nu = (|\gamma_e| \pm \gamma_n)H_0$, where ν is the microwave frequency and γ_e and γ_n are the electronic and nuclear gyromagnetic ratios. H_0 is the external (dc) magnetic field. These forbidden transitions involve simultaneous flips of a nucleus and an electron. Saturation of the transition at $(|\gamma_e| + \gamma_n)H_0$ results in a negative enhancement of the NMR signal (the nuclear polarization is inverted), while that at $(|\gamma_e| - \gamma_n) \times H_0$ produces a positive enhancement. Typically, the forbidden transitions are more easily saturated than the allowed ones, so that much less saturating power is necessary to produce the solid effect than the Overhauser effect, if it is present.

The Overhauser effect in the organic free radical diphenyl picryl hydrazyl (DPPH) is relatively well known.[3] The enhancement obtained at 3400 oersteds is, however, small (about 20) at room temperature and at 77°K. It disappears in the liquid helium temperature range, being masked by a collapsing of the Knight shift and by microwave heating effects.[4]

Wurster's blue perchlorate (WB) has an exchange-narrowed electron spin resonance about 3 oersteds wide at room temperature.[5] At 300°K and at 77°K it gives only an Overhauser effect (Fig. 1). In the liquid helium range, it exhibits only a solid effect (Fig. 1). Here the ESR line is 14 oersteds wide and the proton NMR 14 oersteds, giving rise to an effective broadening of the solid effect spectrum. Power dependence of the two effects is shown in Fig. 2, which is typical of Overhauser effects in all the free radicals, and of solid effects in general.

Picryl amino carbazyl (PAC) resembles the other free radicals in its electron spectrum at room temperature.[6] It has one of the larger g-factor anisotropies among the organic free radicals. It exhibits both solid and Overhauser effects at 300°K and 77°K, with a pure solid effect at 4.2°K and below (Fig. 3).

These two free radicals differ from DPPH in the temperature dependence of their susceptibilities (see Fig. 2 of Rhodes et al.[7]). They also are known to show $g=4$ satellite[7] lines below a

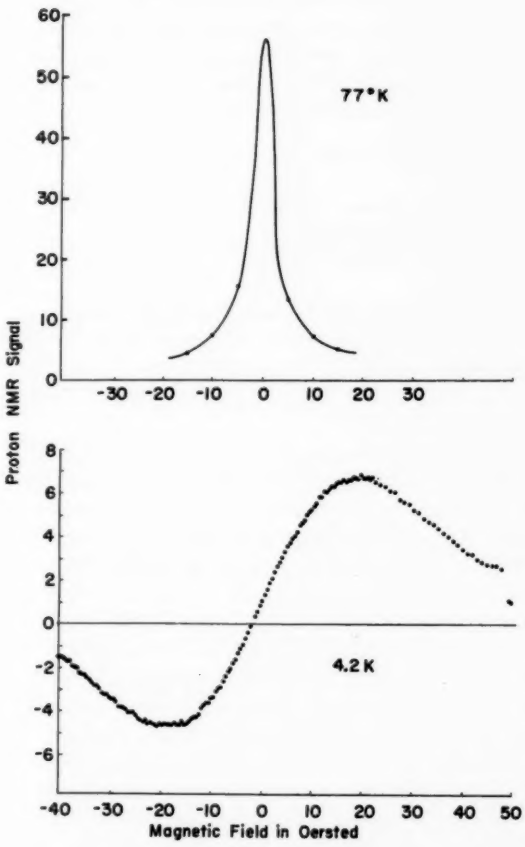

FIG. 1. Proton NMR signal in arbitrary units as a function of magnetic field in Wurster's blue. The microwave frequency is held constant at 9.7 kMc/sec. ESR occurs at $H_0 = 0$.

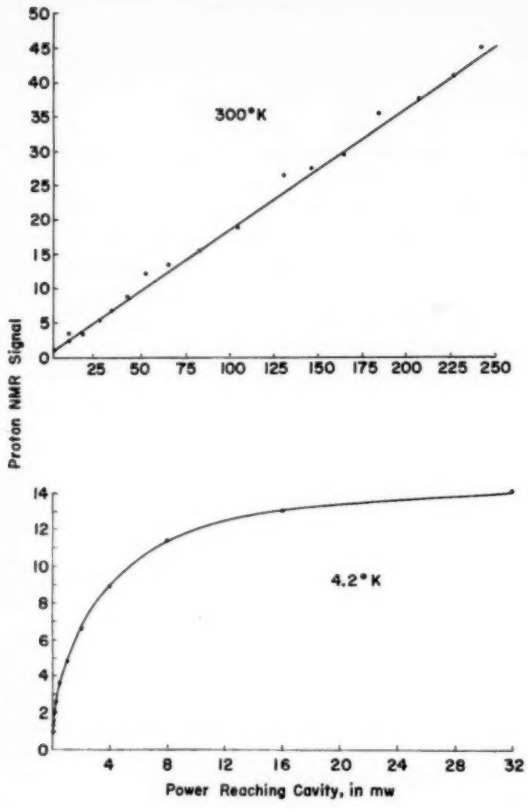

FIG. 2. Proton NMR signal in arbitrary units as a function of saturating power, at the peak of the enhancements in WB.

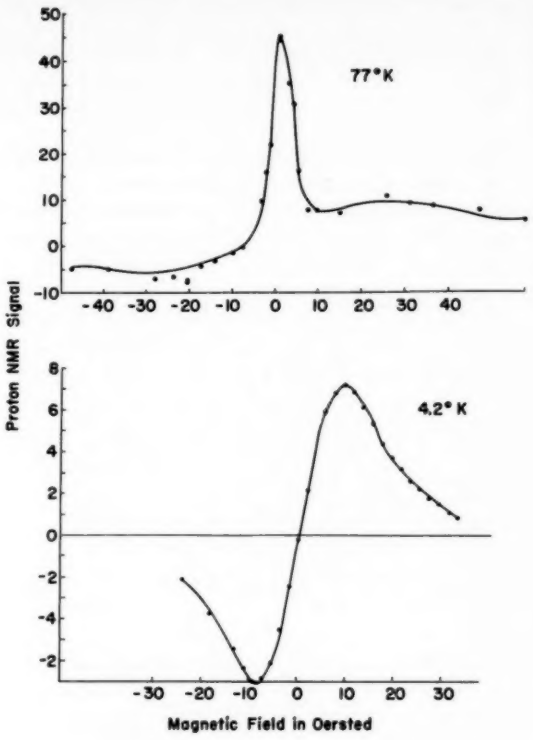

FIG. 3. Proton NMR signal in arbitrary units as a function of magnetic field in PAC. The microwave frequency is held constant at 9.7 kMc/sec. ESR occurs at $H_0 = 0$.

characteristic temperature T^* which is higher in WB. The transition between the two types of dynamic polarization which we observe comes above T^* in PAC, below it in WB. However, the existence of the $g = 4$ lines is apparently due to the presence of dipolar coupling, which is in turn related to the decrease in susceptibility and its consequent effective magnetic dilution. It is this effective magnetic dilution which we suggest may provide the nuclear-electron dipolar coupling which gives rise to the solid effect. It does not follow that the transition temperature for the nuclear-electron effects need be the same as that for the purely electronic phenomenon. Support for this is provided by a fourth free radical, 1-3-bis-diphenylene-2-phenyl allyl (BDPA) which shows a $g = 4$ line below 2°K,[7] but retains a reduced proton Knight shift[8] at this temperature—showing that the proton-electron coupling is still primarily scalar (hyperfine). No solid effect has been observed in this substance at the lowest temperatures so far employed (about 1.8°K), and we have some evidence of a residual Overhauser effect at 4.2°K.

We are continuing our investigations of these materials in an effort to understand the nature of the susceptibility anomalies and the influence of exchange on the interactions among electrons and between electrons and nuclei in solids.[9]

The author wishes to thank Professor G. E. Pake for his help and interest in this work. Discussions with R. S. Rhodes have also been invaluable.

---

*Supported by the Air Force Office of Scientific Research.

[1]A. W. Overhauser, Phys. Rev. 92, 411 (1953). For further references see R. H. Webb, Am. J.

Phys. (to be published).
[2]A. Abragam and W. G. Proctor, Compt. rend. 246, 2253 (1958). For further references see R. H. Webb, Am. J. Phys. (to be published).
[3]H. G. Beljers, L. van der Kint, and J. S. van Wieringen, Phys. Rev. 95, 1683 (1954).
[4]R. H. Webb (to be published).
[5]S. I. Weissman, J. Townsend, D. E. Paul, and G. E. Pake, J. Chem. Phys. 21, 2227 (1953).
[6]C. Kikuchi and V. W. Cohen, Phys. Rev. 93, 394 (1954).
[7]R. S. Rhodes, J. H. Burgess, and A. S. Edelstein, Phys. Rev. Letters 6, 462 (1961).
[8]M. E. Anderson (to be published).
[9]Note added in proof. The solid effect in BDPA has now been seen at 1.4°K.

THERMAL CONDUCTIVITY OF NORMAL AND SUPERCONDUCTING LEAD ALLOYS*

Peter Lindenfeld
Rutgers University, New Brunswick, New Jersey
(Received April 18, 1961)

The thermal conductivity of lead specimens containing 3% indium, 6% indium, and 6% bismuth has been measured in the normal and superconducting states. The data are shown in Fig. 1. Their analysis shows that the addition of impurity leads to an increase in thermal resistance in both states, but that near 2°K the ratio of increase in the resistance to lattice heat transport is 40 times greater in the normal state than in the superconducting state. Since in superconducting lead, at 2°K and below, the electronic conductivity and the effect of the electrons on the lattice conductivity are expected to be negligible, it is seen that the large change in lattice thermal resistance with impurity in the normal state depends on the presence of the electrons.

In the normal state the electronic thermal conductivity is equal to αT, where the coefficient α is related to the residual electrical resistivity ρ_0 by the Wiedemann-Franz law, $\alpha = L_0/\rho_0$ ($L_0 = 2.445\times10^{-8}$ volt^2/deg^2).[1] At sufficiently low temperatures the lattice conductivity is equal to βT^2. The total thermal conductivity $K = \alpha T + \beta T^2$ is most easily separated into its components graphically, on a plot of K/T versus T which will then be a straight line. In Fig. 2 the experimental data for the normal state have been plotted on such a graph. For each specimen the intercept α has been calculated from a measurement of the electrical resistance near 4.2°K, and a straight line drawn through this point and through the low-temperature thermal conductivity points. The slope β of each line is shown in Table I. In addition Table I lists the values of ρ_0 for our specimens and of β and ρ_0 for a specimen of lead with 0.7% bismuth measured by Montgomery.[2] The deviation of the data from the straight lines at higher temperatures is likely to be caused by the increased importance of impurity scattering at these temperatures.

The effect of adding impurity may be calculated roughly by comparing the thermal resistances of specimens containing different amounts of impurity. The lattice resistances at 2°K are

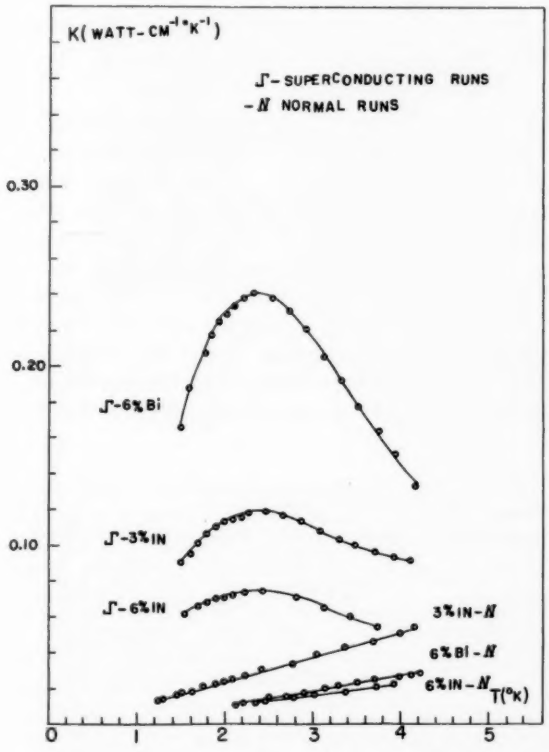

FIG. 1. Thermal conductivity of lead alloys versus temperature.

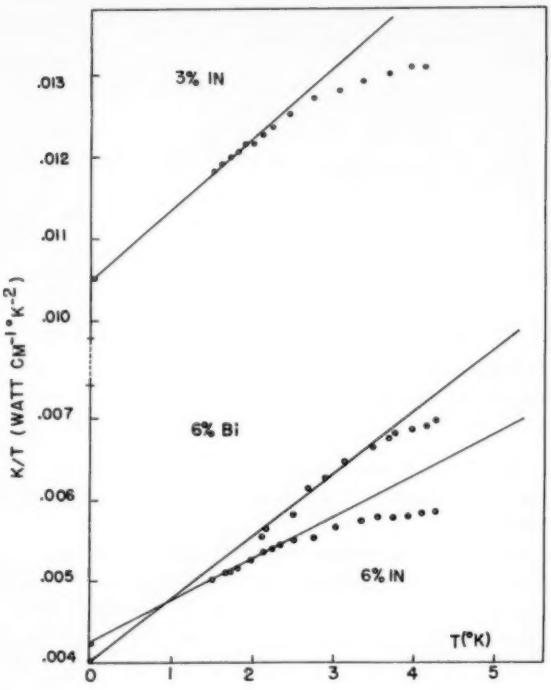

FIG. 2. Normal state thermal conductivity divided by temperature versus temperature.

listed in Table II. It is seen that the extra resistance of the 6% indium specimen compared to the 3% indium specimen is 190 cm-deg/watt in the normal state, and 4.9 cm-deg/watt in the superconducting state; i.e., the extra resistance is 40 times as large in the normal state as in the superconducting state. If the resistances of the 6% bismuth and 0.7% bismuth specimens are compared in the two states, the same ratio between the extra resistances is obtained. Supporting evidence may be inferred from a comparison of Montgomery's data with those of Olsen[3] for a specimen of lead with 10% bismuth.

The results for the superconducting state are similar to those found in insulating crystals where boundary and point defect scattering predominate. The difference between the effects of indium and bismuth may be at least partially accounted for by the difference in the mass of the impurity atoms. On the high-temperature side of the maximum, conduction and scattering by electrons will, of course, begin to affect the conductivity.

That the lattice conductivity in normal metals decreased in an anomalously strong fashion with increasing impurity content has been known from work on other metals.[1] The present measurements underscore our previous conclusion[4] that this change is not related to a large change in dislocation density since this would be expected to affect the conductivity in both states in the same way. The measurements show that the large increase in resistance with added impurity depends on the presence of the electrons, since it is greatly reduced in the superconducting state.

This added resistance could, in principle, be caused by a change in the electronic density of states or the electron-phonon interaction. It seems more reasonable, however, that the presence of the electrons as scattering centers leads to an interference between impurity scattering and electron scattering similar to that discussed for a different case by Berman et al.[5] In that case the interference between isotope scattering and phonon scattering was such that the process of smaller magnitude turned out to dominate the thermal resistance. If a similar enhancement can occur for impurity scattering in metals, the anomalously large effect of impurities on lattice conduction in lead as well as in other metals might be explained.

Table I. Values of lattice conductivity coefficient β and residual resistivity ρ_0.

	β (watt/cm-deg^3)	ρ_0 (ohm-cm)
6% In	0.52×10^{-3}	5.77×10^{-6}
3% In	0.86×10^{-3}	2.33×10^{-6}
6% Bi	0.77×10^{-3}	6.09×10^{-6}
0.7% Bi[a]	1.3×10^{-3}	0.750×10^{-6}

[a]See reference 2.

Table II. Lattice resistance at 2°K in the normal state ($1/K_{gn}$) and in the superconducting state ($1/K_{gs}$).

	$1/K_{gn}$ (cm-deg/watt)	$1/K_{gs}$ (cm-deg/watt)
6% In	480	13.7
3% In	290	8.8
6% Bi	320	4.4
0.7% Bi[a]	190	1.1

[a]See reference 2.

The measurements were made with the help of J. S. Brown and W. B. Pennebaker. I would also like to acknowledge helpful conversations with Dr. P. G. Klemens and Dr. B. Serin.

---

*Work supported by the National Science Foundation.

[1]P. G. Klemens, in Solid State Physics, edited by F. Seitz and D. Turnbull (Academic Press, Inc., New York, 1958), Vol. 7.

[2]H. Montgomery, Proc. Roy. Soc. (London) A244, 85 (1958).

[3]J. L. Olsen, Proc. Phys. Soc. (London) A65, 518 (1952).

[4]P. Lindenfeld and W. B. Pennebaker, Proceedings of the Seventh International Conference on Low-Temperature Physics (University of Toronto Press, Toronto, 1960).

[5]R. Berman, P. T. Nettley, F. W. Sheard, A. N. Spencer, R. W. H. Stevenson, and J. M. Ziman, Proc. Roy. Soc. (London) A253, 403 (1959).

DIRECT OBSERVATIONS OF ION DAMAGE IN CADMIUM

P. B. Price
General Electric Research Laboratory, Schenectady, New York
(Received May 3, 1961)

Pashley and Presland[1] have recently found that, during the normal operation of the Siemens electron microscope, the filament gives off negative ions (of unknown origin) which are accelerated and strike the specimen. The measured flux density at the specimen ranged between 10^7 and 10^9 ions/cm^2 sec. They studied the effect of these ions on a number of metal films, particularly gold,[2] and observed microstructural defects similar to those produced by fast neutron irradiation,[3] namely, tiny dot-like features which were sometimes resolvable as dislocation loops.

This Letter reports evidence that ion damage in cadmium crystals irradiated in the electron microscope results in the nucleation and growth of vacancy-type dislocation loops. Dislocation-free platelets of cadmium, thin enough ($\lesssim$2000 A) to be transparent to 100-kv electrons, were grown from the vapor[4] and examined in transmission in the Siemens Elmiskop I, on a cold stage, at temperatures in the range +25° to -100°C. After a few minutes at high beam current, tiny, isolated dislocation loops appeared and began to grow in the region illuminated by the beam. They were first detectable as dots of about 40A diameter (the minimum size resolvable by the transmission technique). At low temperature the rate of formation was high and the growth rate of individual loops was low, leading to a defect distribution like that in Fig. 1, which is a transmission electron micrograph, taken at -90°C about five minutes after the dots began to appear. At room temperature the rate of production was low, but those loops formed grew quite rapidly and eventually intersected one another to form dislocation networks. Figure 2 shows a typical distribution of loops (a) 5 minutes and (b) 10 minutes after the beginning of irradiation of the same area at +25°C.

FIG. 1. Vacancy-type dislocation loops due to ion damage in cadmium at -90°C. Several of the smallest loops, clearly visible on the original micrograph, are indicated by arrows.

The nature of the loops was determined by tilting a specimen and obtaining selected area diffraction patterns from individual loops in several different reflecting conditions. Virtually all of the loops were circular and oriented in the basal plane, which was parallel to the large platelet faces and perpendicular to the beam.

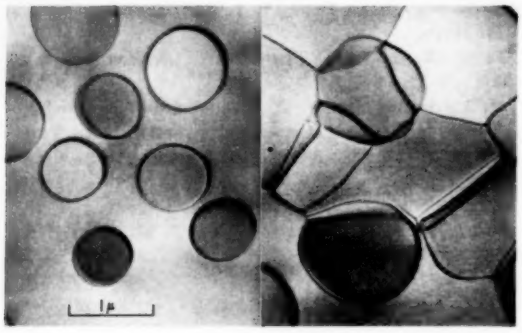

(a) (b)

FIG. 2. (a) Vacancy-type dislocation loops due to ion damage at +25°C after 5 minutes of irradiation. (b) Same area after 10 minutes. Note the dislocation reactions which take place when expanding loops meet.

The Burgers vector of all of the loops was found to be of the type $\frac{1}{2}c+p$, where p denotes a "half-dislocation" in the basal plane. It was inferred, from the observation that p could lie in any one of six equivalent $\langle 10\bar{1}0\rangle$ directions, that each loop was formed by the collapse of a single layer of vacancies, together with a shear in the basal plane.[5] Each loop thus enclosed a single layer stacking fault which, when viewed in a $10\bar{1}0$ reflection, was visible because of the difference in contrast inside and outside of the loop. In Fig. 1 the faults are not visible. In Fig. 2, taken in a $10\bar{1}0$ reflection, the loops have different degrees of contrast, indicating that they were formed at different distances from the surface of the crystal.[6] The uniformity of the contrast inside each loop implies parallelism to the surface and therefore to the basal plane.[6]

The following model is proposed to explain the nucleation and growth of the loops:

The ions, which have an initial energy of 10^5 ev, behave in about the same way as the primary knock-ons of fast neutrons, losing their energy almost entirely by elastic collisions with cadmium atoms. Because of their small range, ≤ 200 A,[7] the damage is limited to a volume close to the surface of the specimen. It is estimated that about 200 Frenkel pairs are produced by each ion.[8] Of these, the interstitials have an extremely high mobility even at -100°C; the first few in the cascade are probably sputtered out of the crystal and the others diffuse rapidly to the surface, which in these thin crystals is an excellent sink.

This leaves about 200 vacancies, clustered in the path of each ion, which may precipitate as a dislocation loop about 40 A in diameter.[3,9,10] Because of its large curvature and line tension, such a small loop will be subjected to a very large radial stress tending to shrink it by the emission of vacancies, which will diffuse to the crystal surface. In the absence of any local vacancy supersaturation due to the presence of other clusters, it is calculated[11] that a 40 A loop will disappear in $\sim 10^{-3}$ sec at +25°C, but only after $\sim 10^5$ sec at -75°C. A 100°C difference in irradiation temperature will therefore have a large influence on the kinetics of loop growth.

At -75°C it is expected that a large proportion of the clusters will precipitate as stable loops, which will grow slowly as a result of the rather low mobility of vacancies arriving from nearby clusters. At room temperature fewer stable loops will be formed, due to the difficulty of maintaining a high local supersaturation, but these will grow rapidly because of the longer diffusion distance of vacancies.

The transmission electron microscope technique provides a means of studying ion damage directly and can therefore be used to study radiation hardening if stress-strain curves are taken of thin films before and after irradiation. It should be borne in mind by those who use the electron microscope to study dislocation distributions in thin specimens that point defects are created during observation and may, at suitable temperatures, create new dislocations (loops and/or tetrahedra[2]) and cause the existing dislocations to climb. The latter effect has recently been observed in cadmium by the author,[12] in zinc by Fourdeux and Berghezan,[13] and in magnesium by Lally.[14]

Thanks are due to Dr. R. H. Pry, Dr. W. G. Johnston, Dr. R. M. Walker, and Dr. A. Howie for useful discussions, and to Dr. D. W. Pashley for communicating his results to me prior to publication.

---

[1]D. W. Pashley and A. E. B. Presland, Phil. Mag. (to be published).

[2]D. W. Pashley and A. E. B. Presland, Proceedings of the European Regional Conference on Electron Microscopy, Delft (to be published).

[3]J. Silcox and P. B. Hirsch, Phil. Mag. 4, 1356 (1959).

[4]P. B. Price (to be published).

[5]A. Howie (private communication).

[6]P. B. Hirsch, A. Howie, and M. J. Whelan, Phil.

Trans. Roy. Soc. (London) 252, 499 (1960).
[7]K. O. Nielsen, in Electromagnetically Enriched Isotopes and Mass Spectrometry, edited by M. L. Smith (Academic Press, Inc., New York, 1956), p. 68.
[8]G. J. Dienes and G. H. Vineyard, Radiation Effects in Solids (Interscience Publishers, New York, 1957), p. 28.
[9]A. H. Cottrell, Metals Rev. 1, 479 (1956).
[10]J. A. Brinkman, Am. J. Phys. 24, 246 (1956).
[11]J. Silcox and M. J. Whelan, Phil. Mag. 5, 1 (1960).
[12]P. B. Price (to be published).
[13]A. Fourdeux and A. Berghezan, Compt. rend. 250, 3019 (1960).
[14]J. S. Lally (private communication).

DE HAAS–VAN ALPHEN EFFECT IN POTASSIUM*

A. C. Thorsen and T. G. Berlincourt
Atomics International, Division of North American Aviation, Canoga Park, California
(Received April 28, 1961)

A study of the alkali metals is of particular interest for an understanding of the electronic structure of metals since these metals should conform most closely to an idealized metallic model of free conduction electrons. Previous measurements of transport properties[1] and specific heats[2] of the alkali metals are in fair accord with this model. In the free-electron picture, a spherical Fermi surface in $\vec{k}$ space gives rise to de Haas–van Alphen oscillations whose period is given simply by $P=(2e/\hbar c)(3\pi^2N)^{-2/3}$, where e, $\hbar$, c have their usual meanings and N is the number of valence electrons per unit volume. The period of the oscillations is related to the extremal cross-sectional area A of the Fermi surface perpendicular to the magnetic field by $P=2\pi e/c\hbar A$. For the case of potassium with 1.32×10^{22} electrons per cm^3 (at room temperature), one would expect a period of 5.69×10^{-9} gauss^{-1} corresponding to an extremal area of 1.68×10^{16} cm^{-2}. Such a short period is of the same order of magnitude as those found in the noble metals,[3] and one would expect to observe such an effect utilizing the high-field pulse technique.[4]

In this paper we report on the observation of de Haas–van Alphen oscillations in a single crystal of potassium in pulsed magnetic fields up to 160 kilogauss. Figures 1 and 2 show the observed oscillations as taken directly from the

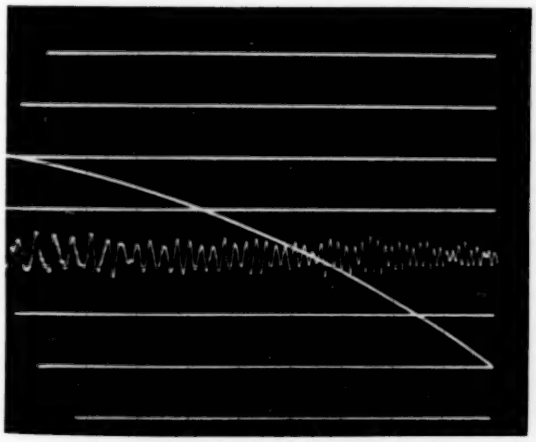

FIG. 1. de Haas–van Alphen effect in potassium at 1.77°K. The oscillating trace (≈ 0.1-mv amplitude) shows the output from a pickup coil containing the sample. The curved trace shows the field increasing from 151.7 to 158.5 kilogauss during a sweep time of about 1.0 millisecond (time increasing from right to left). The change in interval occupied by each successive period is due to the decrease of the time derivative of the magnetic field.

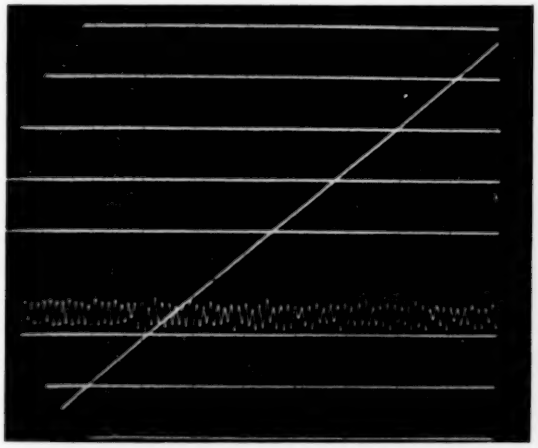

FIG. 2. de Haas–van Alphen effect in potassium at 1.07°K. The diagonal trace shows the field decreasing (from right to left) from 132.8 to 126.9 kilogauss during a sweep time of about 0.9 millisecond.

oscilloscope. The measurements yield a period of $5.75\times10^{-9}\pm1\%$ gauss^{-1}, indicating a cross-sectional area of the Fermi surface of 1.66×10^{16} cm^{-2}, in good agreement with that predicted from the free-electron model. It might be pointed out that the theoretical value is only valid to approximately 2% since no correction for thermal contraction was made. Furthermore, because the measurements were carried out for only one orientation nothing can be said as yet regarding deviations of the Fermi surface from sphericity. A plot of $\ln(a/T)$ versus T, where a is the amplitude of the oscillations and T is the absolute temperature, gives a straight line with slope $-2\pi^2k/\beta H$, where H = magnetic field and $\beta=e\hbar/m^*c$, from which we deduce the effective mass of the electrons as $(0.90\pm10\%)m_0$ (m_0 = free-electron mass). The specific heat data of Douglass et al.[2] give $m^*=1.3\,m_0$.

A brief description of the pulsed-field apparatus used in the present experiment is given elsewhere.[5] The pickup coils used to detect the oscillations in magnetization of the specimen were wound on a 0.79-cm long form using No. 52 copper wire. They consisted of 3050 turns wound series-opposed on top of 4800 turns, so that the effective sensitivity was proportional to the difference in the number of turns. The pure metal was supplied by M. S. A. Research Corporation and had a ratio of room-temperature resistivity to helium-temperature resistivity of approximately 1300. The crystal (0.019 cm diam by 0.81 cm long) was grown by zone-melting techniques in an open-ended Pyrex capillary and was protected from oxidation by a film of mineral oil. Attempts to determine the crystal orientation with x rays were unsuccessful due to the small size of the specimen and the small atomic scattering factor of potassium.

The authors wish to acknowledge the suggestion of D. Shoenberg regarding the use of coaxial pickup coils and valuable discussions with J. Trivisonno, Charles S. Smith, R. Bowers, and A. F. Kip concerning techniques for handling alkali metals.

---

*This research was supported by the U. S. Atomic Energy Commission.

[1]For a review see D. K. C. MacDonald, Handbuch der Physik, edited by S. Flügge (Springer-Verlag, Berlin, 1956), Vol. 14.

[2]R. L. Douglass, W. H. Lien, R. G. Peterson, and N. E. Phillips, Proceedings of the Seventh International Conference on Low-Temperature Physics, 1960 (University of Toronto Press, Toronto, 1960).

[3]D. Shoenberg, Phil. Mag. 5, 105 (1960).

[4]D. Shoenberg, Progress in Low-Temperature Physics, edited by C. J. Gorter (Interscience Publishers, Inc., New York, 1957), Vol. 2.

[5]T. G. Berlincourt, Proceedings of the Seventh International Conference on Low-Temperature Physics, 1960 (University of Toronto Press, Toronto, 1960).

OPTICAL SATURATION OF F-CENTER SPIN RESONANCE*

B. R. McAvoy, D. W. Feldman, J. G. Castle, Jr., and R. W. Warren

Westinghouse Research Laboratories, Pittsburgh, Pennsylvania

(Received May 8, 1961)

The influence of external light on the spin resonance of F centers in KCl has recently been observed,[1,2] with somewhat ambiguous results. This note reports results of preliminary experiments at 9.0 kMc/sec on very pure samples of KCl in which both the steady-state population difference and the spin relaxation time were measured during exposure to light. Irradiation by light in the F band was found to influence the populations of the ground-state sublevels as expected by excitation to a bound state; lattice heating was found to be negligible.

The ground state of F centers in KCl has been described in some detail by Gourary and Adrian.[3] Relaxation[4] of the populations of the two levels of the ground state to the lattice temperature is accomplished by phonons. Absorption of light in the F band equally from both levels and the subsequent random return should drive the populations toward equality and decrease the apparent relaxation time, τ. The rate equations for n electrons in levels 1 and 2 may be written as

$$dn_1/dt = -[2(w_{12}+w_{21})+2W+2\mathfrak{W}+AN]n_1 + (w_{21}+W+\mathfrak{W}+AN_1)n = -dn_2/dt, \quad (1)$$

where[5,6] $n=n_1+n_2$ with no storage in the optically excited states, w_{12} is the probability of transition

from 1 to 2 induced by the lattice, W is the probability of transition induced by the microwave radiation, $\mathfrak{W}$ is the probability of transition from 1 to 2 induced by the optical radiation, and A is the probability of transition by cross-relaxation to one of N impurity spins, of which N_1 spins are capable of flipping in pairs with F electrons in level 1. Since the N impurity spins are more strongly relaxed to the lattice than the F-center spins, N_1 is independent of n_1 and the F-center population difference, $\Delta n(t)$, is given by

$$\Delta n(t) - \Delta n(\infty) = B \exp(-\lambda t), \tag{2}$$

where $\lambda = 2(w_{12} + w_{21}) + 2W + 2\mathfrak{W} + AN = 1/\tau$, $\Delta n(\infty) = [w_{21} - w_{12} + A(2N_1 - N)]/\lambda$, B is the initial perturbation, and $2(w_{12} + w_{21}) + AN = 1/\tau_0$, the reciprocal of the spin relaxation time observed with zero incident light. With low power input, we have found $2W \ll 1/\tau_0$. Therefore, for low temperatures the expected relations between observed quantities are

$$1/\tau = (1/\tau_0) + 2\mathfrak{W}, \tag{3}$$

$$\Delta n(\infty)/\Delta n(\infty)_0 = \tau/\tau_0, \tag{4}$$

where $\Delta n(\infty)_0$ is the steady-state population difference without light.

The samples were prepared from single crystals of pure KCl which had been grown in a horizontal furnace under an atmosphere of HCl. The method of purification will be described elsewhere.[7] The resultant purity was found by ionic conductivity to be about thirty parts per billion. The crystals were colored to saturation by bremsstrahlung from 2-Mev electrons and kept in the dark until used.

In the experiment, light from an Osram *XBO* 2001 lamp is focused into a quartz prism monochromator. Light from the monochromator is directed through the multiple glass walls of a helium-nitrogen double Dewar into a microwave cavity of special design. Details of a similar cavity design are reported elsewhere.[8] The cavity is resonant in the TE_{103} mode with the sample mounted at one end of the cavity near a window. The transmission of the window to light is ~0.8, and to microwave is $\sim 10^{-4}$. Light transmission of the sample is monitored through a second window by a phototube. The power in the light beam incident on the Dewar is measured by a thermopile. The optical absorption spectrum of each sample is measured at 2.1°K. The absolute photon absorption rate is obtained from the measured absorbance of the sample with corrections for reflection losses at nine surfaces, transmission of the cavity window, and estimated scattering. The heat absorbed in the sample and cavity from the beam is found by the change in heater power required by the temperature regulator[6] to be in agreement with the thermopile values. The heat input (~20 microwatts into the sample) gives a negligible rise in temperature in the center of the sample whose outer surfaces are bathed in liquid helium II. A microwave signal power of 10^{-8} watt is employed together with a rapid field sweep of 100 μsec duration twice each second. Resulting average microwave power gives $2W$ much less than $1/\tau_0$. Resonance absorption signals without saturation are observed in this way. Spin relaxation times are measured by the inversion-recovery technique[6]; for no light conditions, room light is excluded from the sample.

Optical saturation is evident in Fig. 1 where the appearance of the resonance absorption signals on the oscilloscope is given for the conditions with and without F-band light. Since the resonance line shape remains constant under

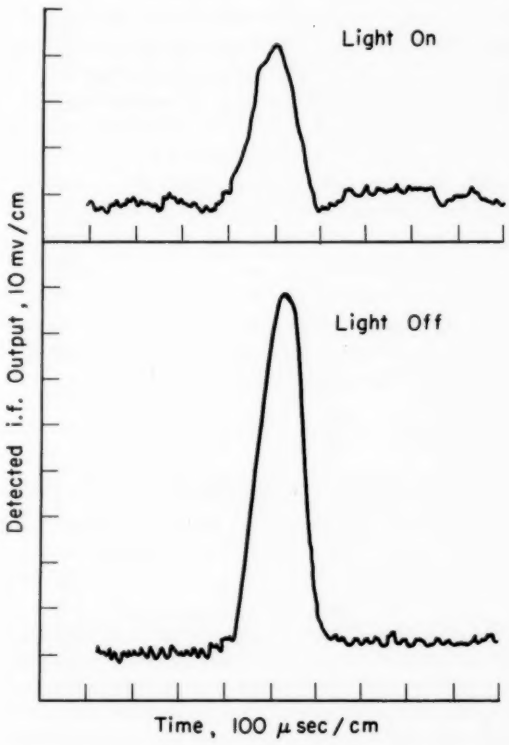

FIG. 1. Microwave resonance absorption by F centers in a crystal of KCl at 2.1°K and 3 kgauss with and without F-band light.

Table I. Effects of F light on ground-state properties of F centers in a γ-irradiated sample of pure KCl at 2.1°K.

Photon absorption rate (10^{14} sec^{-1})	Observed spin absorption signal (relative)	Observed spin relaxation time (sec)	Calculated absorption signal [Eq. (4)]
0	1.0	1350[a]	1.0
1	0.5	540	0.4
2	0.2	270	0.2

[a]This rather long time appears to be the characteristic spin-lattice relaxation time and is under further study by Feldman, Warren, Castle, and Gourary.

optical saturation, the signal height is sufficient for the comparison of Eq. (4).

The observed resonance signals and relaxation times are given in Table I for one sample irradiated to a total dose of 5×10^5 r and having 1×10^{16} F centers. Proportionality between the effective relaxation time and the steady-state population difference is found for two intensities of F light. This agreement confirms the model for optical saturation in which the excitation of isolated F centers occurs to these bound excited states and there is essentially no preferential pumping.

In addition the data allow a comparison of absolute rates. For 1×10^{14} photons absorbed per second and two photons absorbed for every optically induced spin flip, an effective relaxation time of 60 seconds is expected on the basis of Eq. (3) and 1×10^{16} F centers. The number of F centers measured by spin resonance absorption agrees with the number calculated from optical absorbance[9] within a factor of two. Uncertainties in the optical measurements probably account for the discrepancy from the observed τ of 270 seconds.

*Work supported in part by a contract with the Air Force Research Division.

[1]J. Lambe and J. Baker, in Quantum Electronics, edited by C. H. Townes (Columbia University Press, New York 1960), p. 93.

[2]I. Wieder and J. S. Hyde, Bull. Am. Phys. Soc. 5, 497 (1960).

[3]B. S. Gourary and F. Adrian, Advances in Solid-State Physics, edited by F. Seitz and D. Turnbull (Academic Press, Inc., New York, 1960), Vol. 10, p. 127.

[4]Relaxation near room temperature for F centers in NaCl has been analyzed by W. E. Blumberg, Phys. Rev. 119, 1842 (1960).

[5]N. Bloembergen, S. Shapiro, P. S. Pershan, and J. O. Artman, Phys. Rev. 114, 445 (1959).

[6]J. G. Castle, P. F. Chester, and P. E. Wagner, Phys. Rev. 119, 953 (1960).

[7]R. W. Warren (to be published).

[8]B. R. McAvoy, Rev. Sci. Instr. (to be published).

[9]J. H. Parker, Jr. (to be published); and R. H. Silsbee, Phys. Rev. 103, 1675 (1956).

EXTREMELY LOW LOSS ACOUSTIC RESONANCE IN SINGLE-CRYSTAL GARNET SPHERES

R. C. LeCraw, E. G. Spencer, and E. I. Gordon
Bell Telephone Laboratories, Murray Hill, New Jersey
(Received May 10, 1961)

An acoustic resonance has been observed at room temperature and ~9.2 Mc/sec in single-crystal spheres of yttrium iron garnet (YIG) with losses nearly an order of magnitude lower than any other known material at the same temperature and frequency. Until now, quartz crystals vibrating in shear modes were recognized as having the lowest acoustic losses at this temperature and frequency.[1]

The above observation was first made on a YIG sphere using magnetoacoustic resonance (MAR). With this technique a microwave pump signal is used to excite parametrically into acoustic oscillation a small spherical sample of YIG biased with a dc magnetic field near ferromagnetic resonance.[2] At a critical rf mag-

netic field, h_{crit}, the sample oscillates in one of the acoustic modes of the sphere.[3]

Using MAR the Q's of a number of the acoustic modes of a YIG sphere have been obtained by observing the decay time of the acoustic amplitude after the microwave pump has been turned off, Q being defined by the decay factor $\exp[-(\omega/2Q)t]$. The modes S_1, R_1, and R_2, shown in Fig. 1, have been studied in particular.[4]

Although MAR was used for the original measurements, it was realized that a method permitting the selective excitation of a given acoustic mode was desirable. Thus the direct drive scheme shown in Fig. 2 was devised. Here the sphere is driven magnetostrictively at a frequency $F/2$, exciting a particular acoustic mode at a frequency F. The Q of the driven mode is then determined from the frequency difference ΔF between the points of one-half power transmission, using the relation $Q = F/\Delta F$. It was established that the input and output coils contributed negligible loading. Acoustic oscillations have also been excited by driving at F. This is probably due to a "bias effect" in which the dc magnetization is not exactly parallel to the applied dc magnetic field. The bias can be caused by several different kinds of slight sample imperfections or bottom effects. In most cases the response when driving at F is greater than at $F/2$. At higher amplitudes, when driving at F, parametric excitation has been observed in which the measured Q depends strongly on the drive amplitude.

The transmitted signal is monitored by a narrow band superheterodyne receiver connected to the output coil. The response is square law when driving at $F/2$ and linear when driving at F. The input frequency must be highly stable, since the linewidths are of the order of one part in 10^7 of the resonant frequency. It may be noted that the output coupling is primarily through near-field effects, since mode R_1, for example, has no oscillating dipole moment.

The results obtained using direct drive and measuring transmission vs frequency are in good agreement with those obtained using MAR and observing the exponential decay. These results are tabulated in Table I for the sample both in air and in vacuum and are compared with the highest published Q's for quartz[1] and silicon.[5]

At present the physical implications of these data are somewhat obscured by the fact that contact losses at the bottom of the quartz tube have not yet been eliminated. A levitation scheme is being developed to remedy this. We should like, however, to make several suggestions concerning these quite unexpected results: Most YIG crystals grown to date are known to contain relatively large numbers of imperfections such as dislocations,[6] small inclusions, tube-like voids,[7] and chemical impurities. Hence by the usual criteria for lattice perfection, the crystals used in these experiments are quite poor. Thus, it is not surprising that

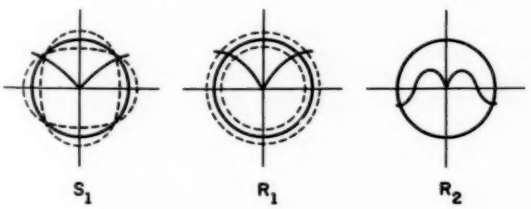

FIG. 1. Schematic representations of three of the acoustic modes of a sphere. The letters S and R refer to spheroidal and radial modes, respectively. The subscripts refer to the number of zeros along a radius. The dashed lines indicate the extremes of the motions (omitted in R_2). The solid curves show the relative amplitudes along the radius (for $\theta = 0$ in S_1). Both R_1 and R_2 are radially symmetric, R_1 having a "breathing" type motion, and R_2 having an inner sphere and an outer shell with opposite radial displacements.

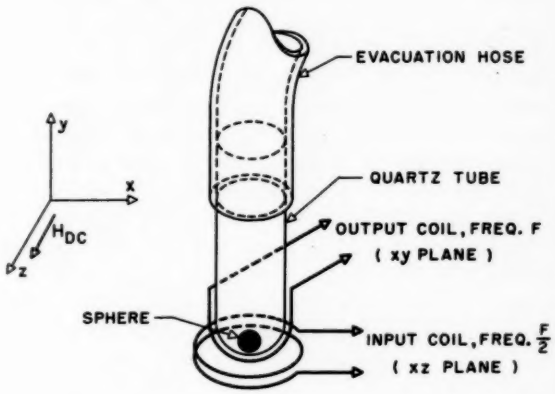

FIG. 2. Schematic diagram of the direct drive method. The sphere rests loosely on the bottom of the quartz tube and is oriented by the dc magnetic field along the [111] crystal axis. The principal purpose of the dc field is to saturate the sample and eliminate the domains. (Below saturation the observed Q's are very low.) The input and output coils are adjusted to give minimum direct coupling when the sphere is not acoustically vibrating.

Table I. Comparison of the Q's for several modes in a single-crystal YIG sphere 0.060 inch in diameter and the highest published Q's for quartz and silicon. The frequencies are tabulated here to only three significant figures, and are quite close to those given for an isotropic sphere by Love.[a] The velocities used were measured on polycrystalline YIG by H. J. McSkimin and are $v_t = 3.87 \times 10^5$ cm/sec and $v_l = 7.17 \times 10^5$ cm/sec. Contact losses due to the quartz tube are contained in these data. Essentially the same results have been observed on more than one sample.

	Freq. (Mc/sec)	Q (air)	Q (vac)
YIG (S_1)	2.10	0.07×10^6	1.2×10^6
YIG (R_1)	3.97	0.26×10^6	0.45×10^6
YIG (R_2)	9.22	2.5×10^6	9.5×10^6
Quartz	9.22		1.5×10^6
Silicon	9.22		0.42×10^6

[a]See reference 3.

mode S_1, which has both shear and compressional components and is quite analogous to similar modes observed in quartz, has a lower Q than quartz at the same frequency.[1]

The radial modes R_1 and R_2, however, are not analogous to any motion thus far observed in quartz or silicon. In these modes the crystal unit cell experiences no shearing stress; and the motion, to first order, is purely "hydrostatic" in form. It is possible that this has a twofold effect: Damping due to several types of dislocations vanishes, or is greatly reduced, when no shear is present.[8] Also, even in a perfect crystal, certain phonon-phonon relaxation terms may vanish or be considerably reduced when the motion is such that the unit cell remains cubic.[9] With respect to the latter point, it is worth noting that YIG has an unusually isotropic sound velocity, there being only about one percent variation in the longitudinal velocity along various crystal axes.[10] This fact is probably quite significant, particularly in the radial modes where dislocation effects are less. Quartz, for example, due to its large elastic anisotropy would not remain nearly as radially symmetric as YIG under motion such as in the R modes. Information about the change in velocity with hydrostatic pressure in YIG would be very helpful but is unavailable at present.

We cannot explain why the Q for R_1, the first-order radial mode, is so much lower than for R_2, especially since its frequency is even lower than R_2 (the normal frequency dependence for Q above a few Mc/sec is $Q \sim f^{-1}$). This large difference has been observed on more than one sample, and must await levitation experiments before being resolved. Although contact losses are undoubtedly greater for R_1 than for R_2, calculations show that the ratio of the surface velocity squared to the stored energy is only approximately twice as great in R_1 as in R_2.

It is important to determine if the unusually large Q observed for mode R_2 is due primarily to the material or to the radial symmetry; and if it is the material, whether it is the whole class of garnets or YIG in particular. Detailed studies are in progress to achieve a greater understanding of this new acoustic material and little-investigated type of motion.

[1]H. E. Bömmel, W. P. Mason, and A. W. Warner, Jr., Phys. Rev. 99, 1894 (1955).

[2]E. G. Spencer and R. C. LeCraw, Phys. Rev. Letters 1, 241 (1958); J. Appl. Phys. 30, 149S (1959).

[3]A. E. H. Love, The Mathematical Theory of Elasticity (Dover Publications, New York, 1944), 4th ed., Chap. 12.

[4]In the notation of P. M. Morse and H. Feshbach, Methods of Theoretical Physics (McGraw-Hill Book Company, New York, 1953), p. 1873, the S and R mode amplitudes can be written $\vec{s} = \vec{L}_{mln} + A\vec{N}_{mln}$, where $m \leq l$ and n is added to indicate the number of zeros along the radius. The function L is derivable from a scalar potential and N from a vector potential. Mode S_n corresponds to $m = 0$ and $l = 1$. Mode R_n corresponds to $l = 0$, for which $N_{00n} \equiv 0$.

[5]J. Lamb, M. Redwood, and Z. Shteinshleifer, Phys. Rev. Letters 3, 28 (1959). The value here is extrapolated and is for longitudinal waves. These authors report in private communication a somewhat higher Q for shear waves.

[6]T. H. Ramsey, Jr., J. Am. Ceram. Soc. 42, 645 (1959).

[7]J. Nielsen and J. F. Dillon, Jr. (private communication).

[8]W. P. Mason, Physical Acoustics and the Properties of Solids (D. Van Nostrand Company, Inc., Princeton, New Jersey, 1958), p. 238.

[9]T. Kasuya (private communication).

[10]A. E. Clark and R. E. Strakna, Naval Ordnance Laboratory, Washington, D. C. (to be published).

OBSERVATION OF FORBIDDEN RESONANCES IN OPTICALLY DRIVEN SPIN SYSTEMS

William E. Bell and Arnold L. Bloom

Instrument Division, Varian Associates, Palo Alto, California

(Received May 1, 1961)

In a recent Letter[1] we described experiments in which a macroscopic moment precessing at the Larmor frequency was induced in a spin system by the synchronous modulation of an incident beam of optical pumping radiation. It was pointed out there that this resonance effect does not involve a perturbation directly coupling the magnetic substates; instead it may be regarded as an indirect effect employing the coupling of each of the magnetic sublevels to a common optically excited state. This statement carries the important corollary that such a resonance might be observed even if a direct coupling between the sublevels does not exist, i.e., even if there is no possible matrix element for the direct transition. We report here the observation of such a forbidden resonance in the $\Delta m = 2$ ($g = 4$, 5.6 Mc sec^{-1} gauss^{-1}) transition between the sublevels $m = 1$ and $m = -1$ in the $2\,^3S$ metastable state of helium. It is clear that the method is generally applicable to other optically pumped systems having more than two sublevels.

In order to describe the experiment, we bear in mind that the transformation properties of triplet state wave functions under rotations are the same regardless of whether the angular momentum is spin or orbital. It is therefore convenient to take advantage of the spatial representation afforded by the orbital functions, whose angular parts can be written as follows:

$$m = 1, \quad \psi_1 = (x + iy)\exp(-i\omega_0 t),$$

$$m = 0, \quad \psi_0 = \sqrt{2}\,z,$$

$$m = -1, \quad \psi_{-1} = (x - iy)\exp(i\omega_0 t),$$

the functions being suitably normalized on a sphere of radius r. ω_0 is the Larmor angular frequency in a field H_0 parallel to the z axis for the usual magnetic transition $\Delta m = 1$. If an ensemble of triplet helium metastables is irradiated by resonance radiation, then, as shown by Colegrove and Franken,[2] optical pumping results in an alignment process tending to populate the state described by $\sqrt{2}\,z$, the effect being a maximum when the axis of the light beam is in the z direction. (The axis of the light is either the direction of propagation of unpolarized light or the direction of the electric vector of plane-polarized light. For our purposes it is immaterial whether the actual alignment results in an excess or a deficit in the specified state.)

Consider now what happens if the light axis is rotated so that it is perpendicular to H_0, specifically if it is in the x direction. Instantaneously the light pumps a small alignment in the state described by $\sqrt{2}\,x$. This alignment immediately proceeds through a time development given by

$$\sqrt{2}\,(x\cos\omega_0 t + y\sin\omega_0 t) = (\psi_1 + \psi_{-1})/\sqrt{2},$$

whose expectation value for population excess in the x direction varies as $\cos^2\omega_0 t$ and is therefore periodic at twice the Larmor frequency. If the light is left on continuously, then the successive smearing-out of phases still results in a net alignment, but much weaker than the maximum.[2] However, let the light be modulated at frequency $2\,\omega_0$; then the result is a synchronous reinforcement of the time-dependent effect resulting in a relatively large precessing alignment. By a treatment exactly analogous to that used in reference 1, it can be shown that the observable effect should be an increase in intensity of the transmitted light when the light modulation frequency ω is within about one linewidth of $2\,\omega_0$.

The possibility of obtaining double-frequency optical effects upon driving a spin-1 system at its Larmor frequency has been pointed out elsewhere.[3] However, the unique feature of the present experiment is the fact that the time-dependent alignment defined by the state $(\psi_1 + \psi_{-1})/\sqrt{2}$ does not correspond to any kind of directly observable macroscopic moment in the case of helium. Furthermore, note that the $m = 0$ level does not enter in the description of the resonant state. Thus the resonance should occur as described even if the $m = 0$ level is displaced from its median position between the $m = \pm 1$ levels for any reason. The resonance linewidth is expected to be about the same, in frequency units, as that of the Larmor resonance and therefore only half as large in terms of magnetic field changes.

The experiment was performed with substantially the same apparatus described in reference 1 but without the circular polarizer. Since alignment effects in He are much smaller than the orientation obtained with a circular polarizer,[4] it was necessary to assure virtually 100% modulation of the light beam in order to make the sig-

nal detectable. This was accomplished most simply by operating in a weak field $H_0 \approx 0.01$ gauss and an observed Larmor frequency $\omega_0/2\pi$ of 24 kc/sec. The $g=4$ resonance at 48 kc/sec was clearly observable on the oscilloscope with or without a linear polarizer in the light beam. Rotation of the linear polarizer verified, within signal-to-noise limitations, that the signal amplitude obeyed the $\sin^2\theta$ dependence to be expected by generalizing the above arguments (θ is the angle between light axis and H_0).

We are indebted to N. Steiger for assistance in performing the experiment and to R. G. Aldrich, of the U. S. Naval Postgraduate School, for pioneering in the production of large signals by modulated light.

[1]W. E. Bell and A. L. Bloom, Phys. Rev. Letters 6, 280 (1961).
[2]F. D. Colegrove and P. A. Franken, Phys. Rev. 119, 680 (1960).
[3]A. Kastler, Compt. rend. (to be published).
[4]L. D. Schearer, Second International Conference on Quantum Electronics (to be published).

PION-PION INTERACTION IN PION PRODUCTION BY π^+-p COLLISIONS*

D. Stonehill, C. Baltay, H. Courant, W. Fickinger, E. C. Fowler, H. Kraybill, J. Sandweiss, J. Sanford,† and H. Taft
Yale University, New Haven, Connecticut and Brookhaven National Laboratory, Upton, New York
(Received May 12, 1961)

Since the first conjectures[1] that rise in the total π^--p cross section between 300 and 600 Mev might be caused by a pion-pion interaction, this subject has received considerable attention. Theoretical analysis[2] of high-energy electron scattering on protons and neutrons has predicted a resonance in the pion-pion interaction at a total di-pion energy (ω) of 4 to 5 pion masses, with isotopic spin and angular momentum both equal to one. Several analyses of π^--p experiments[3] in the 1-Bev energy range have tended to confirm this prediction, and application[4] of the Chew-Low method has indicated a steep rise in the pion-pion cross section above $\omega=4$. Recent work[5] with 1.9-Bev π^--p collisions shows a peak in the pion-pion interaction at $\omega \sim 5.5$. We report here evidence of pion-pion interaction in π^+-p collisions at three separate energies, which show striking effects attributable to a pion-pion resonance with ω of about 5.5 pion masses.

The data presented are results of a systematic study of pion-proton reactions at kinetic energies of 910 Mev, 1090 Mev, and 1260 Mev, which is still in progress. Photographs taken at the Cosmotron in the Brookhaven 20-inch hydrogen bubble chamber have been scanned for all interactions. All two-pronged collisions have been measured on a projection microscope of the Franckenstein type and have been processed by the Yale spatial reconstruction and kinematical fitting programs on the IBM 704 of the New York University Computing Center. Each possible identification assigned by the computation has been compared by a physicist with other information (including ionization densities) available from the photographs, to establish the final identification. Cross sections for the various reactions, based upon the first compilation of these events, are shown in Table I.

The influence of pion-pion interaction will appear most readily in the single pion production processes: $\pi^+ + p \to p + \pi^+ + \pi^0$ and $\pi^+ + p \to n + \pi^+ + \pi^+$. Accordingly, the Q value of the two outgoing pions (that is, the kinetic energy of their relative motion in their mutual center of momentum) has been computed for each individual occurrence of single pion production. The distribution of Q values at each energy is shown in Fig. 1. This figure includes all identified events, without additional selection.

In the reaction $\pi^+ + p \to p + \pi^+ + \pi^0$, a definite peak appears at each energy in the Q-value region of 400-500 Mev, extending well above the number of events to be expected from a uniform momentum-space distribution of secondary particles. The peaks also extend well above the distribution to

Table I. π^+-p cross sections (in mb) at 910-Mev, 1090-Mev, and 1260-Mev kinetic energy.

	910 Mev	1090 Mev	1260 Mev
σ_{total}	24.5±1.3	30.1±1.6	40.3±2.2
σ_{elastic}	10.3±0.9	12.6±1.1	16.5±1.4
$\sigma(p\pi^+\pi^0)$	10.4±0.9	10.8±1.0	11.9±1.2
$\sigma(n\pi^+\pi^+)$	2.6±0.4	2.5±0.5	4.6±0.7
$\sigma_{\text{multiple }\pi\text{ prod.}}$	1.3±0.3	3.9±0.6	6.9±0.9
$\sigma(\Sigma\text{-}K)$	$0.034^{+0.018}_{-0.012}$	0.25±0.02	0.42±0.07

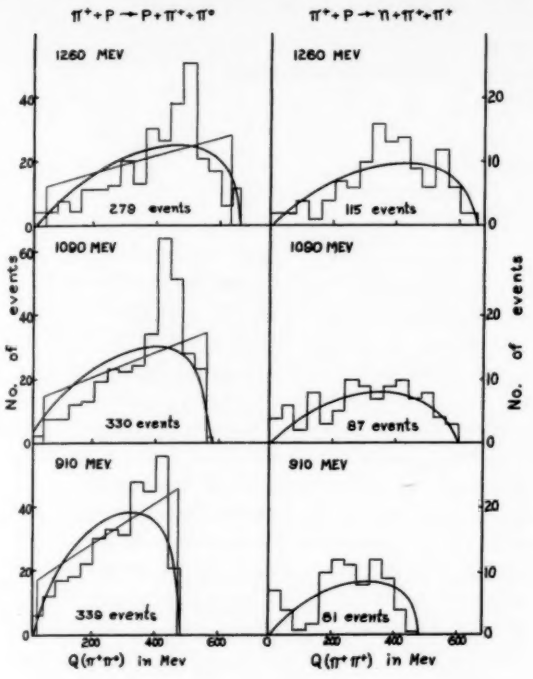

FIG. 1. Distribution of pion-pion Q values (that is, kinetic energy of the two outgoing pions in their mutual center-of-momentum system) for the reactions $\pi^+ + p \rightarrow p + \pi^+ + \pi^0$ and $\pi^+ + p \rightarrow n + \pi^+ + \pi^+$ at 910-Mev, 1090-Mev, and 1260-Mev laboratory kinetic energy of the incident pion. The curved lines are the Q distribution resulting from uniform distribution of the secondary particles in momentum space. The straight lines give the Q distribution resulting from isotropic decay of a pion-proton isobar of unique mass 1230 Mev.

be expected from isotropic decay of the $\frac{3}{2}$-$\frac{3}{2}$ pion-nucleon isobar, which is known to influence this reaction.[6]

In the pion-pion Q distributions for $\pi^+ + p \rightarrow n + \pi^+ + \pi^+$, on the other hand, no peaks appear in the region 400 to 500 Mev. (There may be a peak for the 1260-Mev pion energy in the vicinity of 350 Mev, but this is not statistically certain.)

Now, two π^+ mesons can only have a total isotopic spin of 2, whereas the π^+-π^0 combination contains isotopic spin values of 1 and 2. Therefore, a resonance in the $I=1$ state can only appear in the $p\pi^+\pi^0$ reaction. On the other hand, if charge independence is assumed, a resonance in the $I=2$ state should appear 80% as $n\pi^+\pi^+$ reactions and 20% as $p\pi^+\pi^0$. We conclude that the interaction responsible for the observed peaks is overwhelming in the state $I=1$, and possibly not at all in the state $I=2$. This is consistent both with theoretical predictions[1,2] and with the conclusions of Walker et al.[5]

At present, only an approximate estimate of the pion-pion resonance energy can be made from these data. At 910 Mev, the peak is attenuated and shifted to lower energies by the lack of available momentum space at higher Q values. The peak at 1090 Mev also seems to be about 50 Mev lower than at 1260 Mev. However, the data are not inconsistent with a single resonance with ω between 5.0 and 5.5, corresponding to a total dipion mass of 700 to 770 Mev. The full width at half maximum appears to be ~90 Mev. (The rms error in the determination of Q values is less than 10 Mev.)

We are pleased to acknowledge the considerable help we have received from the regular Brookhaven staff, especially at the Cosmotron and with the Bubble Chamber Group.

---

*This work was partially supported by the U. S. Atomic Energy Commission.

†Part of the work reported here was done by J. R. Sanford who held a National Science Foundation Cooperative Graduate Fellowship.

[1]R. Cool, O. Piccioni, and D. Clark, Phys. Rev. 103, 1082 (1956); F. J. Dyson, Phys. Rev. 99, 1037 (1955); G. Takeda, Phys. Rev. 100, 440 (1955).

[2]W. R. Frazer and J. R. Fulco, Phys. Rev. Letters 2, 365 (1959); J. Bowcock, W. N. Cottingham, and D. Lurié, Phys. Rev. Letters 5, 386 (1960); S. Bergia, A. Stanghellini, S. Fubini, and C. Villi, Phys. Rev. Letters 6, 367 (1961).

[3]I. Derado, Nuovo cimento 15, 853 (1960); F. Selleri, Nuovo cimento 16, 775 (1960); P. Carruthers and H. A. Bethe, Phys. Rev. Letters 4, 536 (1960); E. Pickup, F. Ayer, and E. O. Salant, Phys. Rev. Letters 5, 161 (1960); D. Robinson, B. Munir, E. Pickup, and E. Salant, Bull. Am. Phys. Soc. 6, 301 (1961).

[4]J. Anderson, V. Bang, P. Burke, D. Carmony, and N. Schmitz, Phys. Rev. Letters 6, 365 (1961).

[5]W. Walker, H. Fechter, R. March, D. Lyon, P. Satterblom, and A. Erwin, Bull. Am. Phys. Soc. 6, 311 (1961), and private communication from W. D. Walker.

[6]Private communication.

EMISSION OF CARBON GROUP HEAVY NUCLEI FROM A 3+ SOLAR FLARE

Herman Yagoda
Air Force Cambridge Research Laboratories, Bedford, Massachusetts

and

Robert Filz and Katsura Fukui
Emmanuel College, Boston, Massachusetts
(Received May 8, 1961)

Discoverer satellite XVII was launched into a polar orbit 2042 U.T. on November 12, 1960, about 37 minutes after ground-level neutron monitors indicated their maximum cosmic-ray increase following a 3+ solar flare which commenced at 1325 U.T. During the 50 hours between launching and successful recovery, it is estimated that the outside of the capsule received a bombardment of $\sim 2\times 10^9$ protons of energy $E \geq 30$ Mev.[1] The instrument capsule, which carried a 772-gram block of Ilford G5 emulsion, had an apogee of 993 ± 4 km and a perigee of 188 ± 3 km. The average latitude of apogee was 20°S and the perigee occurred at 18°N. Of the 31 orbits of 96.44-min duration, a total of 0.766 day was spent above geomagnetic latitude 55°N and S.

The 10×15 cm face of the emulsion block was placed adjacent to one wall of the aluminum capsule and radiation arriving perpendicular to this plane penetrated 2.2 g cm^{-2} of condensed matter composed of light nuclei. This admitted carbon nuclei with energies in excess of 88 Mev per nucleon over a solid angle of 1.8 steradians. Owing to other instrumentation in the capsule, the rear of the block was shielded by approximately 21 g cm^{-2} of condensed matter.

After several unsuccessful attempts at full development, which caused almost every grain of silver bromide to be reduced to metallic silver, the bulk of the emulsion stack could be processed to a point where the preparations transmitted light (Fig. 1) by employing a very dilute amidol developer at near 0°C temperature and adjusted by means of a sulfite-bisulfite buffer to a pH of 6.5. Details of the processing, of the flare exposure, and of further measurements on long-lived radioactive nuclides produced in the metallic components are available in a preliminary report on the Discoverer XVII flight.[2,3]

The final ability to discern the tracks of slow, highly charged nuclei above the dense, random, single-grain background is not due in its entirety to the extremely weak development. Owing to the rapid diminution of the flare radiation following maximum, we estimate that about 50% of the total dose was delivered during the first hour in orbit. This intense radiation appears to have destroyed the basic sensitivity of the G5 emulsion, It is very likely that the hydrogen peroxide produced by the radiochemical decomposition of the water retained by the gelatin played a significant role. It is known that hydrogen peroxide[4] has a powerful destructive action on the latent image produced by ionizing radiations. By diffusion into the silver bromide grains all surface latent images would be destroyed, but in the case of the largest or most sensitive grains a residual internal latent image might persist if the nuclear particle crossing the grain had a very high rate of energy loss.

Prior to development, the flown emulsion and a control piece from the same batch were exposed to polonium alpha particles. The tracks of the 5-Mev rays were readily visible on the

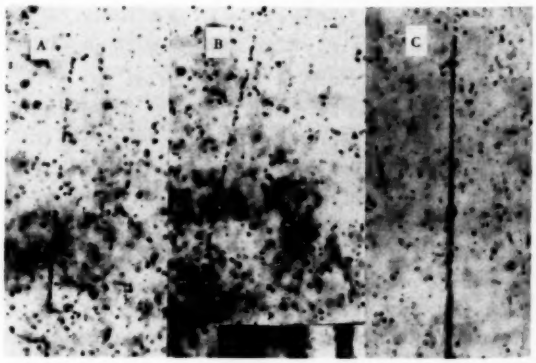

FIG. 1. Photomicrographs of three terminating flat tracks recorded in the Discoverer XVII emulsion block. The black bars define 10-micron intervals. The integral grain densities in the terminal 300 microns are as follows. A: 192 grains ($Z = 4$ or 5); B: 308 grains ($Z = 6$ or 7); and C: 871 grains ($Z \sim 20$).

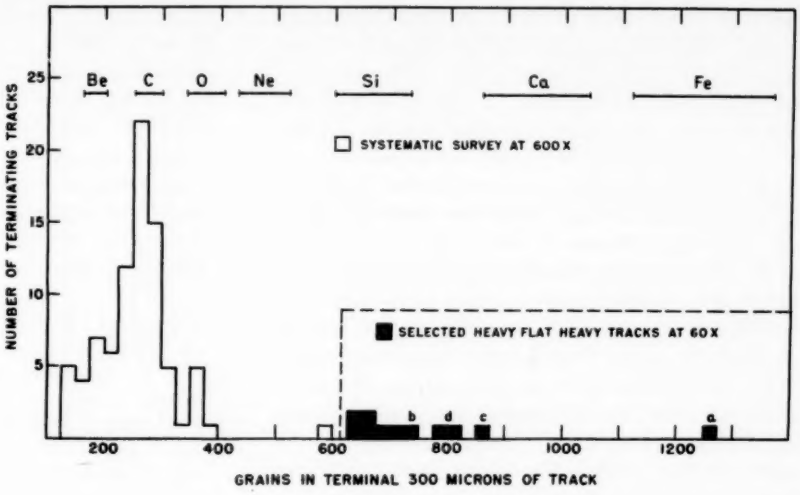

FIG. 2. Histogram of relative abundance of particles based on a scale of grains in terminal 300 microns of track. The insert is not a part of the systematic survey and is included to show the gambit of the charge spectrum.

control sheet, but could not be discerned on the flare-irradiated recording medium. Examination of the desensitized emulsion at 2000× magnification shows star-like structures of 3 to 6 tracks originating from a common center. The grain density and range of these associated tracks clusters suggests that they are the spallation products of $Z \geq 3$ commonly produced when Br, Ag, or I emulsion target nuclei are evaporated.

Systematic examination of the first three 600-micron emulsion sheets facing the thin window at 600× magnification shows a group of tracks which enter the stack and terminate their range by ionization. For particles making small dip angles with the emulsion plane the grain density can be measured after suitable correction for coincident background grains. The histogram of the grain density in the terminal 300 microns of range (Fig. 2) shows a pronounced peak at 275 ± 25 grains. Most all of the light tracks have the same sense of direction and make a spatial angle with respect to the longitudinal axis of the rocket of $\leq 50°$.

If we plot the logarithm of the integral grain count N as a function of the logarithm of the residual range R, tracks of varying grain density yield linear functions of essentially the same slope. This indicates that the strongly irradiated emulsion is still serving as a quantitative tool for measuring ionization. It can be shown that a line of constant grain density intersects these functions at ranges R roughly inversely proportional to the charge Z. If we assign $Z = 4$ to the tracks with an average count of 183 ± 17 grains, then the peak at 275 ± 25 grains yields a charge of 5.9. The charge assignments for heavier nuclei, following this model, are indicated in Fig. 2.

Table I is a summary of the frequency of heavy primary nuclei terminations as observed on Discoverers XVII, XVIII, and at balloon elevations. The Discoverer XVIII block was exposed during

Table I. Comparison of heavy primary terminations in balloon and satellite exposures.

Flight	Date	Altitude (km)(apogee)	$Z \geq 6$ terminations (cc^{-1} day^{-1})
Bemidji 532	July 29, 1960	42.5	7.78 ± 1.15
Bemidji 533	August 5, 1960	42	8.60 ± 1.04
Discoverer XVIII	December, 1960	638	8.65 ± 0.93
Discoverer XVII	November, 1960	993	900 ± 300

a relatively quiescent period of solar activity and could be developed normally. It exhibits essentially the same frequency of terminating $Z \geq 6$ particles as the balloons launched at 55°N, and the tracks enter isotropically. A comparison of the two satellite exposures indicates that during the 3+ flare the flux of $Z \geq 6$ particles capable of terminating in the detectors increased about 100-fold. The greater part of the 900 ± 300 cc^{-1} day^{-1} termination frequency is due to the $Z = 6 \pm 2$ group. If we assume that our low-magnification estimate[5] of 13 ± 3 cc^{-1} day^{-1} applies to the more conspicuous tracks of $Z \geq 10$, then the M/H ratio during a flare is ~70 as compared with a value of 3 for the galactic heavy primaries. The large uncertainty in the $Z \geq 6$ population is not statistical in character, but originates from the sampling position, which reaches a maximum in the first emulsion sheet facing the thin window. The over-all evidence indicates that a beam of particles of $Z = 6 \pm 2$ was emitted from the sun during the 3+ flare.

This identification is consistent with the observation by Fichtel and Guss[6] of a flux of carbon, nitrogen, and oxygen nuclei associated with a flare of magnitude 3, detected by nuclear emulsions flown to 130 km at 1480 U.T. on September 3, 1960. On the other hand, Kurnosova and co-workers[7] report an anomalously large flux of nuclei with $Z \geq 15$ associated with a Class 1$^-$ flare which occurred at 1127 U.T. on September 12, 1959. Their observations are based on two Čerenkov counters carried on the second U.S.S.R. cosmic rocket which responded to heavy particles with energies exceeding 1.5 Bev/nucleon. During the 17-minute period when the flux of $Z \geq 15$ increased about twelvefold, the fluxes of particles with $Z \geq 2$ and $Z \geq 5$ remained essentially normal.

[1]J. A. Van Allen, Bull. Am. Phys. Soc. 6, 276 (1961).

[2]H. Yagoda, Geophysical Research Note No. 54, Air Force Cambridge Research Laboratories, Bedford, Massachussets, March, 1961 (unpublished).

[3]H. Yagoda, Proceedings of the Second International Space Science Symposium, Florence, Italy, April 10-14, 1961 (to be published).

[4]H. Yagoda and N. Kaplan, Phys. Rev. 73, 634 (1948).

[5]K. Fukui and H. Yagoda, Bull. Am. Phys. Soc. 6, 276 (1961).

[6]C. E. Fichtel and D. E. Guss, Phys. Rev. Letters 6, 495 (1961).

[7]L. V. Kurnosova, L. A. Razorenov, and M. L. Fradkin, Priroda (Moscow) 1, 94-96, January, 1961.

EVIDENCE FOR A π-π RESONANCE IN THE $I=1$, $J=1$ STATE*

A. R. Erwin, R. March, W. D. Walker, and E. West

Brookhaven National Laboratory, Upton, New York and University of Wisconsin, Madison, Wisconsin

(Received May 11, 1961)

Since the earliest data became available on pion production by pions, certain features have been quite clear. The main feature which is strongly exhibited above energies of 1 Bev is that collisions are preferred in which there is a small momentum transfer to the nucleon.[1] This is shown by the nucleon angular distributions which are sharply peaked in the backward direction. These results suggest that large-impact-parameter collisions are important in such processes. The simplest process that could give rise to such collisions is a pion-pion collision with the target pion furnished in a virtual state by the nucleon. The quantitative aspects of such collisions have been discussed by a number of authors. Goebel, Chew and Low, and Salzman and Salzman[2] discussed means of extracting from the data the π-π cross section.

Holladay and Frazer and Fulco[3] deduced from electromagnetic data that indeed there must be a strong pion-pion interaction. In particular, Frazer and Fulco deduced that there probably was a resonance in the $I=1$, $J=1$ state. A qualitative set of π-p phase shifts in the 400-600 Mev[4] region were used by Bowcock et al.[5] to deduce an energy of about 660 Mev in the π-π system for the resonance. The work of Pickup et al.[6] showed an indication of a peak in the π-π spectrum at an energy of about 600 Mev.

The present experiment was designed to explore the π-π system up to an energy of about 1 Bev. The π^- beam was produced by the external proton beam No. 1 at the Cosmotron. A suitable set of quadrupole and bending magnets focussed the pion beam on a Hevimet slit about 10 ft from the Adair-

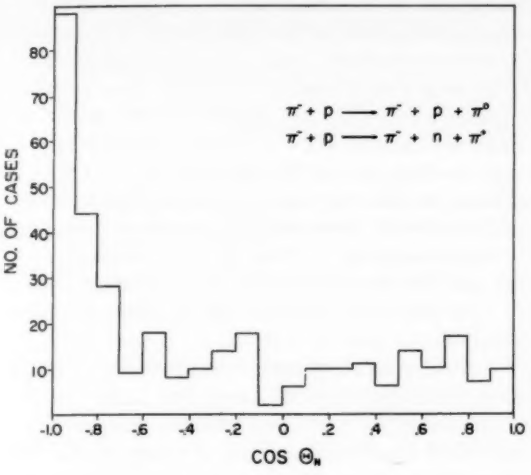

FIG. 1. The angular distribution of the nucleons from the processes $\pi^- + p \rightarrow \pi^- + \pi^0 + p$ and $\pi^- + p \rightarrow \pi^- + \pi^+ + n$.

Leipuner 14-in. H_2 bubble chamber. The pions were guided into the chamber by another bending magnet. The measured momentum was 1.89 ± 0.07 Bev/c.

Events selected for measurement were taken in a fiducial volume of the chamber. The forward-going track was required to be at least 10 cm long. Measurements were made on a digitized system and the output was analyzed by use of an IBM-704. The events were analyzed by means of a program based on the "Guts" routine written by members of the Alvarez bubble chamber group.

Figure 1 shows the combined angular distribution for the nucleons from the two processes, $\pi^- + p \rightarrow \pi^- + \pi^0 + p$ and $\pi^- + p \rightarrow \pi^- + \pi^+ + n$, which appear to be identical within statistics. The results indicate a large number of events with small momentum transfer to the nucleons.

We concentrate our interest on those events with small momentum transfer since these events satisfy the qualitative criterion of being examples of π-π collisions. Somewhat arbitrarily, we center our attention on cases in which the momentum transfer to the nucleon is less than 400 Mev/c. Table I gives the ratios of the three possible final states $\pi^-\pi^+n$, $\pi^-\pi^0p$, and $\pi^0\pi^0n$, assuming the π-π scattering to be dominated, respectively, by the $I=0$, 1, 2 scattering states of the π-π system.

The experimental results in the last column indicate a strong domination by $I=1$ state. For the $I=1$ state the basic π-π scattering cross sections $\sigma(\pi^-\pi^0 \rightarrow \pi^-\pi^0)$ and $\sigma(\pi^-\pi^+ \rightarrow \pi^-\pi^+)$ are equal.

Table I. Ratios of final states.

	$I=0$	$I=1$	$I=2$	Experiment ($\Delta \leq 400$ Mev/c)
$\pi^-\pi^+n$	2	2	2/9	1.7 ± 0.3
$\pi^-\pi^0p$	0	1	1	1
$\pi^0\pi^0n$	1	0	4/9	$<0.25 \pm 0.25$

The nucleon four-momentum transfer spectrum seems to be in qualitative agreement with the theory for the process in which a π is knocked out of the cloud. Figure 2 shows ideograms for the mass spectrum of the di-pions for cases with $\Delta \leq 400$ Mev/c and $\Delta > 400$ Mev/c, where Δ is the four-momentum transfer to the nucleon. The curve for $\Delta \leq 400$ Mev/c clearly shows a peak at 765 Mev/c. In the ideogram for $\Delta > 400$ Mev/c the peak is still present but seems to be smeared to higher values of the di-pion mass, m^*. One worries that diagrams other than the one involving

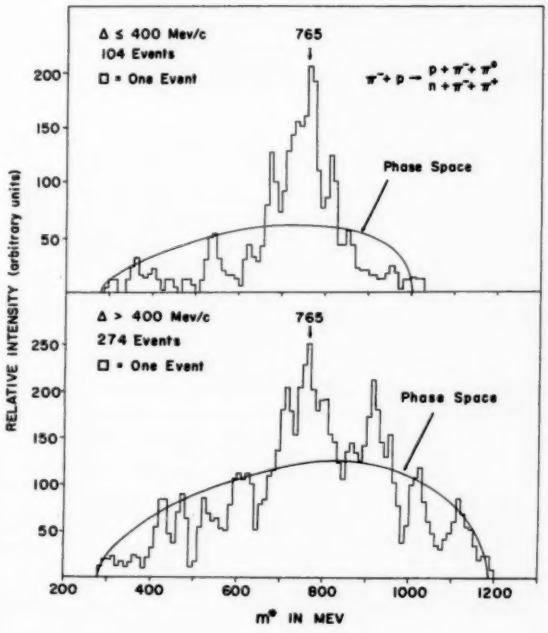

FIG. 2. The combined mass spectrum for the $\pi^-\pi^0$ and $\pi^-\pi^+$ system. The smooth curve is phase space as modified for the included momentum transfer and normalized to the number of events plotted. Events used in the upper distribution are not contained in the lower distribution.

one-pion exchange might be contributing to the observed peak in this m^* spectrum. In particular, an important contribution at lower energies comes from a diagram in which one of the π's rescatters off the nucleon and ends up in the 3-3 state with respect to the nucleon. If one restricts the data to cases with $\Delta \leq 400$ Mev/c this diagram does not seem to be very important, but if one takes cases with $\Delta > 400$ Mev/c many cases consistent with rescattering are found.

In order to deduce values of the π-π cross section, we use the formula[2]

$$\frac{d^2\sigma}{dm^* d\Delta^2} = \frac{3f^2}{\pi} \frac{\Delta^2}{(\Delta^2+1)^2} \left(\frac{m^*}{q_{iL}}\right)^2 K \bar{\sigma}_{\pi-\pi},$$

where $\bar{\sigma}_{\pi-\pi}$ is the mean of $\sigma(\pi^-\pi^0 \to \pi^-\pi^0)$ and $\sigma(\pi^-\pi^+ \to \pi^-\pi^+)$. In the above formula all momenta and energies are measured in units of pion masses. q_{iL} = momentum of the incoming pion measured in units of the pion mass. K = momentum of the pions in the di-pion center-of-mass system. Then

$$\delta\sigma = \frac{3f^2}{\pi} \left(\frac{m^*}{q_{iL}}\right)^2 K \bar{\sigma}_{\pi-\pi} \delta m^* \int_{\Delta_{\min}(m^*)}^{\Delta_{\max}} \frac{\Delta^2 d\Delta^2}{(\Delta^2+1)^2}.$$

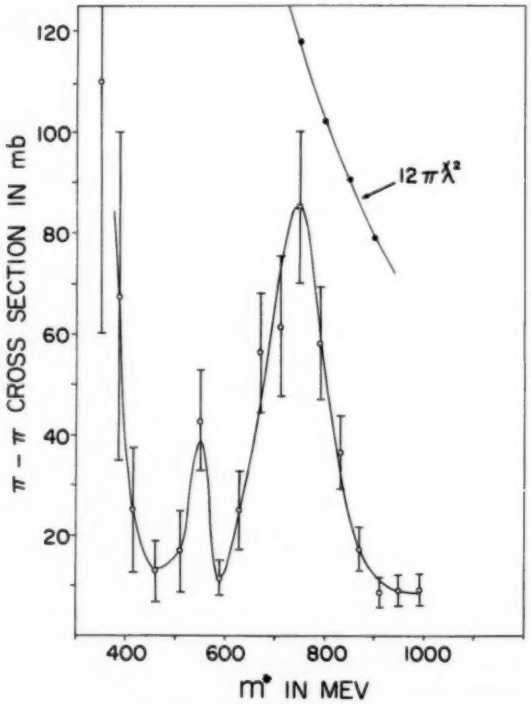

FIG. 3. The π-π cross section as deduced from cases with the four-momentum transfer less than 400 Mev/c.

The results of this calculation using the experimentally determined $\delta\sigma$'s are shown in Fig. 3. The results indicate a peak in the neighborhood of 750 Mev with a width of 150-200 Mev, which is about 3/4 of what it would be ($12\pi\lambda^2$) for a resonance in the $I=1$, $J=1$ state. Since this cross section was determined off the energy shell, it is difficult to estimate the effect of the interference of other diagrams and also the effect of line broadening.[7] Whether or not the other peak and the S-wave scattering indicated in Fig. 3 are real will have to await better statistics for verification.

We wish to acknowledge with gratitude the help and cooperation of R. K. Adair and L. Leipuner in the use of their bubble chamber, and to the latter also for his assistance in adapting the "Guts" routine to our use. We also acknowledge the help of J. Boyd, J. Bishop, P. Satterblom, R. P. Chen, C. Seaver, and K. Eggman in measuring, scanning, and tabulating. We were greatly aided by Dr. J. Ballam and Dr. H. Fechter in setting up the beam. We have had helpful conversations with Dr. R. K. Adair, Dr. C. J. Goebel, Dr. M. L. Good, and in particular Dr. G. Takeda.

---

*Work supported in part by the U. S. Atomic Energy Commission and Wisconsin Alumni Research Foundation.

[1]L. M. Eisberg, W. B. Fowler, R. M. Lea, W. D. Shephard, R. P. Shutt, A. M. Thorndike, and W. L. Whittemore, Phys. Rev. 97, 797 (1955); W. D. Walker and J. Crussard, Phys. Rev. 98, 1416 (1955).

[2]C. Goebel, Phys. Rev. Letters 1, 337 (1958); G. F. Chew and F. E. Low, Phys. Rev. 113, 1640 (1959); F. Salzman and G. Salzman, Phys. Rev. 120, 599 (1960).

[3]W. Holladay, Phys. Rev. 101, 1198 (1956); W. Frazer and J. Fulco, University of California Radiation Laboratory Report UCRL-8880, August, 1959 (unpublished).

[4]W. D. Walker, J. Davis, and W. D. Shephard, Phys. Rev. 118, 1612 (1960).

[5]J. Bowcock, N. Cottingham, and D. Lurie, Nuovo cimento 19, 142 (1961), and Phys. Rev. Letters 5, 386 (1960).

[6]E. Pickup, F. Ayer, and E. O. Salant, Phys. Rev. Letters 5, 161 (1960); Proceedings of the Tenth Annual International Conference on High-Energy Physics at Rochester (Interscience Publishers, Inc., New York, 1960); see also F. Bonsignori and F. Selleri, Nuovo cimento 15, 465 (1960).

[7]Deductions made by extrapolations seem to give different values of the cross section. Also the position of the maximum is not determined very well. J. A. Anderson, Vo. X. Bang, P. G. Burke, D. D. Carmony, and N. Schmitz, Phys. Rev. Letters 6, 365 (1961).

INELASTIC ELECTRON-DEUTERON SCATTERING AND THE ELECTROMAGNETIC STRUCTURE OF THE NEUTRON*

Loyal Durand, III
Brookhaven National Laboratory, Upton, New York
(Received April 25, 1961; revised manuscript received May 11, 1961)

Recent experiments on elastic electron-proton scattering performed at Stanford[1] and Cornell[2] have provided detailed information on the behavior of the Dirac (charge) and anomalous magnetic moment form factors F_{1p} and F_{2p} of the proton for electron 4-momentum transfers up to $q^2 = 36$ f^{-2}. Corresponding information on the form factors F_{1n} and F_{2n} of the neutron has been obtained from studies of the cross section $d^2\sigma/(d\Omega_e dE_e')$ for the inelastic scattering of electrons from the deuteron, $e + d \rightarrow e + n + p$.[3-5] Analysis of the recent Stanford data on this process, using the theoretical cross section calculated by Jankus[6] with the modifications introduced by Hofstadter and others,[7] leads to two interesting conclusions. First, F_{2n} and F_{2p}, which were thought on the basis of earlier work to be approximately equal for $q^2 \leq 10$ f^{-2},[5] were found to differ markedly for $q^2 \gtrsim 5$ f^{-2},[4] reflecting a difference in the spatial distribution of the anomalous magnetic moment in the two nucleons. Second, the Dirac form factor of the neutron F_{1n} was found to differ from zero for $q^2 \gtrsim 5$ f^{-2}, this result providing the first evidence for an extended distribution of charge in the neutron.[4] The values of the form factors F_{1n} and F_{2n} obtained from Fig. 1 of Hofstadter and Herman[4] are given in Table I for representative values of q^2. The values of F_{1n} are also shown in Fig. 1.

We wish to report in the present Letter on the marked changes in the neutron form factors which result from a reanalysis of the Stanford data on inelastic electron-deuteron scattering[4] using a theoretical cross section obtained from a completely covariant theory.[8] This work, which extends considerably the semirelativistic theory given in a previous paper,[9] is based on the techniques of dispersion relations. Calculation of the cross section $d^2\sigma/(d\Omega_e dE_e')$ is especially simple in the region of the large peak which corresponds to the quasi-elastic scattering of the electron by a single nucleon. The dominant terms in the transition amplitude then arise from single-nucleon pole terms which can be calculated exactly. Retention of these pole terms alone would correspond to the replacement of the complete deuteron wave function in the nonrelativistic theory by its asymptotic form. The largest remaining terms arise at the quasi-elastic peak from anomalous regions in the dispersion relations. The spectral functions in these regions are closely related to the short-range parts of the nonrelativistic deuteron wave function. The proximity of the single-nucleon poles to the physical region for the transition results in a relatively weak dependence of the peak cross section on the high-mass regions of the spectral functions, or alternatively, on the short-range structure of the deuteron wave function. It is consequently a good approximation to use in the dispersion relations spectral functions calculated directly from a nonrelativistic model for the wave function. The denominators in the dispersion relations may nevertheless be retained in covariant form; the usual ambiguities[7,9] with respect to the kinematics and the relativistic treatment of the deuteron wave function are thereby eliminated. We may also remark that the nucleon form factors appear

Table I. Changes in the neutron form factors F_{1n} and F_{2n} which result from changes in the theoretical peak value of $d^2\sigma/(d\Omega_e dE_e')$. The form factors with the superscript J result from an analysis of the experimental cross sections[a] based on the modified Jankus theory.[b] The form factors without superscripts are obtained when the data are reanalyzed using the present theory. The calculations were based on the method of intersecting ellipses.[c] The tabulated values of the form factors denoted by asterisks correspond to the point of closest approach[d] in those cases in which the ellipses failed to intersect.

q^2 (f^{-2})	F_{1n}^J	F_{1n}	F_{2n}^J	F_{2n}
5.1	0.16	0.09	0.76	0.75
10.0	0.12	-0.09*	0.49	0.38*
11.5	0.03	-0.11*	0.46	0.34*
15.0	0.18	-0.08*	0.40	0.28*
18.0	0.25	-0.02	0.40	0.28
21.0	0.17	0.00	0.33	0.22

[a] See footnote 13.
[b] See reference 7.
[c] See reference 4.
[d] See footnote 14.

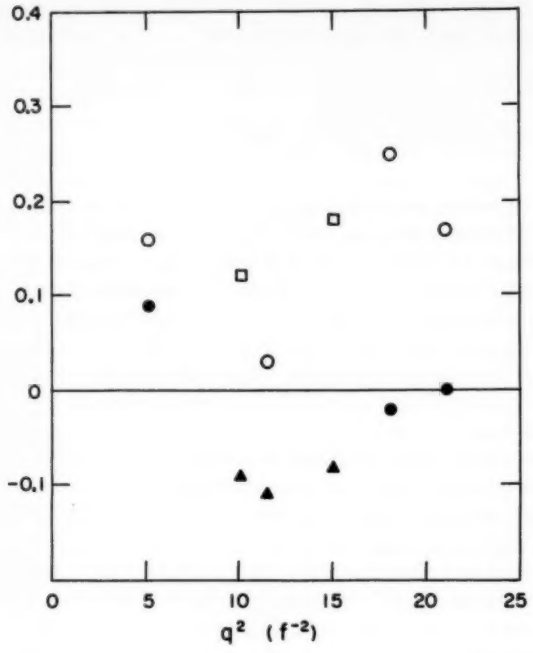

FIG. 1. Values of the Dirac form factor F_{1n} for the neutron obtained by analyzing the data of Hofstadter et al. (reference 4) by the method of intersecting ellipses using the modified Jankus result for $d^2\sigma/(d\Omega_e dE_e')$ (open circles) and the improved result of the present paper (solid circles). For the points indicated by open and solid squares, "experimental" cross sections were constructed using the smoothed values of the nucleon form factors given in Table I and footnote 13. The points indicated by solid triangles represent cases for which no intersection was obtained unless allowance was made for possible experimental errors. The uncertainty in these points is very large. It is expected that the tabulated values of F_{1n} for these points are too large in magnitude, $F_{1n} \approx 0$ being possible within the accuracy of the data.

naturally in the present theory, and are evaluated on the mass shell in the dominant pole terms. Off-mass-shell corrections have been estimated in the remaining expressions, and are thought to be small.

The cross section $d^2\sigma/(d\Omega_e dE_e')$ is well represented in the neighborhood of the quasi-elastic peak by the approximate expression:

$$d^2\sigma/(d\Omega_e dE_e') = \sigma_{\text{Mott}} m p \pi^{-1} (m/E) M(p,q)(G_n + G_p), \tag{1}$$

where

$$\sigma_{\text{Mott}} = \tfrac{1}{4}\alpha^2 E_e^{-2} \sin^{-4}(\tfrac{1}{2}\theta)\cos^2(\tfrac{1}{2}\theta), \tag{2}$$

and

$$G_i = F_{1i}^2 + (q^2/4m^2)\kappa_i^2 F_{2i}^2 + (q^2/2m^2)(F_{1i} + \kappa_i F_{2i})^2 \tan^2(\tfrac{1}{2}\theta). \tag{3}$$

Here E_e is the energy of the incident electron, θ is the electron scattering angle in the laboratory system, m is the nucleon mass, κ_n and κ_p are the anomalous parts of the nucleon magnetic moments, and p is the momentum and E the energy of either of the outgoing nucleons in their center-of-mass system. The effects on the scattering of the structure of the deuteron are contained entirely in the function $M(p,q)$.

The cross section given in Eq. (1) neglects the following: (1) the effects of interactions between the outgoing nucleons; (2) scattering involving the D-state component of the deuteron wave function; (3) small corrections involving interference between scattering by the neutron and by the proton (< 0.5% error); (4) the effects on the functions G_n and G_p of the initial Fermi momentum of the nucleons in the deuteron (< 0.5% error). The effects of final-state interactions have been calculated[8] by the methods of reference 9 using approximate final-state wave functions matched to the neutron-proton scattering phase shifts of Bryan, Signell, and Marshak,[10] and are found to decrease the peak cross section by roughly 1.5-2.5%, depending on q and θ. We have adopted as a reasonable approximation to these effects a uniform 2% decrease of the peak cross section. The D-state component of the deuteron wave function scatters less efficiently than the S-state component, and the peak cross section is decreased by an additional 3% for a large range of q when this effect is included. The function $M(p,q)$ may be shown to reduce for $q \gtrsim 1$ to the form (constant)$/p^2$ at the quasi-elastic peak. Evaluating the constant for a repulsive core wave function,[8] and incorporating the foregoing corrections, one then obtains for the peak value of $d^2\sigma/(d\Omega_e dE_e')$ only

$$[d^2\sigma/(d\Omega_e dE_e')]_{\text{peak}} = \sigma_{\text{Mott}}(4.57\times10^{-3})(1\pm0.05) \times (m^2/pE)(G_n + G_p). \tag{4}$$

The factor (1 ± 0.05) represents our estimate of the uncertainties in the theoretical cross section associated with the foregoing effects, with the contributions to the scattering of meson currents in the deuteron, and of off-mass-shell corrections to the form factors. This result is essentially equivalent in form to that given by Goldberg[11] as an approximation to his impulse-type calculations, but includes some additional corrections, and is furthermore free of the ambiguities attendant on the impulse approximation.

The results obtained from Eq. (4) differ from the peak value of the modified Jankus cross section[7] in three respects: (1) The value of the overall numerical factor 4.57×10^{-3} in Eq. (4) includes the corrections discussed above; (2) Eq. (4) contains a factor (m/E) originating in the three-body phase space which is absent in the Jankus cross section, and decreases the peak value significantly for large values of p; (3) the functions G_i are replaced in the modified Jankus cross section by functions G_i',

$$G_i' = G_i - (q^2/2m^2)F_{1i}^2 + O[(q^2/4m^2)^2].$$

The terms of order $(q^2/4m^2)^2$ in G_i' cannot be retained consistently in the nonrelativistic theory,[9] and should be omitted from the modified Jankus cross section. The appearance of the extra term $-(q^2/2m^2)F_{1i}^2$ in G_i' may be traced to an incorrect modification of the Jankus theory intended to make the peak cross section reduce for large q^2 to a sum of Rosenbluth cross sections[12] for the scattering of electrons from free nucleons. The resulting errors in the theoretical value of $d^2\sigma/(d\Omega_e dE_e')$ are quite large, especially at small scattering angles.

The effect of the foregoing results on the values of the neutron form factors F_{1n} and F_{2n} determined from the Stanford electron scattering experiments, has been investigated by reanalyzing the experimental data of Hofstadter et al.[4] for representative values of q^2. The calculations were based on the theoretical expression for the peak value of the inelastic deuteron cross section $d^2\sigma/(d\Omega_e dE_e')$ given in Eq. (4). The function G_p which appears there was evaluated when possible using the Rosenbluth cross section for elastic electron-proton scattering,[12]

$$(d\sigma/d\Omega_e)_p = \sigma_{\text{Mott}}[1 + (2E_e/m)\sin^2(\tfrac{1}{2}\theta)]^{-1}G_p, \quad (5)$$

in conjunction with experimental values of the elastic scattering cross sections.[1] This result was combined with the experimental electron-deuteron scattering cross sections of Hofstadter et al.[4,13] using Eq. (4) to obtain the Rosenbluth factor G_n for the neutron. The values of F_{1n} and F_{2n} were determined by combining values of G_n corresponding to a fixed q^2, but different energies and scattering angles, using the method of intersecting ellipses.[7] For $q^2 = 10$ f^{-2} and 15 f^{-2}, values of $d^2\sigma/(d\Omega_e dE_e')$ and $(d\sigma/d\Omega_e)_p$ at properly matched energies and scattering angles were not available in the published data. In these cases we have constructed "experimental" cross sections using the Rosenbluth and the modified Jankus theories with smoothed values of the nucleon form factors taken from references 1 and 4.[13] Corrected values of the neutron form factors were then obtained by reanalyzing these "data" using the corrected theoretical cross section of Eq. (4). We note finally that the ellipses failed in three cases [$q^2 = 10$, 11.5, and 15 f^{-2}] to intersect unless allowance was made for possible errors in the cross sections.[14] In these cases, we have determined rough values of F_{1n} and F_{2n} by choosing as the "intersection" the midpoint of the region of closest approach. It is expected from an examination of the effects of possible experimental errors that the value of F_{2n} so determined is slightly too small, and that of F_{1n}, considerably too negative. $F_{1n} \approx 0$ would be consistent with the data within the possible errors.

The results of this analysis are summarized in Table I. The corrected values of F_{1n} are in addition plotted in Fig. 1 along with the values obtained by Hofstadter et al.[4] using the modified Jankus theory. The changes in F_{1n} are quite striking. The results of Hofstadter et al.[4] suggested that this form factor was a positive increasing function for $q^2 \geq 5$ f^{-2}, with a value $F_{1n} \approx 0.2$ for $q^2 = 20$ f^{-2}. The present results favor small or zero values of F_{1n} over the entire range of q^2 which was considered. This result, if substantiated by the analysis of newer experimental data,[15] would indicate that the outer structure of the neutron is more nearly neutral than has been supposed.[3,4] The changes in F_{2n} are less striking, but range up to 30% for large values of q^2, and bring this form factor closer in magnitude to F_{2p}. A detailed analysis of the relevant data will be necessary before the variation of the neutron form factors with increasing q^2 can be specified with any assurance. We wish in particular to emphasize that the corrected values of F_{1n} and F_{2n} given in Table I are quite sensitive to changes in the cross sections $d^2\sigma/(d\Omega_e dE_e')$ and $(d\sigma/d\Omega_e)_p$, and may be altered when the results of recent ex-

periments are analyzed.[15]

The author would like to thank Professor R. R. Wilson, Professor R. Hofstadter, Dr. R. Herman, and Dr. C. deVries for valuable discussions with regard to the electron-deuteron scattering experiments, and I. Cole and E. Windschauer for computational assistance.

---

*Work performed under the auspices of the U. S. Atomic Energy Commission.

[1]F. Bumiller, M. Croissiaux, and R. Hofstadter, Phys. Rev. Letters 5, 261 (1960); R. Hofstadter, F. Bumiller, and M. Croissiaux, Phys. Rev. Letters 5, 263 (1960).

[2]R. R. Wilson, K. Berkelman, J. M. Cassels, and D. N. Olson, Nature 188, 94 (1960).

[3]D. N. Olson, H. F. Schopper, and R. R. Wilson, Phys. Rev. Letters 6, 286 (1961).

[4]R. Hofstadter, C. deVries, and R. Herman, Phys. Rev. Letters 6, 290 (1961); R. Hofstadter and R. Herman, Phys. Rev. Letters 6, 293 (1961).

[5]M. R. Yearian and R. Hofstadter, Phys. Rev. 110, 552 (1958); 111, 934 (1958). S. Sobottka, Phys. Rev. 118, 831 (1960).

[6]V. Z. Jankus, Phys. Rev. 102, 1586 (1956).

[7]R. Herman and R. Hofstadter, High-Energy Electron Scattering Tables (Stanford University Press, Stanford, California, 1960), pp. 40-45. The modified Jankus cross section as given in this reference does not include the effects of a nonvanishing Dirac form factor F_{1n} for the neutron, but the necessary modifications are easily made.

[8]L. Durand, III, Phys. Rev. (to be published).

[9]L. Durand, III, Phys. Rev. 115, 1020 (1959).

[10]P. S. Signell and R. E. Marshak, Phys. Rev. 106, 832 (1957); 109, 1229 (1958). P. S. Signell, R. Zinn, and R. E. Marshak, Phys. Rev. Letters 1, 416 (1958); R. A. Bryan, Bull. Am. Phys. Soc. 5, 35 (1960). The author is indebted to Dr. Bryan for supplying values of the neutron-proton scattering phase shifts.

[11]A. Goldberg, Phys. Rev. 112, 618 (1958). The principal advantage of the present procedure relative to the simple impulse approximation is the possibility of examining in detail such questions as the effects of binding on the current operators, the effects of final-state interactions and neutron-proton interference terms in the scattering, and of relativistic corrections involving the deuteron wave function.

[12]M. N. Rosenbluth, Phys. Rev. 79, 615 (1950).

[13]For $q^2=11.5$, 18.0, and 21.0 f^{-2}, we have used the experimental peak values of $d^2\sigma/(d\Omega_e dE_e')$ given by Hofstadter, deVries, and Herman[4] in conjunction with the experimental proton cross sections $(d\sigma/d\Omega_e)_p$ for the same scattering angles and energies given by Hofstadter, Bumiller, and Croissiaux.[1] For $q^2=5.1$, the values of $d^2\sigma/(d\Omega_e dE_e')$ interpolated from the data of Sobottka[5] by Hofstadter, deVries, and Herman[4] were combined with proton cross sections calculated from the exponential proton model of E. E. Chambers and R. Hofstadter [Phys. Rev. 103, 1454 (1956)]. This model was used by Sobottka to normalize his deuteron cross sections.[5] The cross sections for $q^2=10$ f^{-2} and 15 f^{-2} were calculated as described in the text, using smoothed values of the nucleon form factors taken from Fig. 1 of Hofstadter and Herman.[4] The values assumed for the neutron form factors $F_{1n}{}^J$ and $F_{2n}{}^J$ resulting from an analysis using the Jankus theory are given in Table I. The values assumed for the proton form factors are as follows: $q^2=10$ f^{-2}, $F_{1p}=0.48$, $F_{2p}=0.39$; $q^2=15$ f^{-2}, $F_{1p}=0.43$, $F_{2p}=0.21$.

[14]The failure of the ellipses to intersect indicates that the input data are not consistent with the theoretical form of $d^2\sigma/(d\Omega_e dE_e')$ given in Eq. (4). However, intersections could be obtained by changing either the large-angle or the small-angle deuteron cross section $d^2\sigma/(d\Omega_e dE_e')$ by 10% or less. An error in the cross sections of this magnitude is consistent with the estimated accuracy of the experiments.[1,4] Furthermore, such errors are undoubtedly present, as indicated by the deviation of the experimental values of G_n from the values calculated for the same q^2 and θ using neutron form factors taken from the smooth curve drawn through the points in reference 4. The deviations are of both signs, and range up to about 50% of G_n, but are generally smaller. Since scattering by the proton contributes on the order of $\frac{1}{2}$-$\frac{2}{3}$ of the peak deuteron cross section, depending on q^2 and θ, the corresponding errors in $d^2\sigma/(d\Omega_e dE_e')$ are reduced by factors of 2-3, and lie within the expected range. Conversely, it is clear that values obtained for G_n, hence, for the neutron form factors, can be changed significantly by rather small changes in the experimental values of $d^2\sigma/(d\Omega_e dE_e')$ and $(d\sigma/d\Omega_e)_p$.

[15]The Stanford group has recently extended its measurements of the inelastic electron-deuteron, and the elastic electron-proton scattering cross sections to a number of energies and scattering angles not previously considered, with the largest value of q^2 now 25 f^{-2}. Preliminary analyses at several of the new points suggest that F_{1n} may indeed be greater than zero, but somewhat smaller in magnitude than indicated in reference 4. [R. Hofstadter (private communication). The author is greatly indebted to Professor Hofstadter for a number of communications concerning the Stanford experiments.] The Cornell group has also extended considerably its measurements at larger values of q^2 [R. R. Wilson (private communication)].

PROTON-PROTON INTERACTION*

H. Feshbach and E. Lomon

Department of Physics and Laboratory for Nuclear Science
Massachusetts Institute of Technology, Cambridge, Massachusetts

and

A. Tubis

Department of Physics, Purdue University, Lafayette, Indiana

(Received April 12, 1961)

We have investigated the applicability of the modified boundary condition model[1,2] to the extensive proton-proton scattering data in the energy range extending up to 350 Mev. The success obtained with the model using a field-theoretical potential tail indicates at once the validity of the one- and two-pion exchange potentials (TPEP) in their appropriate range, and the physical significance of the energy-independent boundary condition employed to represent the shorter range interaction. The precision fit we have obtained requires only nine parameters plus the acceptance of the usual fourth-order static "perturbation" theory results for the potential tail.

For $r > r_0$ (r_0 is the same in all states), we assume a potential of the form

$$V = V_2 + V_4,$$

$$V_2(r) = f^2 \mu c^2 \frac{\vec{\tau}^1 \cdot \vec{\tau}^2}{3} \left[\vec{\sigma}^1 \cdot \vec{\sigma}^2 + S_{12} \left(1 + \frac{3}{\mu r} + \frac{3}{(\mu r)^2} \right) \right] \frac{e^{-\mu r}}{\mu r},$$

$$V_4(r) = f_1^4 \mu c^2 \left[-\left(\frac{2M\lambda}{\mu} \right)^2 \frac{6}{\pi (\mu r)^2} K_1(2\mu r) + \left(\frac{2M\lambda}{\mu} \right) 6 \left(\frac{1+\mu r}{(\mu r)^2} \right)^2 e^{-2\mu r} - R_1(\mu r) + \vec{\sigma}^1 \cdot \vec{\sigma}^2 R_2(\mu r) + S_{12} R_3(\mu r) \right], \tag{1}$$

where

$$R_1(x) = \frac{2}{\pi} \left\{ \vec{\tau}^1 \cdot \vec{\tau}^2 \left[\frac{12}{x^2} + \frac{23}{x^4} K_1(2x) + \left(\frac{4}{x} + \frac{23}{x^3} \right) K_0(2x) \right] + \xi (3 - 2\vec{\tau}^1 \cdot \vec{\tau}^2) \left[\left(\frac{1}{x^2} + \frac{4}{x^3} + \frac{4}{x^4} \right) K_1(x) + \left(\frac{1}{x} + \frac{2}{x^2} + \frac{2}{x^3} \right) K_0(x) \right] e^{-x} \right\},$$

$$R_2(x) = \frac{2}{\pi} \left\{ -\left[\left(\frac{8}{x^2} + \frac{12}{x^4} \right) K_1(2x) + \frac{12}{x^3} K_0(2x) \right] + \tfrac{2}{3} \xi (3 - 2\vec{\tau}^1 \cdot \vec{\tau}^2) \left[\left(\frac{1}{x^2} + \frac{2}{x^3} + \frac{2}{x^4} \right) K_1(x) + \left(\frac{1}{x^2} + \frac{1}{x^3} \right) K_0(x) \right] e^{-x} \right\},$$

$$R_3(x) = \frac{2}{\pi} \left\{ \left[\left(\frac{4}{x^2} + \frac{15}{x^4} \right) K_1(2x) + \frac{12}{x^3} K_0(2x) \right] - \tfrac{1}{3} \xi (3 - 2\vec{\tau}^1 \cdot \vec{\tau}^2) \left[\left(\frac{1}{x^2} + \frac{5}{x^3} + \frac{5}{x^4} \right) K_1(x) + \left(\frac{1}{x^2} + \frac{1}{x^3} \right) K_0(x) \right] e^{-x} \right\}.$$

f and f_1 are the dimensionless rationalized pseudovector coupling constant, and are approximately $(0.08)^{1/2}$ when evaluated from meson scattering. We distinguish the numerical values of f and f_1 in order to test separately the significance of V_2 and V_4. μ and M are the pion and nucleon masses, respectively. A variable "pair suppression" is provided by the parameter λ. We shall call ξ the "ladder" parameter. The other operators and functions are standard. $\hbar = c = 1$.

For $f_1^2 = f^2$ and $\xi = 1$, V is the TMO potential.[3] For $\xi = 0$ we have the BW potential.[4] Thus the terms proportional to ξ represent the contribution of the iterated (ladder) second-order diagram to the fourth-order potential which has been the subject of so much controversy.[5] It should be noted that pair suppression ($\lambda < 1$) is a nonperturbative result (or at best comes from high-order terms) but is usually included in the perturbative potentials. No spin-orbit term has been included, as both the phenomenological evidence[6] and the theory[7] indicate a very short range behavior. On the basis of earlier results[1,2] the boundary radius r_0 is expected to include the spin-orbit region. The phase shifts and the corresponding experimental uncertainties, as listed in Table I, were taken from Breit et al.[8] and from effective-range parameters. Only 0, 95, 210, and 310 Mev were fitted in the expectation that the results for intermediate energies would interpolate well.

Starting with Coulomb functions at $r = 8$ f, the wave functions at each energy were numerically integrated inwards (on the IBM-709 at M.I.T.) to r_0, for a set of "potential parameters" r_0, f_1^2, λ, and ξ. For some runs f^2 was fixed at 0.08; for others we set $f^2 = f_1^2$ and they were varied together. At r_0, the logarithmic derivative of the wave function $F_{Jls} = r_0[(1/\psi_{Jls})d\psi_{Jls}/dr]_{r=r_0}$ was evaluated. For coupled states,[7] F is a 2×2 Hermitian matrix,

$$\begin{pmatrix} F_{J,J-1,1} & F_J^{\,c} \\ F_J^{\,c*} & F_{J,J+1,1} \end{pmatrix}.$$

At zero energy the scattering length, a_0, was used to determine the asymptotic $^1S_0$ wave function, which was then integrated inward to obtain F_{000}(0 Mev). The singlet effective range r_{eff}(calc)

Table I. Model parameters at minimum.

$f^2 = f_1^2 = 0.0837$; $r_0 = 0.7011$ f; $\lambda = 1.00$; $\xi = 0.50$; $M = 11.10$; $(M_0 = 14)$

Jls	Energy (Mev)	δ (radians)[a]	$\Delta\delta$ (radians)	F	ΔF	$\bar{F}$
000	0	b		1.02	0.06	
	95	0.419	0.026	1.15	0.07	
	210	0.087	0.026	1.05	0.08	
	310	-0.175	0.044	1.12	0.14	1.08
220	95	0.068	0.012	1.63	4.43	
	210	0.140	0.017	3.66	2.39	
	310	0.192	0.017	3.25	0.94	3.14
011	95	0.209	0.044	-7.33	2.42	
	210	-0.035	0.061	-7.14	2.06	
	310	-0.209	0.035	-8.65	1.55	-7.82
111	95	-0.209	0.009	10.11	6.37	
	210	-0.364	0.017	17.34	12.36	
	310	-0.480	0.026	15.21	9.70	13.37
211	95	0.168	0.009	0.11	0.46	
	210	0.311	0.017	-0.78	0.35	
	310	0.291	0.017	-0.19	0.12	-0.26
$J=2$ coupling[c]	95	-0.279	0.070	-0.14	0.17	
	210	0.131	0.035	0.13	0.16	
	310	-0.105	0.035	0.03	0.14	0.01
231	95	-0.003	0.008	-4.04	0.05	
	210	0.003	0.026	-3.98	0.09	
	310	0.017	0.017	-4.43	0.27	-4.06
331	95	-0.026	0.052	-3.04	115.74	
	210	-0.039	0.017	-3.34	0.73	
	310	-0.062	0.017	4.31	55.29	-3.24

[a] Nuclear Blatt-Biedenharn phase shifts.
[b] $a_0 = -7.7 \pm 0.1$ f; $r_{\text{eff}}(\text{exp}) = 2.67 \pm 0.03$ f; $r_{\text{eff}}(\text{calc}) = 2.68$ f.
[c] For δ read the nuclear Blatt-Biedenharn coupling parameter ϵ_2.

was then calculated directly from F_{000} and the potential parameters.

The F_{Jls} so obtained were in general energy dependent and r_{eff}(calc) did not agree with r_{eff}(exp). The potential parameters were then varied to make the f's as energy-independent as possible and to bring r_{eff}(calc) into agreement with r_{eff}(exp). To do this in a statistically significant way, utilizing the experimental uncertainties in the phase shifts $\Delta\delta_{Jls}$ and in the effective-range parameters Δa_0 and Δr_{eff}(exp), the function

$$M = \sum_{JlsE}\left(\frac{F_{Jls}(E) - \bar{F}_{Jls}}{\Delta F_{Jls}(E)}\right)^2 + \left(\frac{r_{eff}(\text{calc}) - r_{eff}(\text{exp})}{\Delta r_{eff}(\text{exp})}\right)^2$$

was calculated and then minimized (using a gradient search) with respect to the potential parameters.

$$\bar{F}_{Jls} = [\textstyle\sum_E F_{Jls}(E)/\Delta F_{Jls}(E)]/\sum_E[\Delta F_{Jls}(E)]^{-1}$$

is the weighted average of the F_{Jls} at all different energies. $\Delta F_{Jls}(E) = (\partial F_{Jls}/\partial\delta_{Jls})\Delta\delta_{Jls}$, where the $\Delta\delta_{Jls}$ are the experimental uncertainties from Table I. Note that $(\partial F/\partial\delta)^{-1}$ measures the sensitivity of δ to F. Those δ's in the sum in (2) which are insensitive to F have a reduced relative importance.

The most probable value of M, corresponding to 50% correlation probability, M_0, is given by the number of phase shifts less the number of F_{Jls} less the number of potential parameters. Counting the relevant states and energies, as seen in Table I, $M_0 = 14$. $M_0 < 14$ implies that if one puts $F = \bar{F}$ at all energies, the corresponding phase shifts will usually lie within their experimental limits. The word "usually" is meant in its appropriate statistical sense.

Equation (2) neglects the effect of correlations between the phase-shift errors because they are difficult to take into account numerically. The effect of including the correlations in M is usually to decrease its value. Thus a "good fit" remains a good fit while a "bad fit" may become a "good fit" if the correlations are very strong. Thus our criterion suffices for an acceptable potential but can only weakly reject one. However, if $M \gg M_0$ an unusual set of correlations would be required to make the potential acceptable. We intend to inquire further into the effect of correlations.

With $f^2 = 0.08$, a minimum of $M = 10.73$ was obtained for $f_1^2 = 0.0863$, $\lambda = 1.000$, $\xi = 0.500$, and $r_0 = 0.7011$ f. With $f^2 = f_1^2$, a minimum of $M = 11.10$ was obtained for $f^2 = f_1^2 = 0.0837$ and no change in the other parameters. The values of the $\bar{F}_{Jls}$, F_{Jls}, ΔF_{Jls}, and r_{eff}(calc) corresponding to the latter case are given in Table I. The values for r_0 and $\bar{F}_{000}$ are very similar to those obtained previously for special forms of the modified boundary condition model.[2]

It is highly significant that the best fit is obtained for the coupling constant determined by pion-nucleon data,[9] $f^2 \approx f_1^2 \approx 0.082$. A variation of $f_1^2 = f^2$ of about 0.002 would increase M by unity. Previous OPEP analysis[10] had determined that $f^2 \simeq 0.08$ was required for the higher angular momenta. We see at once a similar result for the TPEP region and for lower angular momenta, but not independently of the model for the internal region. However, if this model was not a significant description of the scattering, it would be expected that $M \gg M_0$. The parameters λ and ξ fall within the expected range. The sensitivity to λ and ξ is small however. Varying ξ between 0 and 1 only increases M to 12. This is presumably due in part to the negligible difference between TMO and BW in the singlet even state. Putting $\lambda = 0$ while the other potential parameters remain unchanged makes $M = 58$. If we then minimize holding $\lambda = 0$, we obtain $M = 24.8$, but require $f^2 = f_1^2 = 0.093$. This complete pair suppression is not consistent with our model, especially if we require $f^2 \approx f_1^2 \approx 0.08$.

There is then a strong statistical indication of the quantitative correctness of the fourth-order p-p static potential within limits of the order of the size of the "ladder" contribution. Conversely the energy-independent boundary condition is a statistically satisfactory representation of the inner region. If the fourth-order perturbation static potential is accepted on theoretical grounds for $r > r_0$, then the parameters given by the $\bar{F}$'s and r_0 are sufficient to account for all the scattering data. This is a much smaller number of parameters than those inherent in previous proposed phenomenological potentials.[6] The fact that $r_0 = 0.7$ f indicates that the TPEP approximation breaks down at this distance and implies the onset of nonlocal or energy-dependent effects. In more conventional representations the short-range spin-orbit potential has the same implication.

For $l > 3$ the phase shifts are independent of

F_{Jls} except for a very narrow range which gives rise to a sharp resonance.[11] Thus these phase shifts can in general be considered to depend only on TPEP. For example, a test of TPEP independent of the boundary condition can be made by examining the ΔF's for high angular momenta at low energy.[12] The extremely large value of $\Delta F_{331} \times (95\ \text{Mev})$ is such a verification of TPEP, and the decrease of ΔF_{220} with increasing energy is also significant.

The following calculations are now in progress: (1) The phase shifts for higher l are being evaluated with our potential to further test TPEP. (2) The phase shifts at interpolating energies are being calculated. (3) The nonperturbative potentials KMO[13] and Klein-McCormick[14] are also being tried in place of Eq. (1). (4) The neutron-proton phase-shift data[15] are under analysis employing the modified boundary condition model with the potential forms used in the p-p analysis. Here the triplet even potential depends strongly on the ladder ambiguity so that one may hope to obtain a better value of ξ.

The above extensions of the analysis will be published elsewhere together with a more detailed discussion of the method and results of this paper. We conclude from the present analysis that the field-theoretic fourth-order static potential combined with an energy-independent boundary condition is a simple and accurate, physically significant representation of the data.

We are grateful to the IBM-709 staff and in particular to Miss M. Wirt.

*This work is supported in part by the U. S. Atomic Energy Commission, the Office of Naval Research, and the Air Force Office of Scientific Research.

[1]A. Tubis, Massachusetts Institute of Technology thesis, 1959 (unpublished). See also T. C. Griffith and E. A. Power, Nuclear Forces and the Few Nucleon Problem (Pergamon Press, New York, 1960), p. 83 ff.

[2]E. Lomon and M. Nauenberg, Bull. Am. Phys. Soc. 3, 183 (1958), and Nuclear Phys. (to be published). D. P. Saylor, R. A. Bryan, and R. E. Marshak, Phys. Rev. Letters 5, 266 (1960).

[3]M. Taketani, S. Machida, and S. Ohnuma, Progr. Theoret. Phys. (Kyoto) 6, 683 (1951); 7, 45 (1952).

[4]K. A. Brueckner and K. M. Watson, Phys. Rev. 92, 1032 (1953).

[5]A. Klein, Progr. Theoret. Phys (Kyoto) 20, 257 (1958).

[6]J. L. Gammel and R. M. Thaler, Phys. Rev. 107, 291 (1957); R. A. Bryan, Nuovo cimento (to be published).

[7]E. Butkov, Nuovo cimento 13, 809 (1959); C. K. Iddings and P. M. Platzman, Phys. Rev. 120, 644 (1960).

[8]G. Breit et al., Phys. Rev. 120, 2227 (1960). The numbers chosen correspond closely to the fit labeled YLAM in this reference.

[9]J. Hamilton and W. S. Woolcock, Phys. Rev. 118, 291 (1960).

[10]M. H. MacGregor, M. J. Moravcsik, and H. P. Stapp, Phys. Rev. 116, 1248 (1959). G. Breit et al., Phys. Rev. Letters 4, 79 (1960).

[11]H. Feshbach and E. Lomon, Phys. Rev. 102, 891 (1956).

[12]G. Breit et al., Phys. Rev. Letters 6, 138 (1961).

[13]M. Konuma, H. Miyazawa, and S. Otsuki, Progr. Theoret. Phys. (Kyoto) 19, 17 (1958).

[14]A. Klein and B. H. McCormick, Progr. Theoret. Phys. (Kyoto) 20, 876 (1958).

[15]G. Breit et al. (private communication).

CONSEQUENCES OF A SCALAR $\Sigma\Lambda\pi$ COUPLING

Jeremy Bernstein*† and Reinhard Oehme‡
Institute for Theoretical Physics, University of Vienna, Vienna, Austria
(Received May 2, 1961)

It is the purpose of this note to point out some new experimental and theoretical possibilities which follow from the assumption that the relative $\Sigma\Lambda$ parity is odd.[1] Using a crude dispersion-theoretic estimate of the scalar $\Sigma\Lambda\pi$-coupling constant, we discuss the rates for the decay processes $\Sigma^{\pm} \to e^{\pm} + \nu + \Lambda^0$ and $\Sigma^0 \to \gamma + \gamma + \Lambda^0$, and we remark briefly upon some other consequences of a possibly strong scalar $\Sigma\Lambda\pi$ coupling.

Let us begin with the evaluation of the constant $g_{\Sigma\Lambda\pi}$. Because the $\Sigma\Lambda$ parity is odd, the Σ can be considered as a composite $\Lambda\pi$ system in an s state.[2] The s-wave amplitude for $\pi\Lambda$ scattering, which is defined by $f_0(s) = q^{-1}(s) \sin\delta_0(s) \times \exp i\delta_0(s)$, with $q^2(s) = (4s)^{-1}[s - (m_\Lambda + m_\pi)^2] \times [s - (m_\Lambda - m_\pi)^2]$, has a pole at $s = m_\Sigma{}^2$. The residue of this pole may be expressed in terms of $g_{\Sigma\Lambda\pi}$; we find

$$f_0(s) = \frac{g_{\Sigma\Lambda\pi}{}^2}{4\pi} \frac{(m_\Sigma + m_\Lambda)^2 - m_\pi{}^2}{2m_\Sigma} \frac{1}{m_\Sigma{}^2 - s} + \text{other (nonpole) terms.} \quad (1)$$

In order to make a simple first approximation, let us assume that $f_0[s(q)]$ is a regular function of the c.m. momentum q, except for the Σ pole at $q = q(s = m_\Sigma{}^2) \equiv i\kappa \approx i(2m_{\text{red}}B)^{1/2}$. From the unitarity condition we find

$$f_0(s) = \frac{-\kappa + iq(s)}{q^2(s) + \kappa^2}. \quad (2)$$

If we compute the residue[3] of the pole at $s = m_\Sigma{}^2$ from Eq. (2) and compare the result with Eq. (1), we obtain[4]

$$\frac{g_{\Sigma\Lambda\pi}{}^2}{4\pi} \approx \frac{16 m_\Sigma{}^5 \kappa}{[(m_\Sigma + m_\Lambda)^2 - m_\pi{}^2][m_\Sigma{}^4 - (m_\Lambda{}^2 - m_\pi{}^2)^2]} \approx 1.8. \quad (3)$$

How good is this "zero-range" approximation? Presumably the most important correction is due to the Σ pole in the crossed reaction, the residue of which is again determined by $g_{\Sigma\Lambda\pi}{}^2$. For the s-wave amplitude $f_0(s)$, the relevant contribution from this pole appears in the form of a short logarithmic branch cut,[5]

$$(m_\Lambda{}^2 - m_\pi{}^2)^2/m_\Sigma{}^2 \le s \le 2m_\Lambda{}^2 + 2m_\pi{}^2 - m_\Sigma{}^2. \quad (4)$$

Preliminary estimates seem to indicate that the effect of this branch line is to increase the value (3) of the coupling constant. Aside from the $\pi\Sigma$ and $\bar{K}N$ thresholds for $s > (m_\Lambda + m_\pi)^2$, we have also left out the circular branch line $|s| = m_\Lambda{}^2 - m_\pi{}^2$, which is due to the intermediate pion states of the reaction $\pi + \bar{\pi} \to \Lambda + \bar{\Lambda}$. This neglect seems to be reasonable, provided there are no low-mass two-pion resonances with $T = 0$.

In what follows we make the working assumption that the scalar coupling constant is of the order one, say $g_{\Sigma\Lambda\pi}{}^2/4\pi = 1.5$. As a first application, we estimate the rate for the decay $\Sigma^- \to \Lambda^0 + e^- + \bar{\nu}$ on the basis of several assumptions.

We assume that the strangeness-conserving vector current is conserved. Therefore we may neglect the vector contribution to the decay rate since the $\Sigma\Lambda$ transition has $\Delta T \neq 0$. The vector part vanishes in the allowed approximation in accordance with the selection rule $\Delta T = 0$. If the vector current is not conserved, one would expect that its over-all contribution amounts to an increase of the total decay rate.

The matrix element of the axial vector current may be written in the form (noting the assumption of odd $\Sigma\Lambda$ parity),

$$\langle \Lambda | P_\alpha | \Sigma^- \rangle = \tfrac{1}{\sqrt{2}} \bar{u}_\Lambda [\gamma_\alpha a(-p^2) - ip_\alpha b(-p^2) + \sigma_{\alpha\beta} p_\beta c(-p^2)] u_\Sigma, \quad (5)$$

where $p = p_\Sigma - p_\Lambda$, and $a(0) = G_A{}'$ is the corresponding renormalized axial coupling constant. The coefficients in Eq. (5) are real analytic functions which are regular in the complex p^2 plane except for the branch lines[6] $-p^2 \ge (3m_\pi)^2$ and, in the case of $b(-p^2)$, the pion pole at $-p^2 = m_\pi{}^2$. We assume that in the neighborhood of the interval $0 < -p^2 \le (m_\Sigma - m_\Lambda)^2$ the function $(m_\Sigma - m_\Lambda)a(-p^2) - p^2 b(-p^2)$ is dominated by this pion pole. By well-known methods we find the relation[7]

$$(1/\sqrt{2}) G_A{}' = g_{\Sigma\Lambda\pi} F(m_\pi{}^2)/(m_\Sigma - m_\Lambda), \quad (6)$$

where $F(m_\pi{}^2)$ is determined by the pion lifetime. We may compare Eq. (6) with the Goldberger-Treiman formula for nuclear β decay. Denoting the usual axial vector coupling constant by G_A,

we can write

$$G_A'/G_A = (g_{\Sigma\Lambda\pi}/\sqrt{2}\, g_{NN\pi})[2m_N/(m_\Sigma - m_\Lambda)].$$

According to our zero-range calculation we may take $g_{\Sigma\Lambda\pi}^2/g_{NN\pi}^2 \approx 1/10$ and find $G_A'/G_A \approx 6$. We assume that in the region of interest the function $a(-p^2)$ is slowly varying so that $a(-p^2) \approx G_A'$; then we obtain

$$b(-p^2) \approx G_A'(m_\Sigma - m_\Lambda)/(m_\pi^2 + p^2). \quad (8)$$

In the computation of the decay rate for $\Sigma^- \to \Lambda^0 + e^- + \bar{\nu}$, we can neglect the b term in Eq. (5) because its contribution becomes proportional to the electron mass. The c term in Eq. (5) is difficult to estimate; it is unlikely to make a very large contribution, and we neglect it. With these assumptions, the rate is given in terms of our constant G_A' by the "allowed" β-decay formula,

$$\Gamma_{\Sigma^- \to \Lambda^0 + e^- + \bar{\nu}} = (G_A'^2/60\pi^3)(m_\Sigma - m_\Lambda)^5. \quad (9)$$

We compare this decay rate with the experimental rate for the strangeness-changing process $\Sigma^- \to n + e^- + \bar{\nu}$, which is taken to be about 1/10 of the rate obtained from a straightforward calculation using the universal constant. With our value $G_A' \approx 6G_A$ we find $\Gamma_{\Sigma^- \to \Lambda^0 + e^- + \bar{\nu}}/\Gamma_{\Sigma^- \to n + e^- + \bar{\nu}} \approx 1/10$, a number which is about 30 to 40 times larger than one would predict on the basis of phase-space considerations. This larger rate is a reflection of the renormalization effects due to the rather large scalar $\Sigma\Lambda\pi$ coupling. We believe that, as far as our approximations are concerned, we have consistently underestimated this effect. We note that the states $|\bar{\Sigma}^-\Lambda^0\rangle$ and $|\Sigma^+\bar{\Lambda}^0\rangle$ are related by G conjugation. If the current P_α is such that it transforms like $\bar{n}\gamma_\alpha\gamma_5 p$ under G conjugation, then we have $G_A'(\Sigma^- \to \Lambda^0 + e^- + \bar{\nu}) = -G_A'(\Sigma^+ \to \Lambda^0 + e^+ + \nu)$. Consequently, within our approximations, the rate for the decay $\Sigma^+ \to \Lambda^0 + e^+ + \nu$ should be the same as that for the Σ^- decay.

We hope that there will soon be enough data on β decays of Σ hyperons to make possible a serious test of our considerations.[8]

It has been mentioned by Okun and Rudik[9] that for odd $\Sigma\Lambda$ parity an intermediate π^0 state may play an important role in the calculation of the process $\Sigma^0 \to \Lambda^0 + \gamma + \gamma$. Since we propose a rather large value for the scalar $\Sigma\Lambda\pi$ coupling, it seems reasonable to estimate the rate on the basis of this contribution. We have

$$\Gamma_{\Sigma^0 \to \Lambda^0 + \gamma + \gamma} = (4/945)(1/\pi)(g_{\Sigma\Lambda\pi}^2/4\pi)\Gamma_{\pi^0 \to 2\gamma} + \text{magnetic terms},$$

and with a π^0-decay rate[10] of 0.3×10^{16} sec^{-1} we see that, even for $g_{\Sigma\Lambda\pi}^2/4\pi \approx 10$, the rate for the decay $\Sigma^0 \to \Lambda^0 + \gamma + \gamma$ is negligible compared to that for the decay $\Sigma^0 \to \Lambda^0 + \gamma$, which may be of the order of 10^{19} sec^{-1}. The "magnetic terms" have been discussed in reference 9; they do not change the situation.

A strong, scalar $\Sigma\Lambda\pi$ coupling gives rise to a corresponding spin-independent two-pion exchange force between Λ and N. Spin-dependent forces must have a somewhat shorter range because they require the exchange of three pions or a K meson.

Finally we would like to remark that a large value of $g_{\Sigma\Lambda\pi}$ may well give rise to a $J = 1/2$ resonance in the $\pi\Lambda$ system.[11]

It is a pleasure to thank Professor R. Karplus and Professor W. E. Thirring for stimulating conversations.

---

*Permanent address: Brookhaven National Laboratory, Upton, New York.

†National Science Foundation Post-Doctoral Fellow.

‡Permanent address: Enrico Fermi Institute for Nuclear Studies, University of Chicago, Chicago, Illinois.

[1]For a discussion of arguments in favor of odd $\Sigma\Lambda$ parity, as well as for references to the relevant papers, see Y. Nambu and J. J. Sakurai, Phys. Rev. Letters 6, 377 and 506(E) (1961). See also S. Barshay and M. Schwartz, Phys. Rev. Letters 4, 618 (1960).

[2]S. Barshay and M. Schwartz (reference 1).

[3]M. L. Goldberger, Y. Nambu, and R. Oehme, Ann. Phys. 2, 226 (1957); this paper contains an analogous determination of the residue of the deuteron pole in np scattering.

[4]A similar determination of $g_{\Sigma\Lambda\pi}$ has been made by Nambu and Sakurai, reference 1. Essentially, these authors evaluate the pole term in Eq. (1) at threshold and equate it to $-\kappa^{-1}$. It is easily seen from Eq. (2) that the extrapolation to $q = 0$ gives rise to a factor $\frac{1}{2}$ in the expression for $g_{\Sigma\Lambda\pi}^2/4\pi$.

[5]It should be noted that the branch line (4) corresponds to a force with maximal range $r_0 = (2m_\pi)^{-1}$. This is because, for systems of two particles with unequal mass, the "force range" should be determined from the position of the left-hand singularities in the q^2 plane. The branch line (4) lies inside the circle $|s| = m_\Lambda^2 - m_\pi^2$; it is mapped into the second sheet of the q^2 plane and determines the weight function along the cut $-m_\Lambda^2 \leq q^2 \leq -m_\pi^2$ [see R. Oehme, Phys. Rev. Letters 4, 246 (1960)]. The upper limit of this branch line corresponds to a range $r_0 = (2m_\pi)^{-1}$.

[6]We have $\langle 0|\partial_\alpha P_\alpha|2\pi\rangle = 0$ if we assume that $\partial_\alpha P_\alpha$ transforms like the pion field under G conjugation. Note that this requires that P_α contains the $\Sigma\Lambda$ terms in the combination $\bar{\Lambda}\gamma_\alpha\Sigma^+ - \bar{\Sigma}^-\gamma_\alpha\Lambda$.

[7]Equation (6) and related relations have been written down by many authors. See, for instance, L. Okun, J. Exptl. Theoret. Phys. (U.S.S.R.) 39, 214 (1960) [translation: Soviet Phys. – JETP 12, 154 (1961)];

J. Bernstein, S. Fubini, M. Gell-Mann, and W. Thirring, Nuovo cimento 17, 757 (1960); Chou Kuang-Chao, Dubna Report D514, 1960 (unpublished); these papers contain further references. It is the purpose of this note to use Eq. (6) in order to produce a number for the decay rate.

[8]It may be that some of the observed $\Sigma\beta$ events are due to $\Sigma \to \Lambda + e + \nu$; it will be difficult to separate $\Sigma\Lambda$ events from $\Sigma\pi$ events unless the Λ decay is seen.

[9]L. Okun and A. Rudik, J. Exptl. Theoret. Phys. (U.S.S.R.) 39, 378 (1960) [translation: Soviet Phys. - JETP 12, 268 (1961)].

[10]R. F. Blackie et al., Phys. Rev. Letters 5, 384 (1960).

[11]F. Duimio and G. Wolters, Nuovo cimento (to be published) and CERN preprint.

POSSIBLE MECHANISM FOR THE PION-NUCLEON SECOND RESONANCE

Ronald F. Peierls*

Department of Mathematical Physics, The University, Birmingham, England

(Received February 17, 1961)

Several phenomenological models[1] have been proposed to discuss pion-nucleon interactions near the higher resonances. There seems to be considerable evidence from these analyses that final states described by the 33 isobar model[2] play an important role, but so far there has been little quantitative discussion or explanation of the resonant peaks. In the present note it is shown that a simple model can give a good quantitative description of the second resonance, a rough description of the third, and a plausible explanation of the peak above 1.0 Bev. The model consists in taking seriously the concept of the 33 isobar as an unstable particle (N^*) of spin and isospin $\frac{3}{2}$ and having a complex mass. This means that we assume the low-energy pion-nucleon scattering to be dominated by the one N^* direct pole. The position and width of the 33 resonance then enable us to find the mass of the isobar $M(N^*)$:

$$[M(N^*)]^2 = M^2 + i\Delta,$$
$$M = 8.94\,\mu_\pi, \quad |\Delta| = 8.05\,\mu_\pi{}^2, \tag{1}$$

where μ_π is the pion mass.

We consider next the reaction

$$\pi + N \to \pi + N^*. \tag{2}$$

This is strongly coupled to the process

$$\pi + N^* \to \pi + N^*. \tag{3}$$

Let us try to apply the usual formalism to reaction (3), pion-isobar scattering. For the moment we ignore the spin and isospin and assume that the reaction is described by some amplitude $A(s, \bar{s}, t)$ where s, $\bar{s}$, t are defined in terms of the pion energy ω, the real part E of the isobar energy, and the center-of-mass momentum and scattering angle q, θ:

$$s = (E+\omega)^2 + i\Delta(1+\omega/E),$$
$$\bar{s} = (E+\omega)^2 - 2q^2(1+\cos\theta) + i\Delta(1-\omega/E),$$
$$t = -2q^2(1-\cos\theta),$$
$$s + \bar{s} + t = 2M^2 + 2\mu_\pi{}^2 + 2i\Delta. \tag{4}$$

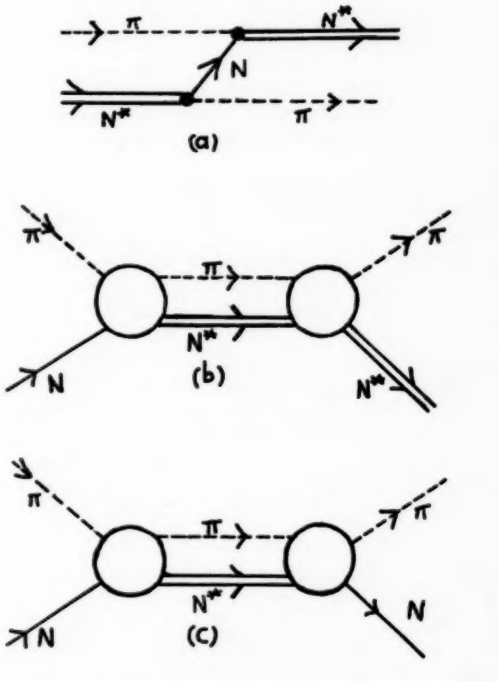

FIG. 1. (a) Crossed one-nucleon diagram for πN^* scattering. (b) Schematic coupling between πN^* scattering and πN^* production in πN collisions. (c) Schematic coupling between πN^* production and πN scattering.

The amplitude A should have a pole whenever s, $\bar{s}$, or t is equal to the mass of a possible intermediate particle. The term represented by Fig. 1(a) has the unusual feature that if $\Delta = 0$, it becomes infinite in the physical region for q, θ. The explicit contribution of this term may be taken empirically to be

$$A_0 = g^2/(\bar{s} - m^2), \tag{5}$$

where m is the nucleon mass and g is the "coupling constant" for the $NN^*\pi$ vertex[3] (determined by the π-N cross section at the 33 resonance). We can rewrite this as

$$A_0(W,\theta) = \frac{g^2}{(W^2 - W_0^2) + i\Delta(1 - \omega/E) - 2q^2(1 - \cos\theta)},$$
$$W_0^2 = 2M^2 + 2\mu_\pi^2 - m^2. \tag{6}$$

The resulting total transition probability is

$$f(W) = \int_{-1}^{+1} |A_0|^2 d\cos\theta$$
$$= \frac{g^4}{2q^2\Delta_1} \tan^{-1}\left(\frac{4q^2\Delta_1}{\Delta_1^2(W^2 - W_0^2)(W^2 - W_0^2 - 4q^2)}\right),$$
$$\Delta_1 = |\Delta|(1 - \omega/E). \tag{7}$$

This is a sharply energy-dependent effect and behaves like a resonance. This interaction is coupled to the πN inelastic scattering [reaction (2)] as indicated in Fig. 1(b) and hence, by unitarity, to the elastic scattering, Fig. 1(c). If the effect is sufficiently strong, it should produce an appreciable contribution to the total πN cross section at pion energies T_π corresponding to the center-of-mass energies W where $f(W)$ is large. Figure 2 shows f plotted as a function of T_π and compared with the experimental results on πN scattering.[4] The agreement with the position and width of the second resonance (N^{**}) in π-N scattering seems very good, in view of the fact that there are no free parameters in the model.

Let us consider the effects of spin and isospin. In the energy range in question, $2q^2 < |\Delta|$; hence we may, as a rough approximation, ignore the θ dependence of $A_0(W,\theta)$ in (6). In other words, the amplitude should contribute mainly to the s state. The only effect of taking account of the spin is to introduce several amplitudes A_i each having some angular factor $\gamma_i(\theta)$ in the numerator. But if the θ dependence of the denominator is not important, this results in multiplying $f(W)$ by some weakly energy-dependent factor, and does not change the main features of the result. Thus, we can say that this effect, looking like a "resonance" in the

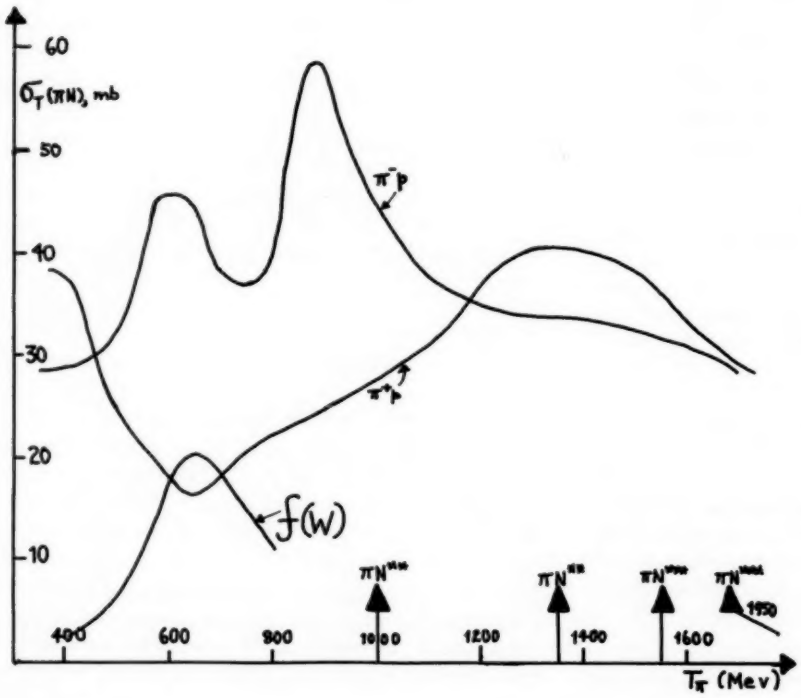

FIG. 2. The function $f(W)$ plotted as a function of the pion lab energy T_π required to produce a total energy W in the center-of-mass system. The approximate positions of the πN^{**} and πN^{***} resonances are also shown and these theoretical predictions are compared with the experimental results for the total cross sections for πN scattering.

s-wave π-N^* scattering, should produce a strong effect in the $(\frac{3}{2}-)$ state of the π-nucleon scattering via the reaction of Fig. 1(b).[5] The isotopic spin dependence is not so clear; however, the contribution of A_0 to the $T=\frac{1}{2}$ state and $T=\frac{3}{2}$ state have opposite signs and the interference of these two contributions with the (appreciable) background may be constructive and destructive, respectively. This might even lead to a dip, rather than a peak, in the π^+p cross section.

The physical interpretation of the mechanism discussed above is easily understood. The isobar, being unstable, can decay into a pion and a nucleon which subsequently absorbs another pion. This [Fig. 1(a)] represents a real process (apart from the finite isobar lifetime) and it is not surprising that it should show up in the physical region. The same phenomenon should be possible whenever an unstable isobar interacts with one of its decay products and may be the explanation of the "resonance" in $\bar{K}N$ scattering due to the possible inelastic excitation of a πY^* state (Y^* being the $\pi\Lambda$ isobar whose mass lies below the $\bar{K}N$ threshold).[6]

The mechanism described corresponds to an s-wave πN^* interaction. The p wave can be studied in the static limit by the conventional effective-range theory which leads to predicted resonances in the $(\frac{1}{2}\ \frac{5}{2}+)$ and $(\frac{3}{2}\ \frac{3}{2}+)$ states. These are the states suggested by Wong and Ross,[7] who consider essentially the iteration of Fig. 1(a), but carry out the calculation in the static-nucleon, rather than static-isobar limit. (The mechanism discussed here does not occur in either static limit.) The third π-N "resonance" (N^{***}) near 900 Mev can be interpreted as the manifestation of these p-wave resonances.

Lastly, the arguments leading to the prediction of N^{**} can be applied to possible πN^{**} and πN^{***} interactions, with intermediate single-nucleon or N^* states, giving rise to four expected peaks in π-N interactions in the energy range indicated in Fig. 2. The situation is much more complex in this energy region, but this may be a partial explanation of the observed broad peak in the πN cross section above 1 Bev.

The model presented here is only approximate; it would be desirable to study it more quantitatively, in particular taking proper account of the spins and of the coupling between the various channels. Further work along these lines is being carried out and will be reported later.

I am very grateful to J. E. Paton for many valuable discussions during the course of this work and wish to acknowledge many stimulating comments and suggestions from L. Castillejo, D. J. Thouless, Professor R. E. Peierls, and Professor S. Mandelstam.

---

*NATO Research Fellow.

[1]L. Landovitz and L. Marshall, Phys. Rev. Letters 4, 474 (1960); H. A. Bethe and P. Carruthers, Phys. Rev. Letters 4, 536 (1960); R. F. Peierls, Phys. Rev. 118, 325 (1960); R. F. Peierls, Phys. Rev. Letters 5, 166 (1960).

[2]S. J. Lindenbaum and R. M. Sternheimer, Phys. Rev. 106, 1107 (1957).

[3]If a one-level formula is assumed for the 33 resonance; then both g^2 and Δ are proportional to the width, so that even if $\Delta \to 0$ the cross section never becomes infinite.

[4]P. Falk-Vairant and G. Valladas, Proceedings of the 1960 Annual International Conference on High-Energy Physics at Rochester (Interscience Publishers, Inc., New York, 1960).

[5]If we assume maximum inelasticity for this reaction, this fixes $\sigma_{\text{total}}(\pi N; J=\frac{3}{2}-) = 4\pi\lambda^2$ which is the normalization used in Fig. 2.

[6]Reported at the Berkeley Conference on Strong Interactions, December, 1960 (unpublished). I am grateful to Professor S. Mandelstam for bringing the $\bar{K}N$ resonance to my attention.

[7]W.-N. Wong and M. Ross, Phys. Rev. Letters 3, 398 (1959). Y. Tomozawa (to be published) has also calculated N^* scattering in the static N^* limit but he discarded the nucleon poles which give rise to the effects considered here.

SCATTERING MATRIX APPROACH TO THE Λ-π RESONANCE*

K. C. Wali, T. Fulton, and G. Feldman
The Johns Hopkins University, Baltimore, Maryland
(Received May 1, 1961)

Recently Dalitz[1] interpreted the Λ-π resonance[2] as a bound state of the $\bar{K}$-N system. His method made use of concepts familiar in low-energy nuclear physics. He was able to obtain the position and width of the resonance independent of the relative Σ-Λ parity.

We attempt, here, to analyze the data involving the three channels $\bar{K}N$, $\Sigma\pi$, $\Lambda\pi$, in the $I=1$ state in the total energy range $m_\Lambda + m_\pi$ to $m_N + m_K$ by means of an effective-range theory derived from a dispersion approach (analogous to the Chew-Low[3] approximation in the one-channel case). If we assume that the Σ-Λ relative parity is odd, and Λ-K odd, we find that there can exist a resonance in the $I=1$, $J=(\frac{1}{2}-)$ state and we can fit all of the known data to a reasonable set of renormalized coupling constants. A similar approach has been used by Amati et al.[4] for the case of even Σ-Λ parity. They include only the π-Λ and π-Σ channels and establish the possibility of a resonance in the $J=(\frac{3}{2}+)$ state. Since the actual position of the resonance is closer (but below) the $\bar{K}N$ threshold than it is to the $Y\pi$ threshold, one might expect (as Dalitz has observed) that the $\bar{K}N$ channel is important.

We next present a brief outline of our method of calculation.

It was shown by Matthews and Salam[5] and by Feldman, Matthews, and Salam[6] that by confining oneself only to the two-particle channels of the S matrix, one can express the unitarity condition nonrelativistically as

$$\mathrm{Im}(T_J^{-1})_{if} = -k_i \delta_{if}, \tag{1}$$

where T_J^{-1} is the inverse of the open-channel T matrix defined in MS,[7] and k_i is the c.m. momentum in the ith channel. The analytic continuation of T_J^{-1} below threshold of one of the channels is easily accomplished.[5] Dispersion relations for the T_J^{-1} matrix elements were postulated in FMS. We use here a modified version of these relations in order to take into account properly the symmetry of T_J^{-1}.

For the case of $J=(\frac{1}{2}-)$, odd Σ-Λ parity, and neglecting terms of order ω/M, Δ/M, where ω is the c.m. energy of the π meson and Δ is the Σ-Λ mass difference, the dispersion relations reduce to the approximate form[8] ($T_{1/2-}^{-1} \equiv T^{-1}$)

$$T_{if}^{-1}(\omega) = B_{if}^{-1}(\omega) + \frac{C_i(\omega)}{\pi}\int_{m_i}^{\infty} \frac{C_i^{-1}(\omega')\,\mathrm{Im}\,T_{if}^{-1}(\omega')}{\omega' - \omega}\,d\omega'. \tag{2}$$

$B^{-1}(\omega)$ is the inverse of the Born approximation matrix in terms of the renormalized coupling constants $g_{N\pi}$, $g_{\Sigma\pi}$, $g_{\Lambda\pi}$, $g_{\Sigma K}$, and $g_{\Lambda K}$. All of the Born matrix elements have a single or double pole at $\omega=0$. $C_i(\omega)$ is a diagonal matrix defined in such a way that

$$T(\omega) \to B(\omega) \text{ as } \omega \to 0. \tag{3}$$

The constant m_i is the physical threshold value for ω in each channel. We estimate that the errors introduced by our approximations are of the order of 10-30% in the energy region of interest.

We now examine the matrix elements obtained from Eq. (2) to see if they give rise to resonance phenomena. In order to do this we make use of certain general properties[8] which are satisfied at resonance. The open-channel K matrix is defined as

$$(T_J^{-1}(\omega))_{if} = (K_J^{-1}(\omega))_{if} - ik_i\delta_{if}, \tag{4}$$

where of course these matrices (T_J^{-1}, K_J^{-1}) are the inverses of the open-channel parts of the T_J and K_J matrices, respectively. The condition for a resonance at $\omega=\omega_\gamma$ is

$$\det K^{-1}(\omega_\gamma) = 0. \tag{5}$$

If a resonance exists at $\omega=\omega_\gamma$ for the $(\Lambda\pi, \Sigma\pi)$ system, then

$$\Gamma_\Lambda/\Gamma_\Sigma = \lim_{\omega\to\omega_\gamma}\left(\frac{k_\Lambda K_{\Lambda\Lambda}}{k_\Sigma K_{\Sigma\Sigma}}\right), \tag{6}$$

$$\Gamma_\Lambda = \lim_{\omega\to\omega_\gamma}\left[k_\Lambda(\omega_\gamma - \omega)K_{\Lambda\Lambda}\right], \tag{7}$$

and

$$\Gamma = \Gamma_\Lambda + \Gamma_\Sigma, \tag{8}$$

where Γ_Λ is the partial $\Lambda\pi$ width and Γ is the full width at half-maximum. $K_{\Lambda\Lambda}$ and $K_{\Sigma\Sigma}$ are the elastic $\Lambda\pi$ and $\Sigma\pi$ K-matrix elements.

The conditions (5) through (8), when applied to the elements obtained from Eq. (2), lead to implicit equations involving the four unknown coupling constants $g_{\Lambda\pi}$, $g_{\Sigma\pi}$, $g_{\Lambda K}$, and $g_{\Sigma K}$ (g). Another relation involving the coupling constants is obtained by setting

$$T_{KK}=A \tag{9}$$

at the $\bar{K}N$ threshold, where A is the complex scattering length defined by Dalitz and Tuan.[9] We have searched for reasonable values of the coupling constants ($g/g_{\pi N}<1.5$) which would lead to the following experimental results[1,2]:

$$\omega_\gamma=2\mu, \quad A=(-1.06+0.2i) \text{ fermis},$$

$$\Gamma_\Lambda/\Gamma_\Sigma>1.5, \quad \Gamma<50 \text{ Mev}.$$

The best known data are for ω_γ and A. Fixing ω_γ at 2μ,[10] we can use Eq. (5) to determine one of the unknown coupling constants in terms of the other three. For A within its quoted experimental error,[1] we find that the constant $g_{\Sigma K}{}^2/4\pi$ is almost uniquely determined to be 1.6 for a wide range of the others:

$$0\leq g_{\pi\Lambda}{}^2/4\pi\leq 5.1; \quad 5.1\leq g_{\pi\Sigma}{}^2/4\pi\leq 32;$$

$$1.3\leq g_{K\Lambda}{}^2/4\pi\leq 32.$$

The demand that we fit ω_γ and A also leads to a narrow width, namely $\Gamma\sim 11$ Mev. If we allow A to have a somewhat larger real part, we obtain the following values for the coupling constants:

$$g_{\pi\Lambda}{}^2/4\pi=5.1, \quad g_{\pi\Sigma}{}^2/4\pi=32.0,$$

$$g_{\Lambda K}{}^2/4\pi=11.5, \quad g_{\Sigma K}{}^2/4\pi=2.1,$$

and the following experimental fits:

$$A=-1.50+0.24i, \quad \Gamma_\Lambda/\Gamma_\Sigma=3.4, \quad \Gamma=38 \text{ Mev}.$$

It is gratifying that the scalar coupling constants $g_{\Lambda\pi}{}^2/4\pi$ and $g_{\Sigma K}{}^2/4\pi$ are a good deal smaller than the pseudoscalar constant $g_{N\pi}{}^2/4\pi$. They are somewhat larger than those obtained by Ferrari and Fonda,[11] using criteria based on hypernuclear physics data, and by Nambu and Sakurai,[12] who treat the Σ as a bound $\pi\Lambda$ system. The fact that the ΣK coupling constant is almost uniquely determined seems to support Dalitz's contention that the $\bar{K}N$ channel is most important in determining the properties of this resonance. In fact, if we neglect the $\bar{K}N$ channels altogether, we find it impossible to fit the resonance data using our method.

We have also briefly examined the $J=(\frac{1}{2}-)$ case for even Σ-Λ parity. In this case the Born approximation matrix elements have no poles near $\omega=0$. This is analogous to the S-wave π-N scattering where we know that the Chew-Low approximation does not explain the results.

From our results, we conclude that a resonance in the $J=(\frac{1}{2}-)$ state can be explained in terms of odd Σ-Λ parity, whereas it would be difficult to understand in terms of even Σ-Λ parity.

In a future publication we intend to present our calculations in greater detail, report on a more refined search program, and present other predictions near thresholds.

We would like to thank Mrs. Doris Ellis and Mr. M. Nussbaum for assisting with the computations.

---

*Work supported in part by the National Science Foundation and the Office of Scientific Research.

[1] R. H. Dalitz, Phys. Rev. Letters 6, 239 (1961).

[2] M. H. Alston, L. W. Alvarez, P. Eberhard, M. L. Good, W. Graziano, H. K. Ticho, and S. J. Wojcicki, Phys. Rev. Letters 5, 520 (1960); O. Dahl, N. Horwitz, D. H. Miller, J. J. Murray, and P. G. White, Phys. Rev. Letters 6, 142 (1961).

[3] G. F. Chew, M. L. Goldberger, F. E. Low, and Y. Nambu, Phys. Rev. 106, 1337 (1957); G. F. Chew and F. E. Low, Phys. Rev. 101, 1570 (1956).

[4] D. Amati, A. Stanghellini, and B. Vitale, Nuovo cimento 13, 1143 (1959).

[5] P. T. Matthews and A. Salam, Nuovo cimento 13, 381 (1959), hereafter referred to as MS.

[6] G. Feldman, P. T. Matthews, and A. Salam, Nuovo cimento 16, 549 (1960), hereafter referred to as FMS.

[7] In the one-channel case, $T_J{}^{-1}=k(\cot\delta_J-i)$.

[8] A more detailed discussion will be the subject of a future publication. In writing a relation of the type of Eq. (2), we seek to satisfy the following properties: unitarity in the physical region, symmetry of the T matrix, and the condition $T\to B$ at the poles of B.

[9] R. H. Dalitz and S. F. Tuan, Ann. Phys. 8, 100 (1959).

[10] The value of the resonance energy has been rounded off. Neglect of the Λ-Σ mass difference makes the precise value of ω_γ to be used somewhat ambiguous in any case.

[11] F. Ferrari and L. Fonda, Nuovo cimento 9, 842 (1958).

[12] Y. Nambu and J. J. Sakurai, Phys. Rev. Letters 6, 377 (1961).

ERRATA

NEW SOLID PHASE IN He^4. J. H. Vignos and H. A. Fairbank [Phys. Rev. Letters 6, 265 (1961)].

The last factor in Eq. (1) should read $(\Delta V_{\alpha,\gamma}/\Delta V_{\gamma,l})$ instead of $(\Delta V_{\gamma,l}/\Delta V_{\alpha,\gamma})$.

LOSS OF C^{11} FROM PLASTIC FOILS AND ITS EFFECT ON CROSS-SECTION MEASUREMENTS. J. B. Cumming, A. M. Poskanzer, and J. Hudis [Phys. Rev. Letters 6, 484 (1961)].

The authors' attention has been called to a paper on the loss of activity from betatron-irradiated samples by diffusion, by H. Fuchs and K. H. Lindenberger, Nuclear Instruments and Methods 7, 219 (1960), which previously reported the same effect for C^{11} produced by a (γ,n) reaction. Their results and ours obtained for C^{11} produced by (p,pn) and $(n,2n)$ reactions are in good agreement which indicates that the effect is not very sensitive to the means of producing C^{11}.

ABSTRACTS

In this section are printed the abstracts of Articles that have been forwarded to The American Institute of Physics for publication in THE PHYSICAL REVIEW. In quoting information obtained from this section before the appearance of the corresponding Article, reference should be made to "Physical Review (to be published)" rather than to this Journal.

ELECTRIC-FIELD-INDUCED ANISOTROPIES IN AN INHOMOGENEOUS PLASMA. Lewis Wetzel, Brown University, Providence, Rhode Island (Received February 21, 1961; revised manuscript received May 1, 1961).

It is shown on the basis of the Boltzmann equation that in the absence of a dc magnetic field, an electric field alone can produce anisotropies in electron diffusion and conductivity in a weak inhomogeneous plasma. These anisotropies have their origin in the ac component of the electron density resulting from the interaction between the electric field and electron density gradients. Electron diffusion is reduced in the direction of the field, while the induced ac current acquires an additional component in the direction of the gradient of the ac electron density. This component will in general lie in a direction different from that of the exciting field. Although these effects are usually small, they may become significant under suitable circumstances.

ION MOTION IN SUPERFLUID LIQUID HELIUM UNDER PRESSURE. Lothar Meyer, Institute for the Study of Metals, University of Chicago, Chicago, Illinois, and F. Reif, Department of Physics, University of California, Berkeley, California (Received March 17, 1961).

Recent investigations of superfluidity by a study of the mobilities of ions in liquid He II have been extended to the liquid under pressure. At a fixed temperature the positive-ion mobility decreases appreciably as the pressure is increased, particularly at low temperatures. At a fixed pressure the mobility increases less rapidly with decreasing temperature at higher pressures. The negative-ion mobility, smaller than that of the positive ion at zero pressure, becomes equal to that of the latter above 7 atm. In high electric fields and at high pressures the drift velocity of the negative ions approaches a limiting value roughly equal to the Landau critical velocity for a body moving through the superfluid. The theory, which discusses the mobility in terms of ion scattering by rotons and phonons, is reviewed. It is pointed out that previously neglected effects concerned with the importance of small-angle scattering of the ion ought to be taken into account; some earlier estimates of scattering cross sections are revised accordingly. It is then shown that this theory, making use only of the known change of the roton dispersion relation with pressure, can account quantitatively for the observed pressure dependence of the positive-ion mobilities.

RADIATION IN A PLASMA. I. ČERENKOV EFFECT. Marshall H. Cohen,* Observatoire de Meudon, Seine et Oise, France (Received March 27, 1961).

We start with the linearized plasma equations containing an isotropic pressure term, plus extra source terms $\vec{J}^S$ and ρ^S in the Maxwell equations. The fields of $(\vec{J}^S, \rho^S)$ can be decomposed into two modes. The electromagnetic (EM) mode has all the magnetic field and no charge accumulation; it is the ordinary EM field of $(\vec{J}^S, \rho^S)$ in a dispersive medium of relative dielectric constant $\epsilon_r = 1 - (\omega_p/\omega)^2$. The plasma ($P$) mode has all the charge accumulation and no magnetic field; at great distances from the source it becomes a longitudinal (radial) plasma wave with the usual dispersion relation for plane plasma waves. Various potentials for the EM and P modes are given by the inhomogeneous Klein-Gordon equation.

The fields of a uniformly moving charged particle are found by a Lorentz transformation. When $(u/v_0) < 1$ (u = particle velocity, v_0 = rms thermal velocity) the EM and P fields are exponentially screened outside oblate spheroids foreshortened in the direction of motion. When $(u/v_0) > 1$ the field exists only within the Mach (Čerenkov) cone trailing the particle. The frequency and angular spectra of the Čerenkov radiation are found, and the total radiated energy is found by assuming an arbitrary high-frequency cutoff due to Landau damping. The expression for total radiated energy agrees with that given by Pines and Bohm, except for the logarithmic terms.

*On leave from Cornell University, Ithaca, New York.

SELF-CONSISTENT PAIR INTERACTION FOR MANY-FERMION SYSTEM. Katuro Sawada* and Toshio Soda, University of California, La Jolla, California (Received August 15, 1960).

The equations which determine the one-particle energy and effective two-body interaction in an interacting Fermi gas are constructed within the approximation which sums up all pair creation-annihilation processes. The equation corresponds to the familiar equation for the K matrix which represents the interaction between particles (or holes) and sums up the particle-particle (or hole-hole) scattering processes. The method of the equation of motion is used in this paper. Our result for the one-particle energy is shown to lead to the result previously obtained by Quinn and Ferrell, and by Rockmore for the case of the electron gas with Coulomb interactions, when we replace screened potentials by bare potential in the self-consistent energy equation. For nuclear matter, it is shown that the presence of an attractive interaction in the equation of motion for number density causes an "enhancement" of exchange forces, whereas in the electron gas repulsive Coulomb interactions lead to "screening" of the exchange force. The strength of the isospin density interaction pseudopotential is enhanced by a factor of two when one solves the self-consistent equation; and a simple estimate shows that the Goldhaber-Teller mode lies about 15% higher than the value $p_F q/m$, previously estimated by Glassgold et al. (q: momentum of the oscillation, p_F: Fermi momentum).

*On leave of absence from Tokyo University of Education, Tokyo, Japan.

LATTICE ANHARMONICITY AND OPTICAL ABSORPTION IN POLAR CRYSTALS. II. CLASSICAL TREATMENT IN THE LINEAR APPROXIMATION. A. A. Maradudin, Westinghouse Research Laboratories, Pittsburgh, Pennsylvania, and R. F. Wallis, U. S. Naval Research Laboratory, Washington, D. C. (Received March 24, 1961).

An expression for the elements of the dielectric susceptibility tensor for an ionic crystal has been derived in a manner analogous to that employed by Kubo in his treatment of magnetic susceptibility. In the high-temperature (classical) limit, this expression reduces to the Laplace transform of the autocorrelation function of the single normal coordinate which interacts directly with the external radiation field. We have applied this formalism to the calculation of the high-temperature linear optical absorption coefficient of an anharmonic ionic crystal for which we have retained only cubic anharmonic terms in the lattice Hamiltonian. We have solved directly for the Laplace transform of the autocorrelation function to lowest order in the anharmonic coupling constant by solving the equations of motion for the normal coordinates after they have been linearized. The linear absorption coefficient obtained from the susceptibility tensor is of Lorentzian form with a frequency-dependent damping constant which varies linearly with temperature. The absorption coefficient for a diatomic linear chain with nearest neighbor interactions has been evaluated.

RECOIL-FREE RESONANT ABSORPTION IN Au^{197}. D. A. Shirley and M. Kaplan, Lawrence Radiation Laboratory and Department of Chemistry, University of California, Berkeley, California, and P. Axel, Physics Department, University of Illinois, Urbana, Illinois (Received March 27, 1961).

The Mössbauer absorption in Au has been measured at 4°K for the 77-kev gamma ray emitted by Au^{197} nuclei embedded in gold, platinum, stainless steel, iron, cobalt, and nickel. In each case, a Doppler-shift curve was measured to find the effective width and the chemical shift. The recoil-free fractions, f, are obtained with the aid of a straightforward analysis, which incidentally shows the errors that can be made in f if the chemical shift and effective width are not taken into account. The observed recoil-free emission fractions were found to be approximately 0.06(Au), 0.34 and 0.14(Pt), 0.24(steel), 0.32(Fe), 0.27(Co), and 0.35(Ni). The relative f values are correct; the correct absolute f values might require a multiplicative correction factor that could be as small as 0.53.

Relatively large f values were obtained when the Au^{197} radioactive nuclei were in high Debye-temperature lattices composed of light nuclei. Particularly low f values were found when the largest radiation-damage effects were expected.

The observed chemical shifts were (in units of 10^{-6} ev) < 0.13(Au), 0.26(Pt), 1.3(steel), 1.4(Fe), 1.3(Co), and 1.1(Ni). These chemical shifts give information more directly interpretable than, but related to, the optical-isotope and isomer shifts,

and the Knight shift; the magnitudes of the shifts measure directly either the depletion or the enhancement of electron density at the radioactive nuclei in the different lattices.

Zeeman splittings of the nuclear energy levels caused by local magnetic fields at Au had relative magnitudes of 1.0:0.43:<0.10 for Fe, Co, and Ni lattices. If the magnetic moment of the 77-kev excited state in Au^{197} is 1.6 nm, the local magnetic fields in Fe and Co were 282 and 122 koe, respectively.

LATTICE DISTORTION DUE TO ISOTOPES IN SOLID HELIUM. P. G. Klemens and A. A. Maradudin, Westinghouse Research Laboratories, Pittsburgh, Pennsylvania (Received March 17, 1961).

Observations of the thermal resistivity of solid helium containing He^3 isotopes have indicated that the phonon scattering cross section of the isotope is three times larger than the theoretical value obtained by one considering only the mass difference. Using as a model a helium atom in the potential well formed by its neighbors, and taking account of the zero-point energy of that atom and of the strain energy in the surrounding solid when the atomic cell is expanded, it is shown that around a He^3 isotope the lattice suffers an outward distortion of about 1-2%. This distortion can account for the discrepancy in the phonon scattering cross section.

MAGNETIC PROPERTIES OF $HCrO_2$ AND $DCrO_2$. R. G. Meisenheimer and J. D. Swalen, Shell Development Company, Emeryville, California (Received March 13, 1961).

Magnetic susceptibility measurements and electron paramagnetic resonance measurements have been made on powdered chromous acid ($HCrO_2$) and deuterated chromous acid ($DCrO_2$). The Curie constants, derived from the susceptibility results, are consistent with three unpaired electrons associated with each chromium ion. In addition, a large Curie-Weiss θ temperature, indicating a strong exchange interaction, is necessary to account for the results. The most unusual feature of this particular exchange is that it is strongly influenced by deuteration.

The electron paramagnetic resonance spectra also show strongly exchange-narrowed lines with a variation between $HCrO_2$ and $DCrO_2$. From a comparison between the calculated and observed linewidths and second moments, a value of the zero-field splitting is estimated.

Although no transition has been observed to an antiferromagnetic state, the Curie-Weiss θ temperatures indicate that the ground state is undoubtedly antiferromagnetic for both $HCrO_2$ and $DCrO_2$. Superexchange through the intervening proton or deuteron is probably the main source of any antiferromagnetic exchange coupling. Some of the various mechanisms proposed for superexchange are discussed in relation to chromous acid.

ABSORPTION SPECTRA OF TRANSITION IONS IN CdS CRYSTALS. R. Pappalardo and R. E. Dietz, Bell Telephone Laboratories, Murray Hill, New Jersey (Received March 21, 1961).

The low-temperature optical absorption spectra of single crystals of wurtzite CdS containing impurity ions of the first transition series and one rare earth ion, ytterbium, were studied in the range of 4.5 to 0.4 μ. The main features of the spectra were found to be in good agreement with a cubic crystal field model, while structure found in the spectral bands of nickel and cobalt impurities could be described by a simple, first-order treatment using the free ion spin-orbit coupling constants. The relevant crystal field parameters, the site symmetry, and the formal charges of the impurity ions were determined where possible.

RECOVERY OF ELECTRON RADIATION DAMAGE IN n-TYPE InSb. F. H. Eisen, Atomics International, a division of North American Aviation, Incorporated, Canoga Park, California (Received March 22, 1961).

The production and recovery of electron radiation damage in n-type InSb has been studied by means of Hall coefficient and electrical conductivity measurements. Irradiations were performed mainly at 80°K, since no recovery was observed between 4°K and 80°K. The damage recovered in five well-defined stages with the recovery nearly complete at 320°K. Isochronal and isothermal recovery was monitored in each of the stages, allowing a determination of the activation energies for recovery and a study of

the recovery kinetics. None of the recovery kinetics fit any simple models. There is evidence that the two lowest temperature recovery stages involve the annihilation of close interstitial-vacancy pairs and that interactions of primary defects with impurities do not occur. However, the first-order kinetics expected for close-pair recovery is not explicitly observed. A possible explanation for the observed kinetics, involving the independent annihilation of two types of close-pair configurations in the same stage with an electrostatic interaction between the interstitial and vacancy, is proposed.

LATTICE ABSORPTION BANDS IN SiC. Lyle Patrick and W. J. Choyke, Westinghouse Research Laboratories, Pittsburgh, Pennsylvania (Received March 29, 1961).

Using four phonon energies, $TA = 0.045$, $LA = 0.067$, $TO = 0.0955$, and $LO = 0.1055$ ev, it is possible to explain, as summation bands, the ten absorption bands lying in the energy range 0.130 to 0.300 ev. Phonon energies close to three of the four given here have been obtained by an analysis of the indirect interband absorption in SiC.

REFLECTION OF NOBLE GAS IONS AT SOLID SURFACES. Homer D. Hagstrum, Bell Telephone Laboratories, Murray Hill, New Jersey (Received March 22, 1961).

A method has been developed for distinguishing the reflection of ions at solid surfaces as ions or as metastable atoms. Results are given for He^+, Ne^+, and Ar^+ ions incident on clean W, Mo, and Si(100) and on contaminated W, Hf, and Ge(111) surfaces. The reflection coefficient of ions to ions (R_{ii}) is found to be small (0.0004 to 0.002) and essentially independent of incident ion energy. The reflection coefficient of ions to metastable atoms (R_{im}) is found to increase with ion energy from values comparable to R_{ii} at 10 ev to values as high as 0.04 at 1000 ev. Discussion of these results is given in terms of the known resonance and Auger transitions which can occur near a solid surface for ions of sufficiently large ionization energy. It is shown that the results can be accounted for only if ions are transformed to metastable atoms very close to the surface and a possible mechanism for this process is proposed.

EFFECT OF HYDROSTATIC PRESSURE ON IONIC CONDUCTIVITY IN DOPED SINGLE CRYSTALS OF SODIUM CHLORIDE, POTASSIUM CHLORIDE, AND RUBIDIUM CHLORIDE. C. Ballard Pierce,* Department of Physics, University of Illinois, Urbana, Illinois (Received January 30, 1961; revised manuscript received May 8, 1961).

The effect of hydrostatic pressure up to 9000 kg/cm^2 on ionic conductivity in NaCl, KCl, and RbCl single crystals doped with divalent impurities has been studied over the temperature range 200°C to 500°C. The conductivity in this temperature range is due almost entirely to the motion of extrinsic cation vacancies. The activation volume, ΔV_m, for motion of the cation vacancies is 7.7 ± 0.5 cc/mole in NaCl doped with $CaCl_2$ and 7.0 ± 0.5 cc/mole in KCl doped with $SrCl_2$. The results are in fair agreement with values predicted on the basis of Keyes's empirical expression relating activation volume to activation energy and isothermal compressibility. Sample materials were chosen with the view of testing for a correlation between activation energy and shear modulus. The small shear modulus in KCl and RbCl decreases with increasing pressure, while the reverse is true for NaCl. However, the data are not adequate to draw definite conclusions about such a correlation. The conductivity of RbCl doped with $BaCl_2$ increases by an order of magnitude at the phase transition from the NaCl to the CsCl structure. At 300°C, the transition occurs at 6100 kg/cm^2.

*Now at Sandia Corporation, Albuquerque, New Mexico.

PHOTOSENSITIVE-ULTRASONIC PROPERTIES OF CADMIUM SULFIDE. Harmon D. Nine, General Motors Research Laboratories, Warren, Michigan, and Rohn Truell, Brown University, Providence, Rhode Island (Received January 9, 1961).

Ultrasonic attenuation in single crystals of CdS has been observed to be a function of light irradiation. Two distinct types of behavior have been observed. Some crystals (type A) show a decrease of attenuation with white light application,

and others (type B) show an increase of attenuation with white light. The ultrasonic attenuation and the conductance of the crystals were measured as a function of temperature. An excellent correlation between the conductance and the ultrasonic attenuation is evident for type B cyrstals. A strong correlation between the directional piezoelectric properties of CdS and the ultrasonic attenuation in both types of CdS is also shown. An interaction between conduction electrons and stress waves coupled by the piezoelectric property of CdS is isolated as the dominant mechanism for the photosensitive ultrasonic attenuation in CdS of type B. Two or more competing effects appear to be responsible for the type A photosensitive attenuation behavior.

LATTICE DYNAMICS OF ALPHA URANIUM. D. O. Van Ostenburg, Argonne National Laboratory, Argonne, Illinois (Received September 14, 1960).

The method developed by Begbie and Born has been applied to alpha uranium, where equations are developed which give the macroscopic elastic constants in terms of the microscopic force constants. Interactions of an atom with its first through fourth nearest neighbors are considered; these involve twelve atoms. Through symmetry considerations, nineteen atomic force constants enter into this force system. An independent determination of the force constants is required before a valid verification of the solutions can be made. However, using measured values of the nine elastic constants, two sets of force constants are evaluated, one based upon central forces and the other upon neglect of fourth nearest neighbors.

Fe^{57} MÖSSBAUER EFFECT IN Cu-Ni ALLOYS. G. K. Wertheim and J. H. Wernick, Bell Telephone Laboratories, Murray Hill, New Jersey (Received March 30, 1961).

The Mössbauer effect of Fe^{57} has been used to study the properties of iron impurity atoms in the complete range of composition of Cu-Ni alloys. The isomer shift indicates a small decrease in the total electronic density at the Fe^{57} nucleus in going from pure Ni to pure Cu. The magnetic field at the iron nucleus at 0°K decreases by 9% in the range from 0 to 40% Cu. Both results show that only minor changes take place in the atomic configuration of the iron. The linewidth, measured in the paramagnetic alloys, is smallest in pure copper and largest near the middle of the composition range. The rapid change in linewidth with small nickel admixture can result from quadrupole splitting due to the field gradients arising from the spatial charge fluctuations around an impurity atom. Some of the broadening can also arise from an inhomogeneous isomer shift due to a range of surroundings of an iron atom in the alloy.

EFFECTIVE X-RAY AND CALORIMETRIC DEBYE TEMPERATURE FOR COPPER. P. A. Flinn, G. M. McManus, and J. A. Rayne, Westinghouse Research Laboratories, Pittsburgh, Pennsylvania (Received March 27, 1961).

The Debye-Waller factor for copper was determined from x-ray intensity measurements on a single crystal over the temperature range 4.2°K-500°K. From a machine calculation of the vibrational spectrum of copper, the values of the specific heat and Debye-Waller factor were obtained and compared with those found by experiment. The agreement indicates that for copper the central force model with nearest and second neighbor interactions is adequate for the interpretation of effects depending on simple averages over the frequency spectrum.

IMAGE OF THE FERMI SURFACE IN SPIN-WAVE SPECTRA OF RARE EARTH METALS. Edwin J. Woll, Jr., and Stephen J. Nettel, Department of Physics, University of California, San Diego, California (Received March 20, 1961).

Calculations of spin-wave spectra in rare earth metals were carried out to find whether images of the electronic Fermi surface might be observable. In the space of spin-wave vectors $\vec{q}$ there should occur surfaces on which the frequencies have an infinite gradient with respect to $\vec{q}$, the location of such abrupt changes, "kinks" in the dispersion curves, being determined by the shape of the Fermi surface. The spin-wave spectrum is found by assuming that the coupling between ionic spins takes place primarily through exchange

scattering of conduction electrons, paralleling the calculation on the coupling of nuclear spins by Ruderman and Kittel. Spin-wave dispersion curves in two directions of high symmetry are computed numerically. The sought-for kinks in the dispersion curves are found to amount to about two percent of the maximum excitation frequency. The development is for ferromagnets, but extension to spiral antiferromagnets is taken up briefly.

ANGULAR DISTRIBUTIONS OF SPUTTERED POTASSIUM ATOMS. R. P. Stein* and F. C. Hurlbut,† Missiles and Space Division, Lockheed Aircraft Corporation, Sunnyvale, California (Received January 19, 1961; revised manuscript received April 24, 1961).

The angular distributions of potassium particles issuing from a potassium surface under bombardment by noble gas ions were observed under moderately good vacuum conditions. Sputtered potassium atoms were detected for incident ion energies above approximately 15 electron volts and useful observations of angular distributions were obtained for incident ion energies in the range 50 to 450 electron volts for all available values of the incident angle. A means was discovered for the discrimination between the total sputtered flux and that fraction of it possessing particle energies above a certain threshold. The apparatus and experimental procedures are described and the observed distribution patterns and a two-collision sputtering mechanism are discussed, along with related observations.

*R. P. Stein, Lockheed Missiles and Space Division, Palo Alto, California.

†F. C. Hurlbut, University of California, Berkeley, California.

FLUORESCENCE AND OPTICAL MASER EFFECTS IN $CaF_2:Sm^{++}$. C. G. B. Garrett, W. Kaiser, and D. L. Wood, Bell Telephone Laboratories, Murray Hill, New Jersey (Received March 17, 1961).

Measurements are reported of absorption, emission, and activation spectra in $CaF_2:Sm^{++}$, and also of fluorescence lifetime. A revised level scheme is proposed. Observations of optical maser effects were made at liquid hydrogen and liquid helium temperatures over a wide range of pumping intensities. For illumination in the 6400A band, the threshold intensity of illumination was about 20 watts cm^{-2}. Observations are reported of the dependence of the intensity of the maser beam on the pumping intensity. Photographic observations, made both with and without a Fabry-Perot etalon, show that on one particular sample five distinct frequencies were present in the maser signal, and that the number of modes excited was of the order of one thousand.

MAGNETIC MOMENT OF LANTHANUM MAGNETOPLUMBITE FERRITE. A. Aharoni and M. Schieber, Department of Electronics, The Weizmann Institute of Science, Rehovoth, Israel (Received March 31, 1961).

The composition $La^{3+}Fe^{2+}Fe_{11}{}^{3+}O_{19}$ was prepared by sintering the oxides, and its magnetic moment was measured from liquid air temperature to the Curie point. At the lowest temperature a value of 17.5 Bohr magnetons per formula weight was obtained, as compared with 19 Bohr magnetons of $BaFe_{12}{}^{3+}O_{19}$. The difference is qualitatively understood if the Fe^{2+} ion is a nearest neighbor to the La^{3+} in the crystal, i.e., in the $[12k]$ site, thus decreasing the total magnetic moment. The Curie temperature is 695°K, compared to 725°K of $BaFe_{12}{}^{3+}O_{19}$. The lower Curie point can again be qualitatively explained by less exchange interaction with the divalent iron of $LaFe^{2+}Fe_{11}{}^{3+}O_{19}$, or possibly by the change in unit-cell dimension which modifies the short-range exchange interaction between the iron ions.

REMANENT STATE IN ONE-DIMENSIONAL MICROMAGNETICS. Amikam Aharoni, Department of Electronics, The Weizmann Institute of Science, Rehovoth, Israel (Received March 1, 1961; revised manuscript received April 20, 1961).

A first integral is found for Brown's nonlinear equations in one dimension. When the external field is zero, another first integral can be found, which enables complete integration of the equations. For a unidirectional anisotropy with an easy direction perpendicular to the plane of the film, one of the integration constants is not determined by the boundary conditions, as if indicating a possibility of continuum of different

remanence values for different histories. However, when a small field in the plane of the film is introduced as a perturbation, this degeneracy is removed, and the magnetization can change only in the plane defined by the field and the direction of anisotropy. There are still many discrete possible values for the remanence, each of which determines uniquely the susceptibility at that state.

DISPERSION OF GYROMAGNETIC RATIOS IN COMPLEX SPECTRA. Norbert Rosenzweig, Argonne National Laboratory, Argonne, Illinois, and C. E. Porter, Brookhaven National Laboratory, Upton, New York (Received March 20, 1961).

It is pointed out that the random-matrix hypothesis, which was previously used to explain the "repulsion" of energy levels in complex atomic and nuclear spectra, leads to a dispersion in the values of the gyromagnetic ratios which depends on the relative strengths of central and spin-dependent interactions and the number of states which interact with one another in the *LS* coupling scheme. The dispersion based on experimentally known atomic g factors is computed in three regions of the periodic table, and the empirical trends are found to be in qualitative agreement with the theoretical analysis.

DECAY OF Tm^{172}. R. G. Helmer and S. B. Burson, Argonne National Laboratory, Argonne, Illinois (Received March 16, 1961).

The radioactive nuclide $_{69}Tm^{172}$ was produced by successive capture of two neutrons in erbium oxide enriched in Er^{170}. The irradiations were made in the Materials Testing Reactor at Arco, Idaho. In addition to three thulium activities, these samples contained six active contaminants. Pure thulium sources were obtained by use of an ion-exchange column. Studies were conducted with a 256-channel coincidence scintillation spectrometer. These measurements indicate the presence of at least 17 gamma-ray and 5 beta-ray transitions. The beta-ray spectrum was studied with a 180° magnetic beta-ray spectrometer. This spectrum was analyzed by use of a computer program compiled by the authors in collaboration with members of the Argonne Applied Mathematics Division. The level scheme proposed for Yb^{172} has states with energies, spins, and parities of $0.0(0^+)$, $0.079(2^+)$, $0.260(4^+)$, 1.17(3), 1.46(2), 1.54(3), 1.60(1), 1.64(?), and 1.73(3) Mev. The total decay energy is found to be 1.88 Mev. The experimental data are consistent with the previously proposed interpretation that the first two excited states are members of a $K=0$ rotational band based on the ground state. The states at 1.46 and 1.54 Mev are interpreted as members of a rotational band with $K=2$. The states at 1.60 and 1.73 Mev are tentatively interpreted as members of a rotational band with $K=0$ and negative parity. It is suggested that the state at 1.17 Mev has $K=3$. From the analysis of the beta spectrum it is concluded that the ground state of thulium has $I=K=2$ and negative parity.

ENERGY LEVELS IN $_{69}Tm^{172}$ FROM THE DECAY OF $_{68}Er^{172}$. R. G. Helmer and S. B. Burson, Argonne National Laboratory, Argonne, Illinois (Received March 27, 1961).

The radioactive nuclide $_{68}Er^{172}$ was produced in the Materials Testing Reactor, Arco, Idaho, by the successive capture of two neutrons in erbium oxide enriched in Er^{170}. In addition to three erbium activities and the radioactive Tm^{172} daughter, these samples contained six active contaminants from which the erbium was separated by use of an ion-exchange column. Scintillation studies, conducted with a 256-channel coincidence scintillation spectrometer, indicate the presence of at least eight gamma-ray transitions. Two of these transitions are either highly K converted or their transition energies are approximately 50 kev. The energies of the other six transitions are about 610, 450, 408, 200, 160, and 125 kev. Beta-gamma coincidence experiments indicate the presence of two beta-ray components at approximately 310 kev (in coincidence with the 610-kev gamma ray) and 370 kev (in coincidence with the 408-kev gamma ray). The level scheme deduced for Tm^{172} has excited states at 408, 450 (or 160), 470 ± 15, 530, and 610 kev. From the beta-ray intensities, the states at 530 and 610 kev are assigned spins of either 0 or 1 with positive parity. The spin and parity (2^-) of the thulium ground state have previously been assigned from the properties of the decay of Tm^{172}.

INTERPRETATION OF EXPERIMENTAL $(n, 2n)$ EXCITATION FUNCTIONS. D. W. Barr, C. I. Browne, and J. S. Gilmore, Los Alamos Scientific Laboratory, University of California, Los Alamos, New Mexico (Received March 6, 1961).

Radiochemically determined $(n, 2n)$ excitation functions for Sc^{45}, Ti^{46}, Ni^{58}, Cu^{65}, Ge^{70}, As^{75}, Sr^{84}, Rb^{85}, Rb^{87}, Y^{89}, Zr^{90}, Sn^{112}, Cd^{116}, Sb^{123}, and U^{238} have been interpreted in terms of the statistical model of nuclear reactions. Values of the level density parameter a are obtained and correlated with mass number. A procedure is outlined for predicting the magnitude of any $(n, 2n)$ cross section from the nuclear content of the target material. Two level density formulations are studied, and approximations customarily made in calculations of this sort are examined quantitatively.

MEASUREMENT OF THE DEUTERON BINDING ENERGY USING A BENT-CRYSTAL SPECTROGRAPH. A. Halim Kazi,* Norman C. Rasmussen, and Hans Mark, Department of Nuclear Engineering and Department of Physics, Massachusetts Institute of Technology, Cambridge, Massachusetts (Received March 20, 1961).

The deuteron binding energy has been determined by measuring the neutron-proton capture gamma-ray energy. This energy has been measured directly, relative to annihilation radiation, with the help of a six-meter radius bent-crystal spectrograph. The spectrograph is of the Cauchois type, in which a collimated but extended gamma-ray beam is incident on the convex side of an elastically bent quartz crystal, is diffracted, and focused onto a focal circle defined by the radius of curvature of the crystal. The neutron-proton capture gamma rays are produced by placing a polyethylene sample in the through port of the MIT research reactor. The (310) planes of quartz are used for diffraction, and the gamma-ray lines are recorded on glass-mounted 600-micron thick Ilford G-5 emulsions. The value of $B(D)$ obtained is 2225.5 $\pm$ 1.5 kev, where the error is the standard deviation. This is the most precise direct measurement reported to date, and is in agreement with previous work. Using recent mass spectroscopic data, the mass of the neutron is found to be $1.008\,984 \pm 0.000\,002$ amu.

The efficiency of the spectrograph is low. At 2225 kev, 6000 curie hours are required to record a line; at 511 kev, 1200 curie hours are necessary. The error in $B(D)$ agrees with the estimated precision which varies from about 0.01% at 100 kev to 0.3% at 4000 kev. The latter energy is close to the practical upper energy limit of the instrument.

*Present address: John Jay Hopkins Laboratory for Pure and Applied Science, General Atomic Division of General Dynamics Corporation, San Diego, California.

NUCLEAR ORIENTATION OF Pm^{143}. C. A. Lovejoy, J. O. Rasmussen, and D. A. Shirley, Lawrence Radiation Laboratory and Department of Chemistry, University of California, Berkeley, California (Received March 24, 1961).

Promethium-143 has been oriented in a crystal of neodymium ethyl-sulfate. The angular distribution of the 740-kev γ ray was found to be $W(\theta) = 1 - (0.060 \pm 0.006)P_2(\cos\theta)$ at 0.02°K. Values for the mixing ratio, δ, of the 740-kev γ ray of Nd^{143} were obtained as a function of the magnetic moment of the ground state of Pm^{143}. The spin of the excited state of Nd^{143} was assigned as 9/2-. An absolute lower limit of $|\mu| > 1.0$ was set on the magnetic moment of Pm^{143}. The mixing ratio of the γ ray of Nd^{143} was found to lie in the range $0.23 < \delta(E2/M1) < 0.35$.

$Ca^{40}(p, \gamma)Sc^{41}$ REACTION. J. W. Butler, Nucleonics Division, U. S. Naval Research Laboratory, Washington, D. C. (Received March 24, 1961).

Proton capture by Ca^{40} has been studied by means of observations on both the prompt gamma rays from resonance states in the compound nucleus and the delayed positrons from the decay of the ground state. Targets of CaO were prepared by the electrodeposition of Ca onto a Pt backing followed by the oxidation of the Ca and the purging of impurities by heat. These targets were bombarded by protons from a 2-Mv Van de Graaff accelerator, producing the reaction $Ca^{40}(p, \gamma)Sc^{41}$. The gamma rays from this reaction were observed with the use of a 3-in. diam by 3-in. NaI(Tl) crystal and a 256-channel pulse-height analyzer. Positrons from the decay of Sc^{41} were detected with the use of a thin plastic phosphor, 1.5 in. diam by 0.012 in. thick. Two resonances in the reaction were observed at bombarding energies of 650 ± 5 kev and 1850 ± 10 kev. Two other possible resonances were observed at 1550 ± 15 kev and

1630 ± 15 kev. The 650-kev resonance corresponds to an excited state in Sc^{41} at 1.723 ± 0.011 Mev, has an integrated cross section of 0.02 ev barn (factor of two uncertainty either way), has a width of less than 5 kev, and involves a gamma ray whose energy was measured to be 1.71 ± 0.03 Mev. The 1850-kev resonance corresponds to an excited state in Sc^{41} at 2.883 ± 0.014 Mev, has an integrated cross section of 0.3 ev barn (factor of two uncertainty either way), has a width of less than 10 kev, and involves a gamma ray whose energy was measured to be 2.89 ± 0.02 Mev.

NUCLIDES Ar^{42} and Cl^{39}. Nelson Jarmie and M. G. Silbert, Los Alamos Scientific Laboratory, University of California, Los Alamos, New Mexico (Received March 27, 1961).

The masses of Cl^{39} and Ar^{42} and the energies of their first excited states have been determined by an investigation of the reactions $Ar^{40}(t,\alpha)Cl^{39}$ and $Ar^{40}(t,p)Ar^{42}$. Charged reaction products were analyzed with a high-resolution magnetic spectrometer. The experimental results for Ar^{42} are: mass excess $(M-A) = -34.423 \pm 0.040$ Mev ($C^{12} = 0$) or -21.990 ± 0.040 Mev ($O^{16} = 0$); energy of first excited state 1.138 ± 0.030 Mev. The experimental results for Cl^{39} are: mass excess $(M-A) = -29.772 \pm 0.040$ Mev ($C^{12} = 0$) or -18.227 ± 0.040 Mev ($O^{16} = 0$); energy of first excited state = 0.364 ± 0.030 Mev. The Q values of $Ar^{40}(t,p)Ar^{42}$ and $Ar^{40}(t,\alpha)Cl^{39}$ were found to be 7.046 ± 0.040 Mev and 7.259 ± 0.040 Mev, respectively.

ELASTIC SCATTERING OF IDENTICAL SPIN-ZERO NUCLEI. D. A. Bromley,* J. A. Kuehner, and E. Almqvist, Atomic Energy of Canada Limited, Chalk River Laboratories, Chalk River, Ontario, Canada (Received March 27, 1961).

Elastic scattering measurements have been carried out on the $C^{12}+C^{12}$ and $O^{16}+O^{16}$ systems in the energy range from 6 to 35 Mev using heavy-ion beams from the Chalk River tandem accelerator and Au-Si surface barrier detectors. At energies below the Coulomb barriers the Mott scattering predictions are in excellent accord with the measurements as functions of both angle and energy. At energies above the barrier the O+O excitation curve drops exponentially below the Mott predictions to a value of 10 mb/sr at $E_{c.m.} = 16.5$ Mev and remains approximately constant thereafter at that value; in contrast, the C+C excitation curve shows marked resonant interference structure. The states involved have $\tau \sim 10^{-21}$ sec, large compound elastic branching ratios Γ_C/Γ, and appear to correspond to resonant absorption of high order partial waves; hence they have high angular momentum. It is suggested that these states reflect a quasi-molecular interaction mechanism which is involved in grazing collisions of these nuclei and which is critically dependent upon the structure of the nuclei involved.

*Present address: Department of Physics, Yale University, New Haven, Connecticut.

"BREAKS" IN THE ACTIVATION CURVES OF THE $P^{31}(\gamma,n)P^{30}$ REACTION. D. Sadeh,* Laboratoire de Synthèse Atomique, Centre National de la Recherche Scientifique, Ivry, France (Received March 17, 1961).

Discontinuities in the slope of the activation curve of the $P^{31}(\gamma,n)P^{30}$ reaction were found while using two large NaI(Tl) crystals to detect the annihilation gammas from P^{30}. These breaks correspond well with resonances found recently in the $Si^{30}(p,n)P^{30}$ reaction.

The correspondence between breaks and known resonances in some light nuclei is discussed. Such a correspondence was found to exist in the case of N^{14}, F^{19}, and P^{31} and is in doubt in the case of C^{12}.

The detection system used allowed accurate measurements of the thresholds of the $P^{31}(\gamma,n)P^{30}$ reaction (12.23 ± 0.04 Mev) and the $Cl^{35}(\gamma,n)Cl^{34}$ reaction (12.66 ± 0.04 Mev).

*Present address: Atomic Energy Commission of Israel, P.O.B. 7056, Hakirya, Tel-Aviv, Israel.

$T = 3/2$ LEVEL IN F^{19} AT 9.07 Mev. G. Amsel and G. R. Bishop, Ecole Normale Supérieure, Paris, France (Received March 24, 1961).

Contrary to previous reports we have detected α particles emitted from the 9.07-Mev state of F^{19} formed by the reaction $O^{18}(p,\alpha)N^{15}$. The α-particle reduced width indicates that the isotopic spin of this state is $T = 3/2$ with an admixture of about 5% of $T = 1/2$. The spin of the state is determined to be 7/2 from the α-particle angular distribution, while odd parity is favored by the proton reduced width.

NEUTRON CAPTURE CROSS SECTION OF GOLD AT 30 kev AND 64 kev. L. W. Weston and W. S. Lyon, Oak Ridge National Laboratory, Oak Ridge, Tennessee (Received January 27, 1961; revised manuscript received May 8, 1961).

The capture cross section of gold has been measured with kinematically collimated neutrons from the $Li^7(p,n)Be^7$ and $T(p,n)He^3$ reactions. The cross sections at 30.2 kev and 63.9 kev were found to be 0.767 ± 0.060 and 0.456 ± 0.040 barn, respectively.

3.14-hr ISOMERIC LEVEL IN Y^{90}. R. L. Heath, J. E. Cline, C. W. Reich, E. C. Yates, and E. H. Turk, National Reactor Testing Station, Phillips Petroleum Company, Idaho Falls, Idaho (Received March 24, 1961; revised manuscript received May 5, 1961).

A previously unreported 3.14-hr isomeric activity has been produced in Y^{90} by thermal neutron irradiation of Y^{89}. The thermal capture cross section for the production of the isomer was measured to be 1.0 ± 0.2 millibarn. The decay of the isomeric level is characterized by the emission of two cascade gamma rays of 0.482 and 0.203 Mev. Conversion coefficient measurements indicated that the isomeric level at 0.685 Mev decays by $M4$ or $E5$ radiation to an intermediate level at 0.203 Mev followed by a predominantly $M1$ transition to the ground state of Y^{90}. Gamma-gamma directional correlation measurements and internal conversion measurements indicated that the level at 0.203 Mev has spin 3 with odd parity and that the level at 0.685 Mev has spin 7 or 8 with even parity. A shell-model configuration of $(g_{9/2}d_{5/2})$ has been assigned to the isomeric state.

(n,d) and (n,p) REACTIONS NEAR $Z = 50$. R. A. Peck, Jr., Brown University, Providence, Rhode Island (Received March 10, 1961).

An emulsion study is reported of charged particles produced by 14-Mev neutron bombardment of Rh^{103}, In^{115}, Sn^{116}, Sn^{120}, Sb, and Te. For all but Te (no detectable yield) cross sections and spectra are presented, with distributions over the first 40° of laboratory angle of energy groups from Rh, In, and Sb. Contrary to an assumption common in earlier work, there is strong evidence that the (n,d) reaction contributes strongly. Five peaks among the Rh, In, and Sb spectra are identified with pickup transitions to known residual levels, four of their angular distributions fitting the predicted Butler forms and the fifth providing the new assignment 0-, 1- for the 1.88-Mev level in Ru^{102}. The wide (n,np) group is found at the expected energy in the Rh, In, Sn^{116}, and Sb spectra; its angular distribution is anomalous for Rh but displays the expected isotropy in the other three cases. Up to at least 6-Mev excitation the (n,p) gross structure is dominated by single-particle effects, the uncontaminated (n,p) yield obeying predictions of the Nilsson model as to spectral concentration and angular distribution; the low collective levels excited in (p,p') are not observed. Systematic behavior of the direct-interaction radius for (n,d) and (n,p) and of the reduced width for pickup are found to be reasonable. It is inferred that the parent state for proton pickup with low residual excitation is almost purely a single-particle state in the case of Sb, has a strong single-particle character in Rh, and a very weak one in In.

PHOTOALPHA REACTION IN Sb^{121}. John H. Wolfe and John P. Hummel, Department of Chemistry and Chemical Engineering and Department of Physics, University of Illinois, Urbana, Illinois (Received March 20, 1961).

The $Sb^{121}(\gamma,\alpha)In^{117-117m}$ reaction has been studied by determining the radioactivities of the product nuclei in samples that were irradiated with bremsstrahlung of maximum energy varying from 15.5 to 24 Mev. Excitation functions for the total cross section and the cross sections to each isomer were obtained. The total cross section rises steadily over the energy range studied, reaching a value of 360 microbarns at 24 Mev. The ratio of the cross section for the direct production of the ground state to the cross section for the production of the isomer is constant over the energy range studied at a value of 2.60 ± 0.40. The total excitation function up to 18 Mev agrees well with cross sections calculated on the basis of a statistical theory for compound-nucleus decay. The cross-section predictions could not be made for higher energies. The observed ground to isomer cross-section ratio is consistent with that expected from a compound-nucleus mechanism and probably inconsistent with that expected from a direct mechanism. Thus, the reaction appears

to involve compound-nucleus processes for the most part.

SHORT-LIVED ISOMERS OF Ge^{71}, As^{74}, Br^{78}, AND Tc. A. W. Schardt* and Albert Goodman,† Los Alamos Scientific Laboratory, University of California, Los Alamos, New Mexico (Received March 20, 1961).

Short-lived isomers have been produced with the pulsed beam of a Van de Graaff generator and observed between pulses with scintillation detectors. The results are summarized in the following table:

Isotope	Half-life	Isomeric transition (kev)	Observed gamma ray (kev)
Ge^{71}	20.3 ±0.3 msec	23 ($M2$)	175
As^{74}	8.0 ±0.3 sec	283 ($M3$)	283 ±5
Br^{78}	118.0 ±1.5 μsec	149 ($M2$)	149 ±2, 32 ±2
Tc	8.15 ±0.20 μsec		177 ±4
Tc	15.5 ±0.8 μsec		43 ±3

*Present address: Advanced Research Project Agency, Washington, D. C.

†Present address: Sandia Corporation, Albuquerque, New Mexico.

ELECTRON-SCATTERING STUDY OF NUCLEAR LEVELS IN COBALT, NICKEL, LEAD, AND BISMUTH. H. Crannell, R. Helm, H. Kendall, J. Oeser, and M. Yearian,* High-Energy Physics Laboratory, Stanford University, Stanford, California (Received March 24, 1961).

We have observed inelastic scattering of 183-Mev electrons through angles of 40°-90° in the laboratory, leading to excitation of discrete nuclear excited states in Ni^{58}, Co^{59}, Ni^{60}, Pb^{208}, and Bi^{209}. The excitation energies were below 8 Mev. Born-approximation analysis of the measured inelastic form factors was used to deduce the multipolarities λ (when not previously known), and, by extrapolation, the transition rates, for 15 corresponding gamma transitions. A number of groups of electric transitions for $\lambda = 2$, 3, and 4 were observed, each group having strikingly similar form factors. In all but one of these groups the ratios G of the observed gamma transition rates to the single-particle predictions were greater than 15, and for some transitions from 30 to over 100. One of the groups, in cobalt and the nickels, contains the 1.33-Mev $E2$ transition to the first excited state of Ni^{60}. Another group consists of fast $E3$ transitions, seen in all five niclei, from states known as the "anomalous levels." They included the transition to the first excited state in Pb^{208} ($G = 31$) and a transition in Bi^{209} identical in energy and form factor. Among three slow $E4$ transitions in cobalt and the nickels was the 2.50-Mev $4^+ \rightarrow 0^+$ transition in Ni^{60}. The $E4$, $E3$, and an $E2$ transition in Co^{59} identify states analogous to the 4^+, 3^-, and 2^+ seen in the neighboring even-even nuclei. The last two transitions are strongly enhanced. A pair of fast 4.30-Mev $E4$ transitions was observed in Pb^{208} and Bi^{209}; their speed ($G = 37$) indicates that they may constitute the lowest energy configuration of 16-pole mode of excitation of the nuclear surface. Values of the collective vibrational parameters C_λ and B_λ and the degree to which some of the transitions exhaust ordinary sum rules support the conclusion that the inelastic scattering process is strongly exciting nuclear collective excitations. Some of the observed results are expected on the basis of the theory of collective vibrational excited states; some are the consequence of unidentified configurations.

ISOMER RATIO FOR THE $Sn^{118}(\gamma,p)$ REACTION. John P. Hummel, Department of Chemistry and Chemical Engineering and Department of Physics, University of Illinois, Urbana, Illinois (Received March 29, 1961).

The relative yields of In^{117} and In^{117m} from the $Sn^{118}(\gamma,p)$ reaction have been measured by counting the gamma rays emitted by a sample of SnO_2 enriched in Sn^{118} that had been irradiated with 24-Mev bremsstrahlung. The measured ground to isomer yield ratio was 0.65 ± 0.15, and is consistent with predictions made on the basis of both the Wilkinson direct mechanism and the compound nucleus mechanism. However, the values of the isomer ratios for the series of even-even tin isotopes (Sn^{118}, Sn^{120}, Sn^{122}, and Sn^{124}, the latter three from the work of Yuta and Morinaga) are not at all consistent with the predictions of the compound nucleus mechanism but can be rationalized on the basis of the Wilkinson model, lending support for that theory for direct photoproton reactions.

ENERGY LEVELS IN Na^{21}. R. E. Benenson* and L. J. Lidofsky, Columbia University, New York, New York (Received March 17, 1961).

The Na^{21} nucleus has been studied through two reactions: the $Ne^{20}(d,n)Na^{21}$ reaction using a fast-neutron spectrometer, and the $Ne^{20}(p,\gamma)Na^{21}$ reaction using both single-crystal and Hoogenboom techniques. $\bar{E}_d$ for the neutron spectroscopy for the major part of the work was centered about 4.87 Mev, while the capturing resonance for the gamma-ray work was at $\bar{E}_p = 1.17$ Mev. Enriched neon was employed as target gas. Energy levels in Na^{21} are found at excitations of 0.33 ± 0.03 Mev, 1.77 ± 0.05 Mev, 2.42 ± 0.04 Mev, 2.80 ± 0.06 Mev, and 3.61 ± 0.06 Mev. From the neutron work level parameters can be assigned to the 0.33- and 2.42-Mev levels, while from the gamma-ray work spin limits and parity may be assigned to the 3.61-Mev level. This latter level corresponds to the 1.17-Mev capture resonance, and a study of the de-excitation cascades has been partially completed. A discussion of the level scheme of Na^{21} in terms of the collective model is given.

*Permanent address: City College, New York, New York.

ANTISHIELDING OF NUCLEAR ELECTRIC HEXADECAPOLE MOMENTS. R. M. Sternheimer, Brookhaven National Laboratory, Upton, New York (Received March 27, 1961).

The antishielding factor η_∞ for a possible nuclear electric hexadecapole moment has been calculated for the Cu^+, Ag^+, and Hg^{++} ions, using the Hartree-Fock wave functions for the $3d$, $4d$, and $5d$ electrons involved. It was found that $\eta_\infty(Cu^+) \cong -1200$, $\eta_\infty(Ag^+) \cong -8050$, and $\eta_\infty(Hg^{++}) \cong -63\,000$. The implication of these results is discussed.

CONFIGURATION MIXING AND THE EFFECTS OF DISTRIBUTED NUCLEAR MAGNETIZATION ON HYPERFINE STRUCTURE IN ODD-A NUCLEI. H. H. Stroke and R. J. Blin-Stoyle,* Physics Department, Laboratory for Nuclear Science and Research Laboratory of Electronics, Massachusetts Institute of Technology, Cambridge, Massachusetts, and V. Jaccarino, Bell Telephone Laboratories, Murray Hill, New Jersey (Received January 16, 1961).

The theory of Blin-Stoyle and of Arima and Horie, in which the deviations of the nuclear magnetic moments from the single-particle model Schmidt limits are ascribed to configuration mixing, is used as a model to account quantitatively for the effects of the distribution of nuclear magnetization on hyperfine structure (Bohr-Weisskopf effect). A diffuse nuclear charge distribution, as approximated by the trapezoidal Hofstadter model, is used to calculate the required radial electron wave functions. A table of single-particle matrix elements of R^2 and R^4 in a Saxon-Woods type of potential well is included. Explicit formulas are derived to permit comparison with experiment. For all of the available data satisfactory agreement is found. The possibility of using hyperfine structure measurements sensitive to the distribution of nuclear magnetization in a semiphenomenological treatment, in order to obtain information on nuclear configurations, is indicated.

*On sabbatical leave from the Clarendon Laboratory, Oxford, England.

ISOTOPIC-SPIN SELECTION RULE VIOLATION IN THE $B^{10}(d,\alpha)Be^8$ REACTION. J. R. Erskine* and C. P. Browne, Department of Physics, University of Notre Dame, Notre Dame, Indiana (Received March 28, 1961).

All previous tests of the isotopic-spin selection rule in (d,α) reactions were obscured by statistical weight factors because in each case the initial and final nuclear states had spin and parity 0^+. The $B^{10}(d,\alpha)Be^8$ reaction provides a test of the isotopic-spin selection rule free from this restriction. The energy levels of Be^8 near the lowest $T=1$ level were studied with the $Li^6(He^3,p)Be^8$ and $Be^9(He^3,\alpha)Be^8$ reactions as well as with the $B^{10}(d,\alpha)Be^8$ reaction. Energy levels in Be^8 were found at 16.623 ± 0.010 Mev, 16.921 ± 0.010 Mev, and 17.637 ± 0.006 Mev. The widths are 95 ± 20 kev, 85 ± 20 kev, and < 15 kev, respectively. The first of these levels is the lowest $T=1$ state whereas the second is $T=0$ and the third probably $T=1$. Energy levels at 16.08 Mev and a $J=2$ level at 17.7 Mev, reported by other laboratories, were not observed. The ratio of the differential cross sections for formation of the 16.62- and 16.92-Mev levels was measured over a range of angles and bombarding energies. The ratio is about 1.4 and is roughly constant for both the $Li^6(He^3,p)Be^8$ and $B^{10}(d,\alpha)Be^8$ reactions. This implies complete violation of the selection rule because the latter reaction should not go to the $T=1$ level. Argu-

ments are given which indicate that the $T=0$ impurities in the 16.62-Mev $T=1$ level are no more than a few percent. Consequently, the failure of the selection rule probably results from the complete intermixing of $T=0$ and $T=1$ states in the C^{12} compound nucleus near 28-Mev excitation. Groups from the $C^{12}(He^3, p)N^{14}$ reaction were seen corresponding to levels in N^{14} at 5.691 ± 0.008, 5.834 ± 0.008, 6.203 ± 0.008, and 6.440 ± 0.008 Mev.

*Present address: Laboratory for Nuclear Science, Massachusetts Institute of Technology, Cambridge, Massachusetts.

PROTONS FROM ALPHA-INDUCED REACTIONS. Wayne Swenson and Nikola Cindro,* Department of Physics and Laboratory for Nuclear Science, Massachusetts Institute of Technology, Cambridge, Massachusetts (Received December 21, 1960).

The results of proton energy spectra measured at several angles from 30.5-Mev alpha-particle-induced reactions on Al^{27}, V^{51}, Co^{59}, As^{75}, Nb^{93}, Rh^{103}, In^{115}, and Ta^{181} were analyzed using the statistical model. The analysis yielded the differential cross section $d^2\sigma/d\Omega dE$ and the relative level density $\omega(E)$ of the residual nucleus as a function of proton and excitation energy of the residual nucleus. The nuclear temperature $1/T \equiv d(\ln\omega)dE$ and the level density parameter a of $\omega = C \exp[(aE)^{1/2}]$ were obtained. The energy and angular dependence of the spectra are adequately described by the statistical model at back angles, with the indication of the presence of a direct reaction mechanism contribution at forward angles, which extends to high excitation energies.

*On leave of absence from the Institute "Rudjer Boskovic," Zagreb, Yugoslovia.

POLARIZATION CORRELATION MEASUREMENTS ON Eu^{154}. C. V. K. Baba, Atomic Energy Establishment, Trombay, Bombay, India, and S. K. Bhattacherjee, Tata Institute of Fundamental Research, Bombay, India (Received March 15, 1961).

The spins and parities of the 1400-kev and 1723-kev levels in Gd^{154} are discussed on the basis of the polarization-directional correlation measurements on the 1277-123 kev and 725-998 kev gamma-gamma cascades following the β decay of Eu^{154}. In the case of the 1277-123 kev cascade, the directional correlation measurements and the polarization correlation measurements of the 1277-kev gamma ray are made with liquid and solid sources. An attenuation in the anisotropy of directional correlation and in the degree of linear polarization correlation has been observed in both the sources, the attenuation in the solid source being more. In the 725-998 kev cascade, the polarization of either of the two radiations has been measured in two separate experiments. On the basis of these measurements, the spins and parities of both the 1400-kev and the 1723-kev levels in Gd^{154} are assigned as 2^-. The performance of the apparatus has been checked by measuring the polarization correlations of the known cascades in Ni^{60}, Ti^{46}, Pd^{106}, and Sr^{88}.

THEORY OF AVERAGE NEUTRON REACTION CROSS SECTIONS IN THE RESONANCE REGION. P. A. Moldauer, Argonne National Laboratory, Argonne, Illinois (Received February 2, 1961).

The scattering matrix for compound-nucleus processes is studied in the R-matrix formalism, using a series expansion which is due to Thomas. It is shown that this series generally converges when (a) the average total resonance width is less than the average resonance spacing, (b) the number of important channels is not too large, and (c) the width amplitudes have random signs. The treatment also suggests strongly that the series does not converge in the continuum region. In the region of convergence the exact relationship between the channel transmission factor T_C and the ratio of partial width to level spacing is found in the absence of direct-scattering reactions to be $T_C = 2\pi\langle\Gamma_{\lambda C}\rangle/D - \pi^2\langle\Gamma_{\lambda C}\rangle^2/D^2$. The quadratic term is shown to be important in the vicinity of optical-model maxima. Correction terms to the Hauser-Feshbach relations for average reaction cross sections arising from the higher order terms of the series are obtained and are found to depend on the statistical properties of both resonance widths and resonance spacings. The effect on average neutron inelastic, compound elastic, and capture cross sections is discussed and an example of a calculation is presented.

RESONANCE MODEL OF Λ-K^0 PRODUCTION. Akira Kanazawa,* Department of Physics, Purdue University, Lafayette, Indiana (Received March 30, 1961).

A resonance model is proposed to explain the excitation function, the angular distribution, and the large polarization of Λ in the reaction $p+\pi^- \rightarrow \Lambda+K^0$. It is assumed that there exists a low angular momentum resonance in the channel $p+\pi^- \rightarrow$ (resonant state) $\rightarrow \Lambda+K^0$. There are five real parameters in this model. Two of these are the coupling constants of the usual interactions. The other three are the position, half-width, and height of the assumed resonance. With reasonable choices of parameters a fairly good fit is obtained, for both a scalar and a pseudoscalar K meson, to the experimental data in the interval 910 to 1300 Mev of the pion kinetic energy in the laboratory system.

*On leave from Hokkaido University, Sapporo, Japan.

PHOTOPRODUCTION OF K^+ MESONS FROM DEUTERIUM. R. L. Anderson, F. Turkot, and W. M. Woodward, Cornell University, Ithaca, New York (Received February 13, 1961).

The differential cross section for the reaction $\gamma+n \rightarrow K^+ + \Sigma^-$ has been measured. The data are obtained by observing the charged K particle with a magnet spectrometer alternately from hydrogen and from deuterium. For γ-ray energy of 1122 Mev and for $\theta_{\text{c.m.}} = 82°$, we get $d\sigma_{n\Sigma^-}/d\sigma_{p\Sigma^0} = 1.6 \pm 0.7$.

PION PRODUCTION AND THE SECOND PION-NUCLEON RESONANCE. Charles J. Goebel* and Howard J. Schnitzer, Department of Physics and Astronomy, University of Rochester, Rochester, New York (Received March 16, 1961).

A model for the reaction $\pi+N \rightarrow 2\pi+N$ at low energies, which includes pion-pion interaction and final-state interactions in the (3, 3) state, is discussed. The theory involves 2 parameters which are related to the S-wave and P-wave π-π scattering lengths. These parameters are chosen from a fit to the total cross section for $\pi^-+p \rightarrow \pi^-+\pi^++n$. Meson production is predicted to be primarily in the $T=1/2$ state. Predictions are made for the total cross sections of the various channels (e.g., $\pi^++p \rightarrow \pi^++\pi^++n$, etc.) in the energy range from threshold to ≈ 500 Mev, in good agreement with experiments. Angular distributions are predicted. These are in qualitative agreement with the π^+ angular distribution for $\pi^-+p \rightarrow \pi^-+\pi^++n$. From these data it is suggested that the S-wave π-π scattering length has opposite sign to the P-wave scattering length. A conjecture concerning rapidly rising inelastic cross sections in a single partial wave is made to connect the large $T=1/2$, $D_{3/2}$ production cross sections with the $T=1/2$, $D_{3/2}$ pion-nucleon resonance. The π-π scattering length found are $a_0 = -0.290\,\mu^{-1}$, $a_1 = 0.122\,\mu^{-1}$, and $a_2/a_0 = 2/5$ by hypothesis.

*On leave of absence 1960-61 at the Institute for Advanced Study, Princeton, New Jersey.

ANNIHILATION PROCESS OF NEUTRINO PRODUCTION IN STARS. H. Y. Chiu, Institute for Advanced Study, Princeton, New Jersey (Received March 31, 1961).

The rate at which the energy of a black-body radiation is converted into neutrinos by the pair annihilation process $e^-+e^+ \rightarrow \nu+\bar{\nu}$ has been calculated. At $T \sim 6\times10^9$ °K, the relaxation time for such conversion process is around 100 seconds for pure radiation. Since neutrinos have very long mean free path ($\gg$ stellar dimensions) they will escape, thus carrying away the energy. This process therefore will be of astrophysical importance. The rate of energy loss dU/dt is tabulated, as a function of temperature and density, together with the chemical potential, the pressure, and the electron-positron energy. This table should be useful for numerical integrations of stellar structure equations in the temperature range $(0.5-10)\times10^9$ °K, and the density range $0-10^9$ gram/cc.

MEAN LIFETIME OF THE NEUTRAL PION. R. G. Glasser, N. Seeman, and B. Stiller, Nucleonics Division, Naval Research Laboratory, Washington, D. C. (Received March 30, 1961).

An estimate of the mean lifetime of the π^0 meson has been obtained from an experiment employing a direct time-of-flight technique first attempted by Harris et al. in 1957. This method is based upon the observation in nuclear emulsion of the decay of the $K_{\pi 2}{}^+$ meson ($K^+ \rightarrow \pi^++\pi^0$) and the subsequent decay of the π^0 via

the Dalitz mode, $\pi^0 \rightarrow e^+ + e^- + \gamma$. In the present experiment we were able to utilize a new fine-grained emulsion (Ilford L.4) that yielded markedly improved resolution. The availability of the separated K^+ beam from the bevatron at Berkeley permitted detection and measurement of 76 Dalitz decays. We obtain for the mean lifetime of the π^0, $\tau = (1.9 \pm 0.5) \times 10^{-16}$ sec.

NUCLEON POLARIZABILITY CORRECTION TO HIGH-ENERGY ELECTRON-NUCLEON SCATTERING. N. R. Werthamer,* University of California, Berkeley, California, and M. A. Ruderman,† New York University, New York, New York (Received March 23, 1961).

The contribution of nucleon polarizability to ultrarelativistic electron-nucleon scattering cross sections is estimated and found to be small for nonforward scattering angles at all energies.

*Present address: University of California, La Jolla, California.

†On leave from the University of California, Berkeley, California.

BROKEN SYMMETRIES AND BARE COUPLING CONSTANTS. Murray Gell-Mann and Fredrik Zachariasen, California Institute of Technology, Pasadena, California (Received March 20, 1961).

There are known cases of symmetry laws valid for one kind of interaction but broken by another. Each symmetry is then supposed to be exact for bare masses and coupling constants but only approximate for the renormalized quantities, like neutron and proton masses. We ask how the equality of unrenormalized constants can be rephrased as a statement about measurable quantities. This question is particularly important in connection with proposed strong-interaction symmetries that are supposed to be badly broken. The answer appears to involve the limits of ratios of experimental quantities at very high momenta. We discuss first the connection between wave function renormalizations and weak and electromagnetic form factors. Then we take up the measurement of strong-interaction vertex renormalization factors by the study of scattering amplitudes at energies and momentum transfers large compared to all masses. The last part of the work is based in part on indications from the perturbation development of pseudoscalar meson theory, but we hope it will point the way to similar results in a better theory.

NOTE ON REARRANGEMENT COLLISIONS. T. B. Day, L. S. Rodberg, G. A. Snow, and J. Sucher, Physics Department, University of Maryland, College Park, Maryland (Received March 29, 1961).

The conventional Born approximation formula for rearrangement collisions is used extensively in both atomic and nuclear physics. This formula contains a direct contribution from the heavy particle or "core" interaction. A straightforward demonstration shows that for the usual case of a massive core this contribution does not appear, so that the only effect of this interaction is to distort the incident and outgoing waves. Such problems as the "post-prior" discrepancy are clarified.

ASYMPTOTIC BEHAVIOR AND SUBTRACTIONS IN THE MANDELSTAM REPRESENTATION. Marcel Froissart,* Department of Physics, University of California, Berkeley, California (Received March 27, 1961).

It is proved that a two-body reaction amplitude involving scalar particles and satisfying Mandelstam's representation is bounded by expressions of the form $Cs \ln^2 s$ at the forward and backward angles, and $Cs^{3/4} \ln^{3/2} s$ at any other fixed angle in the physical region, C being a constant, s being the total squared c.m. energy. This corresponds to cross sections increasing at most like $\ln^2 s$. These restrictions limit the freedom of choice of the subtraction terms to six arbitrary single spectral functions and one subtraction constant.

*On leave of absence from Centre d' Etudes Nucléaires de Saclay, Gif sur Yvette, Seine et Oise, France.

CORRELATIONS BETWEEN CUSPS IN DIFFERENTIAL CROSS SECTIONS AND IN POLARIZATIONS. M. Nauenberg and A. Pais, Institute for Advanced Study, Princeton, New Jersey (Received March 31, 1961).

Experiments have shown that partial waves with

$l > 1$ appear in $\pi^- + p \to \Lambda + K^0$ at the ΣK thresholds. This necessitates a reconsideration of the criteria sufficient to determine the $\Sigma\Lambda$ parity $P(\Sigma\Lambda)$ by the method of cusps. In this paper we start from the usual assumption that contributions which show a cusp in either the differential cross section or the polarization may be ignored beyond some optimal power in $\cos\theta$. On this sole basis, previously stated criteria are rendered inadequate due to the occurrence of Minami and other ambiguities. It is shown that under suitable circumstances there exist unambiguous correlations between certain properties of cross-section cusps and of polarization cusps. These correlations could possibly be of use to determine $P(\Sigma\Lambda)$ and give information as to which states contribute significantly to the ΛK production at ~900 Mev. The finite separation between $\Sigma^0 K^0$ and $\Sigma^- K^+$ thresholds is taken into account. The results are summarized in a table of cusp properties.

ANALYTIC PROPERTIES AND RESCATTERING CORRECTION TO THE BORN APPROXIMATION FOR TRANSITION MATRIX ELEMENTS. B. Bosco,* Institute of Theoretical Physics, Department of Physics, Stanford University, Stanford, California (Received March 22, 1961).

In this paper the analytic properties of a matrix element of a general operator between a bound state and a scattering state are studied in the framework of the Schrödinger theory. It is shown that the singularities of such a matrix element are easily inferred from those of the Born approximation. Finally, using the fact that the possible singularities which are not contained in the Born approximation are located far apart from those included in the lowest approximation, a simple formula is derived which allows one to obtain the rescattering correction to the Born approximation using the phase shifts explicitly.

*Permanent address: Istituto di Fisica dell' Università, Torino, Italy.